Chem, Volume *7*

Supplemental information

Synthetic Na^+/K^+ exchangers promote apoptosis by disturbing cellular cation homeostasis

Sang-Hyun Park, Inhong Hwang, Daniel A. McNaughton, Airlie J. Kinross, Ethan N.W. Howe, Qing He, Shenglun Xiong, Martin Drøhse Kilde, Vincent M. Lynch, Philip A. Gale, Jonathan L. Sessler, and Injae Shin

Supplemental Experimental Procedures

Table of Contents

1. Synthetic Experimental

All solvents and chemicals used were purchased from Aldrich, TCI, Acros, or Fisher Scientific and used without further purification. TLC analyses were carried out using Sorbent Technologies silica gel (200 mm) sheets. Column chromatography was performed on Sorbent silica gel 60 (40–63 mm). NMR spectra were recorded on a Varian Mercury 400 instrument. The NMR spectra were referenced to residual solvent peaks. Spectroscopic solvents were purchased from Cambridge Isotope Laboratories and Aldrich. Electrospray ionization (ESI) mass spectra were recorded on a VG AutoSpec apparatus. X-ray crystallographic analyses were carried out on either a Rigaku AFC12 diffractometer equipped with a Saturn 724+ CCD with a graphite monochromator and a MoKα radiation source (λ = 0.7107 Å) or an Agilent Technologies Super Nova Dual Source diffractometer using a μ-focused Cu Kα radiation source (λ = 1.5418 Å) with collimating mirror monochromators. Further details of the structures and their refinement is given in a later section.

Compounds **3** and **5** were prepared according to reported procedures[1, 2].

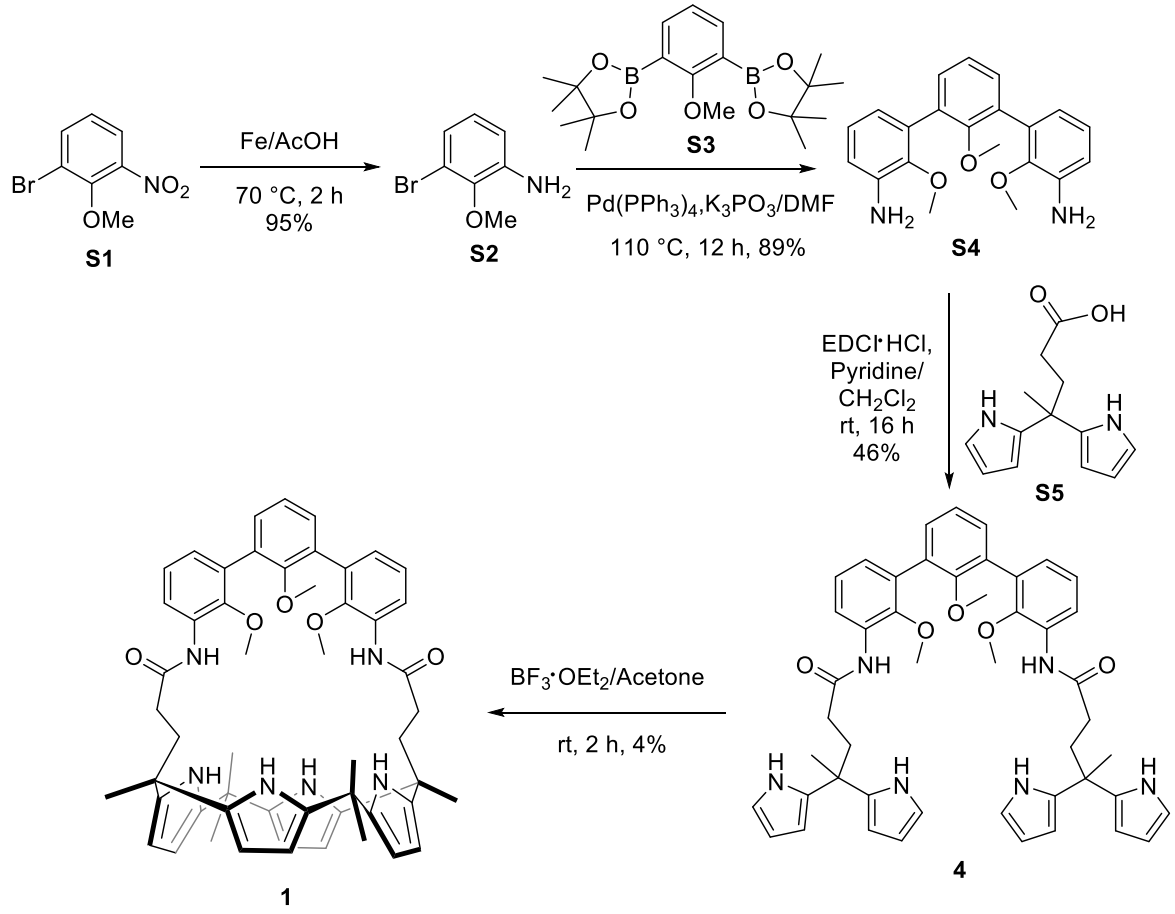

Scheme S1. Synthesis of receptor **1** and control **4**.

Compound S2. To a solution of 1-bromo-2-methoxy-3-nitro-benzene **S1**[3] (45 g, 194 mmol) and acetic acid (AcOH) (450 mL) was added iron powder (65 g, 1.2 mmol). The reaction mixture was then heated to 70 °C for 2 h. The reaction mixture was cooled to room temperature and filtered. The filtrate was washed with ethyl acetate (EtOAc) (1 L) and the combined organics were concentrated. The residue was redissolved in EtOAc (300 mL), washed with water (3 x 200 mL), dried with Na_2SO_4 and concentrated in vacuo, which gave 3-bromo-2-methoxyaniline **S2** (37.4 g, mmol, 95%) as a yellow oil: ^{1}H NMR (400 MHz, $CDCl_3$) δ 6.90 (dd, *J* = 6.4, 1.2 Hz, 1H), 6.78 (t, *J* = 6.4 Hz, 1H), 6.67 (dd, *J* = 6.4, 1.2 Hz, 1H), 3.92 (brs, 2H), 3.83 (s, 3H) ppm. ^{13}C NMR (100 MHz, $CDCl_3$) δ 144.3, 141.6, 125.9, 122.5, 117.3, 115.1, 59.7 ppm. HRMS (ESI) m/z 201.9862 $[M + H]^+$ calcd for $C_7H_9BrNO^+$, found 201.9861.

Compound S4. Compounds **S2** (4.32 g, 21.4 mmol), **S3**[4] (3.64 g, 10.1 mmol), $Pd(PPh_3)_4$ (0.66 g, 0.6 mmol), and K_3PO_4 (12.72 g, 60 mmol) were mixed and dissolved in dry DMF (100 ml) and then heated to 110℃ under an N_2 atmosphere and then stirred for 12 h. After allowing the reaction mixture to cool to room temperature, the mixture was diluted with EtOAc (250 ml). The resulting solution was washed with water (5×100 ml). The combined organic phase was dried over anhydrous Na_2SO_4 for 4 h. After evaporative removal of the volatiles, the residue was subjected to flash column over silica gel eluting with CH_2Cl_2/methanol/triethylamine (2:1, v/v) to obtain the product (3.09 g, 89%) as an off-white solid: ^{1}H NMR (400 MHz, $CDCl_3$): δ 7.22-7.20 (m, 2H, ArH), 7.13-7.07 (m, 3H, ArH), 6.37-6.33 (m, 4H, ArH), 3.75 (s, 6H, OMe), 3.71 (brs., 4H, NH2), 3.21 (s, 3H, Ome); ^{13}C NMR (100 MHz, CDCl3) δ 157.9, 156.6, 147.1, 132.3, 131.9, 131.1, 122.7, 118.8, 107.1, 98.8, 60.3, 55.6; HRMS (ESI) m/z 351.1703 $[M + H]^+$ calcd for $C_{21}H_{23}N_2O_3^+$, found 351.1716.

Compound 4. To a mixture of compound **S4** (1.98 g, 5.6 mmol), **S5**[5] (2.89 g, 12.4 mmol), and EDCI•HCl (3.26 g, 17.0 mmol) in DCM (150 ml) 4 ml of pyridine was added. The resulting solution was stirred at room temperature under an N_2 atmosphere for 16 h. After the volatiles were removed under reduced pressure, the residue was subjected to silica gel column eluting with EtOAc/hexanes (1/3, v/v) to give 2.01 g (46% yield) of **4** as off-white solid: ^{1}H NMR (400 MHz, $CDCl_3$): δ 7.95 (s, 4H, pyrrolic-NH), 7.50 (d, *J* = 2.0 Hz, 2H, ArH), 7.23-7.20 (m, 4H, ArH), 7.15-7.10 (t, *J* = 8.0 Hz, 1H, ArH), 7.04 (brs., 2H, CONH), 6.6-6.62 (dd, *J* = 8.0 Hz, 2.0 Hz, 4H, pyrrole-H), 6.21-6.02 (m, 8H, pyrrole-H), 3.77 (s, 6H, Ome), 3.14 (s, 3H, Ome), 2.50-2.39 (m, 4H, CH_2), 2.30-2.20 (m, 4H, CH_2), 1.62 (s, 6H, CH_3); ^{13}C NMR (100 MHz, $CDCl_3$) δ 171.5, 157.3, 156.3, 138.5, 137.1, 131.5, 131.5, 131.3, 124.0, 122.9, 117.6, 111.1, 108.1, 105.2, 103.2, 60.6, 55.8, 39.1, 36.1, 33.4, 26.7; HRMS (ESI) m/z 801.3735 $[M + Na]^+$ calcd for $C_{47}H_{50}N_6NaO_5^+$ found 801.3743.

Compound 1. A solution of precursor **4** (1.133 g, 1.455 mmol) in acetone (500 ml) was added

dropwise to a solution of BF_3•Et_2O (1.0 ml) in acetone (700 ml) over 8 h at RT. After that, the reaction solution was stirred for further 3 h at RT. Then triethylamine (10 ml) was added to quench the reaction. The volatiles were removed under reduced pressure and the resulting residue was dissolved in chloroform (300 mL) and washed with water (4 × 200 mL). After the volatiles were again removed under reduced pressure, the residue was purified by column chromatography over silica gel (eluent: MeOH/DCM (1/100, v/v) to give 250 mg (0.291 mmol, 20% yield) of **1** as an off-white solid: ^{1}H NMR (400 MHz, CD_2Cl_2) δ 8.43 (brs., 2H, CONH), 8.23 (d, *J* = 4.0 Hz, 2H, ArH), 7.89 (br., 2H, pyrrole-NH), 7.84 (br., 2H, pyrrole-NH), 7.45 (d, *J* = 8.0 Hz, 2H, ArH), 7.33 (t, *J* = 8.0 Hz, 1H, ArH), 7.19 (t, *J* = 8.0 Hz, 2H, ArH), 7.12 (d, *J* = 8.0 Hz, 2H), 5.93-5.90 (m, pyrrole-CH), 3.35 (s, 6H, OMe), 2.90 (s, 3H, OMe), 2.55-2.20 (m, 8H, CH_2), 1.61-1.47 (m, 18H, Me). ^{13}C NMR (100 MHz, CD_2Cl_2) δ 171.4, 157.3, 147.4, 138.9, 138.6, 136.8, 136.7, 132.2, 132.1, 131.9, 130.7, 125.0, 124.7, 124.5, 119.3, 105.4, 104.5, 104.0, 61.4, 61.2, 54.2, 39.3, 37.3, 35.9, 35.7, 34.4, 31.5, 30.6, 29.2, 28.9, 28.0. HRMS (ESI) m/z 881.4361 $[M + Na]^+$ calcd for $C_{53}H_{58}N_6NaO_5^+$ found 881.4366.

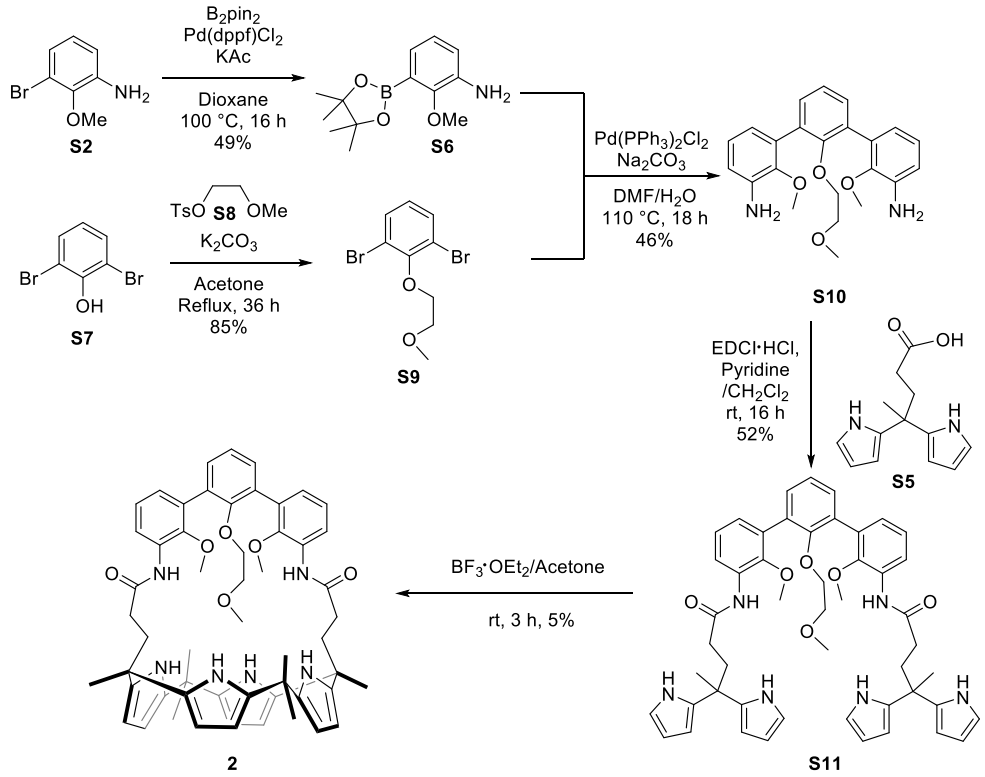

Scheme S2. Synthesis of receptor **2**.

Compound S6. A mixture of **S2** (6.61 g, 32.7 mmol), bis(pinacolato)diboron (12.46 g, 49.1 mmol) potassium acetate (9.62 g, 98.2 mmol) and $Pd(dppf)Cl_2$ (1.05 g, 1.1 mmol) in dioxane (200 ml) was thoroughly degassed with N_2. The resulting solution was heated to 100 °C under

N_2 overnight. The reaction mixture was cooled to room temperature and then quenched with H_2O (200 ml) and diluted with EtOAc (150 mL). The organic phase was separated and washed with brine (3 x 300 mL), dried over anhydrous Na_2SO_4, filtered off and concentrated *in vacuo*. Further purification by flash column chromatography over silica gel (EtOAc/hexanes, 1/3, v/v) gave **S6** (3.81 g, 15.4 mmol) as a white solid in a yield of 49%: ^{1}H NMR (400 MHz, $CDCl_3$) δ 7.11 (dd, J = 6.0, 1.6 Hz, 1H), 6.94-6.91 (m, ArH, 1H), 6.86-6.84 (m, ArH, 1H), 3.81 (s, 3H, CH_3), 1.36 (s, 12H, CH_3) ppm. ^{13}C NMR (126 MHz, $CDCl_3$) δ 152.7, 139.7, 126.1, 124.3, 119.1, 83.7, 61.5, 25.0 ppm. HRMS (ESI) m/z 250.1609 $[M + H]^+$ calcd for $C_{13}H_{21}BNO_3^+$ found 250.1616.

Compound S9. A mixture of 2,6-dibromophenol (**S7**) (10.0 g, 39.7 mmol), 2-methoxyethyl *p*-toluenesulfonate (**S8**) (9.60 g, 41.7 mmol) and K_2CO_3 (16.5 g, 119 mmol) was heated to reflux for 45 h. The reaction mixture was cooled to rt and was filtered through a short silica gel plug (SiO_2 0.43-0.63 μm) using acetone as the eluent. Purification by flash column chromatography over silica gel (SiO_2 0.43-0.63 μm 30% CH_2Cl_2/hexanes to 40% CH_2Cl_2/hexanes, loading on column: hexanes) gave **S9** (10.4 g, 33.6 mmol, 85%) as a colorless oil: ^{1}H NMR (400 MHz, $CDCl_3$) δ 7.50 (d, J = 8.0 Hz, 2H), 6.86 (t, J = 8.0 Hz, 1H), 4.22 – 4.13 (m, 2H), 3.87 – 3.78 (m, 2H), 3.49 (s, 3H) ppm. ^{13}C NMR (101 MHz, $CDCl_3$) δ 153.3, 132.9, 126.5, 118.6, 72.2, 71.7, 59.4 ppm. HRMS (ESI) m/z 330.8940 $[M + Na]^+$ calcd for $C_9H_{10}Br_2NaO_2^+$ found 330.8944.

Compound S10. To a nitrogen degassed solution of **S9** (1.00 g, 3.23 mmol) and **S6** (2.10 g, 8.43 mmol) in a mixture of DMF (40 mL) and H_2O (8 mL) was added $Pd(PPh_3)_2Cl_2$ and Na_2CO_3 and the reaction mixture was then heated to 110 ℃ under an N_2 atmosphere for 18 h. The reaction mixture was cooled to rt and diluted with Et_2O (100 mL) and quenched with H_2O (100 mL). The phases were separated and the aqueous phase extracted with Et_2O (4 x 50 mL). The combined organic extracts were washed with H_2O (3 x 75 mL), brine (100 mL), dried with Na_2SO_4, filtered and concentrated *in vacuo*. Purification by flash column chromatography over silica gel (SiO_2 0.40-0.63 μm, 50% EtOAc/hexanes to 100% EtOAc; loaded on the column using warm $CHCl_3$) gave **S10** (587 mg, 1.49 mmol, 46%) as an off-white solid: ^{1}H NMR (500 MHz, $CDCl_3$) δ 7.35 (d, J = 5.0 Hz, 2H, ArH), 7.20-7.17 (m, 1H, ArH), 6.96-6.93 (m, 2H, ArH), 6.77-6.74 (m, 4H, ArH), 3.89 (brs., 4H, NH_2), 3.54 – 3.45 (m, 8H, OCH_3 and CH_2), 3.04 (t, J = 5.0 Hz, 2H, CH_2), 2.96 (s, 3H, OCH_3) ppm. ^{13}C NMR (126 MHz, $CDCl_3$) δ 155.2, 145.4, 140.0, 132.6, 132.6, 130.8, 124.2, 123.3, 121.3, 115.4, 71.9, 71.3, 59.7, 58.5 ppm. HRMS (ESI) m/z 395.1965 $[M + H]^+$ calcd for $C_{23}H_{27}N_2O_4^+$ found 395.1963, and 417.1785 $[M + Na]^+$ calcd for $C_{23}H_{26}N_2NaO_4^+$ found 417.1783.

Compound S11. To a solution of **S10** (3.36 g, 8.52 mmol), **S5**[5] (6.80 g, 29.3 mmol) and EDC·HCl (7.20 g, 37.6 mmol) in CH_2Cl_2 (250 ml) was added pyridine (20 mL, 248 mmol) and the reaction mixture was stirred under nitrogen atmosphere for 16 h after which the solvents were removed *in vacuo*. Purification by flash column chromatography over silica gel (SiO_2

0.40-0.63 μm, 40% EtOAc/hexanes to 60% EtOAc/hexanes; loaded on column using CH_2Cl_2) gave **S11** (4.04 g, 4.75 mmol, 56%) as a white solid: ^{1}H NMR (500 MHz, $CDCl_3$) δ 8.34 (d, J = 8.0 Hz, 2H), 8.00 (s, 4H), 7.88 (s, 2H), 7.37 (d, J = 7.5 Hz, 2H), 7.27-7.23 (m, 1H), 7.14 (t, J = 8.0 Hz, 2H), 7.05 (d, J = 8.0 Hz, 2H), 6.63 (s, 4H), 6.14 (s, 8H), 3.44 (s, 6H), 3.30 (t, J = 4.5 Hz, 2H), 2.90 (t, J = 5.0 Hz, 2H), 2.84 (s, 3H), 2.45 (t, J = 7.5 Hz, 4H), 2.26 (t, J = 7.5 Hz, 4H), 1.63 (s, 6H) ppm. ^{13}C NMR (126 MHz, $CDCl_3$) δ 171.6, 155.1, 146.6, 137.1, 132.2, 131.4, 131.3, 131.0, 126.2, 124.4, 124.1, 119.9, 117.5, 107.9, 105.1, 72.2, 71.1, 60.9, 58.3, 38.9, 36.2, 33.5, 26.6. HRMS (ESI) m/z 845.3997 $[M + Na]^+$ calcd for $C_{49}H_{54}N_6NaO_6$ found 845.3996.

Compound 2. To a solution of $BF_3{\cdot}OEt_2$ (1.5 mL, 95%) in acetone (1.3 L) was added a solution of **S11** (1.80 g, 2.19 mmol) in acetone (0.5 L) over 8 h and the reaction mixture was stirred for a further 3 h under a nitrogen atmosphere. The reaction mixture was quenched with Et_3N (12 mL), which resulted in a color change from red to yellow, after which the volatiles were removed *in vacuo*, and the result solid was dissolved in chloroform (300 mL) and washed with water (3 × 200 mL), after which the solvents were removed *in vacuo*. Purification by flash column chromatography over silica gel (SiO_2 0.40-0.63 μm, 1% MeOH/DCM; loaded on column using CH_2Cl_2) gave **2** (592 mg, 0.655 mmol, 30%) as a white solid: ^{1}H NMR (400 MHz, CD_2Cl_2) δ 9.04 (br., 2H, CONH), 8.37 (d, J = 8.0 Hz, 2H, ArH), 7.97 (br., 2H, pyrrole-NH), 7.93 (br., 2H, pyrrole-NH), 7.48 (d, J = 8.0 Hz, 2H, ArH), 7.35 (t, J = 8.0 Hz, 1H, ArH), 7.15 (t, J = 8.0 Hz, 2H, ArH), 7.04 (d, J = 8.0 Hz, 2H, ArH), 5.88 (m, pyrrole-CH), 3.34 (s, 6H, Ome), 3.00 (t, J = 4.0 Hz, 2H, CH_2), 2.83 (t, J = 4.0 Hz, 2H, CH_2), 2.78 (s, 3H, OCH_3), 2.29-2.21 (m, 4H, CH_2), 1.94-1.87 (m, 4H, CH_2), 1.71-1.48 (m, 18H, Me) ppm. ^{13}C NMR (101 MHz, CD_2Cl_2) δ 172.5, 155.8, 147.5, 139.9, 139.2, 138.9, 136.2, 132.8, 132.2, 131.2, 130.2, 125.3, 125.2, 124.5, 119.6, 105.2, 104.0, 103.5, 102.6, 71.6, 70.9, 61.7, 57.0, 39.0, 37.8, 35.8, 35.2, 35.2, 30.8, 30.6, 29.0, 27.8, 25.4 ppm. HRMS (ESI) m/z 921.4909 $[M + H_3O]^+$ calcd for $C_{55}H_{65}N_6O_7^+$ found 921.5102, and 925.4623 $[M + Na]^+$ calcd for $C_{55}H_{62}N_6NaO_6^+$ found 925.4628.

2. X-ray Crystal Structures and ^{1}H NMR Spectral Titrations

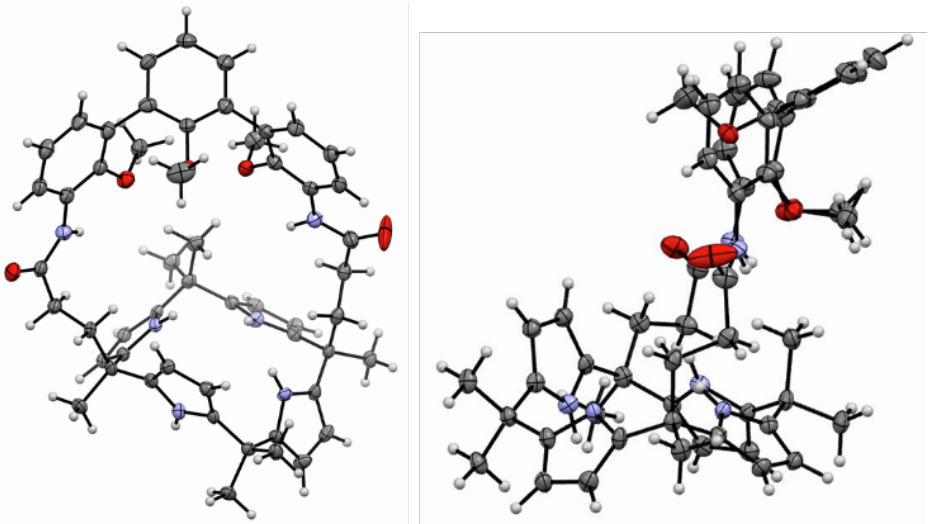

Figure S1. Two views of the single crystal structure of **1**. Displacement ellipsoids are scaled to the 50% probability level. Solvent molecules are omitted for clarity.

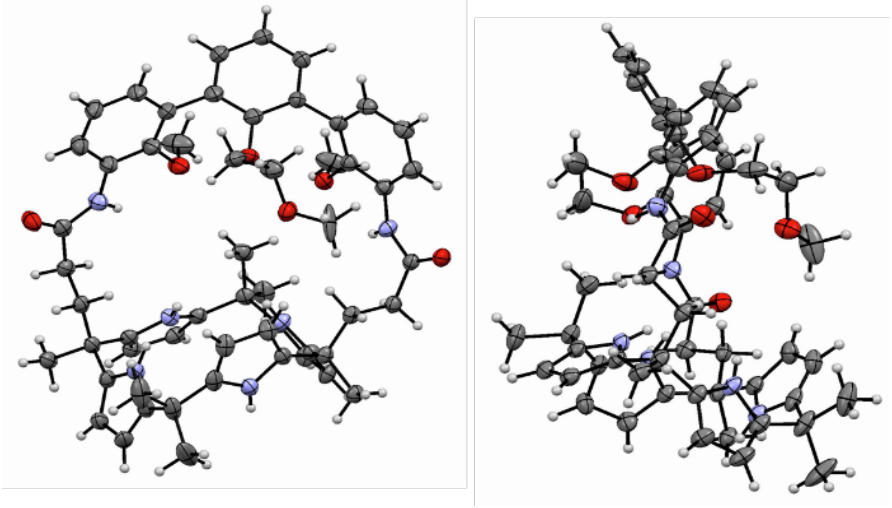

Figure S2. Two views of the single crystal structure of **2**. Displacement ellipsoids are scaled to the 50% probability level. Solvent molecules are omitted for clarity.

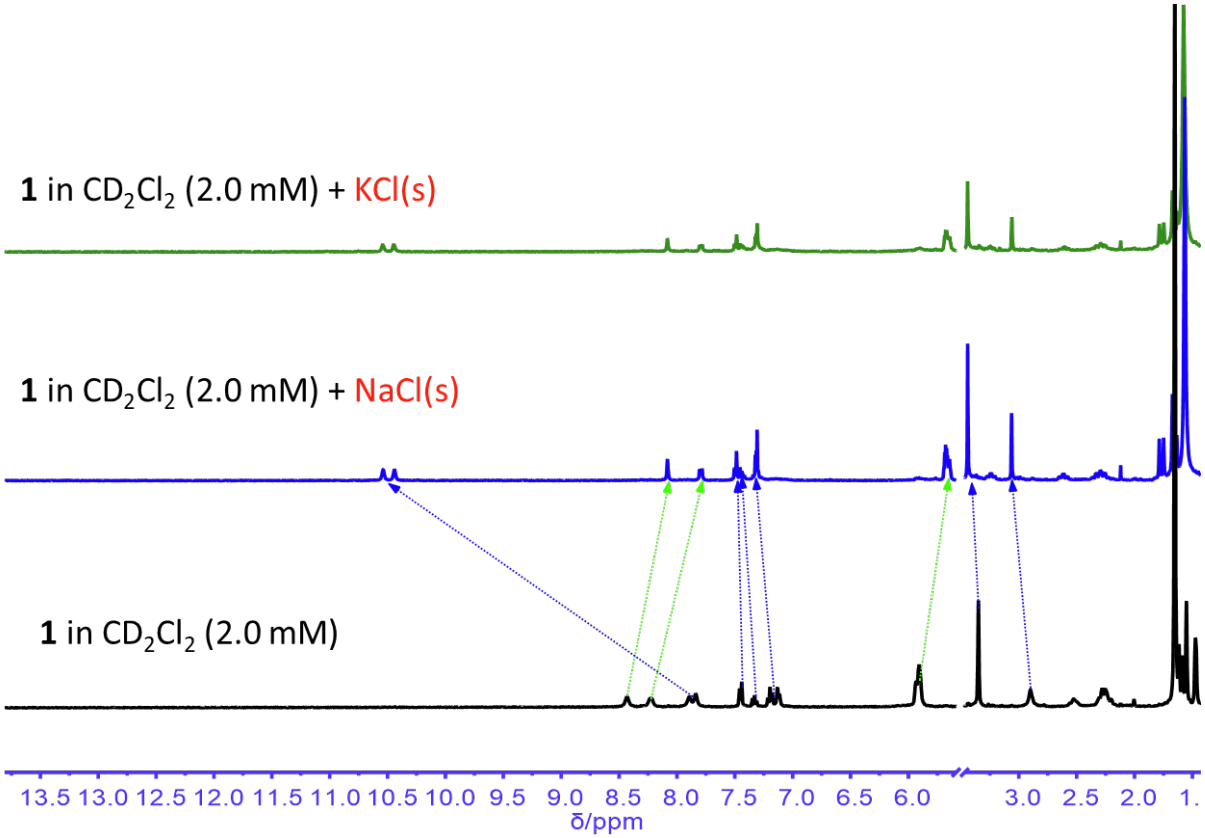

Figure S3. Partial ^{1}H NMR spectra of a 2.0 mM solution of receptor **1** recorded in the absence (bottom) and presence of excess NaCl (middle), and KCl (top) in CD_2Cl_2. All spectra were recorded after allowing the solid phase and the organic phase to equilibrate for 48 h.

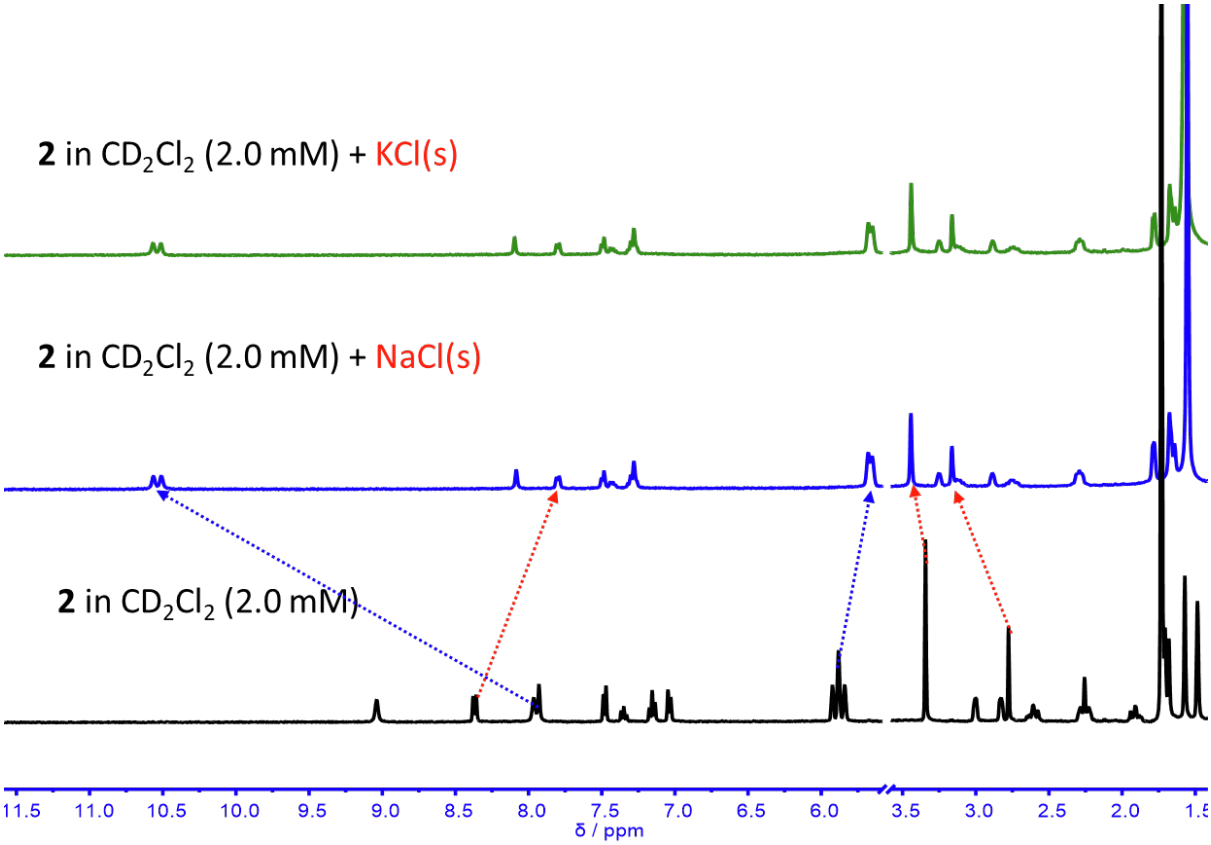

Figure S4. Partial ^{1}H NMR spectra of a 2.0 mM solution of receptor **2** recorded in the absence (bottom) and presence of excess NaCl (middle), and KCl (top) in CD_2Cl_2. All spectra were recorded after allowing the solid phase and the organic phase to equilibrate for 48 h.

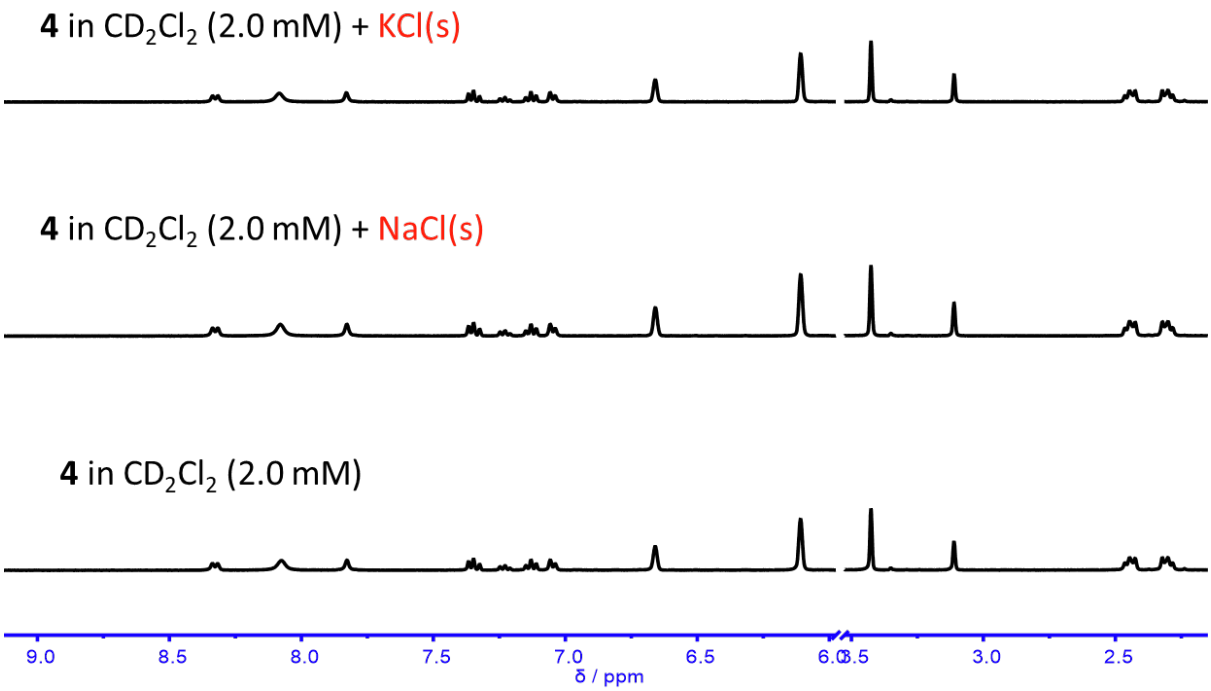

Figure S5. Partial ^{1}H NMR spectra of a 2.0 mM solution of control system **4** recorded in the absence (bottom) and presence of excess NaCl (middle), and KCl (top) in CD_2Cl_2. All spectra were recorded after allowing the solid phase and the organic phase to equilibrate for 48 h. The lack of spectral change is taken as evidence that compound **4** is not able to bind NaCl or KCl effectively.

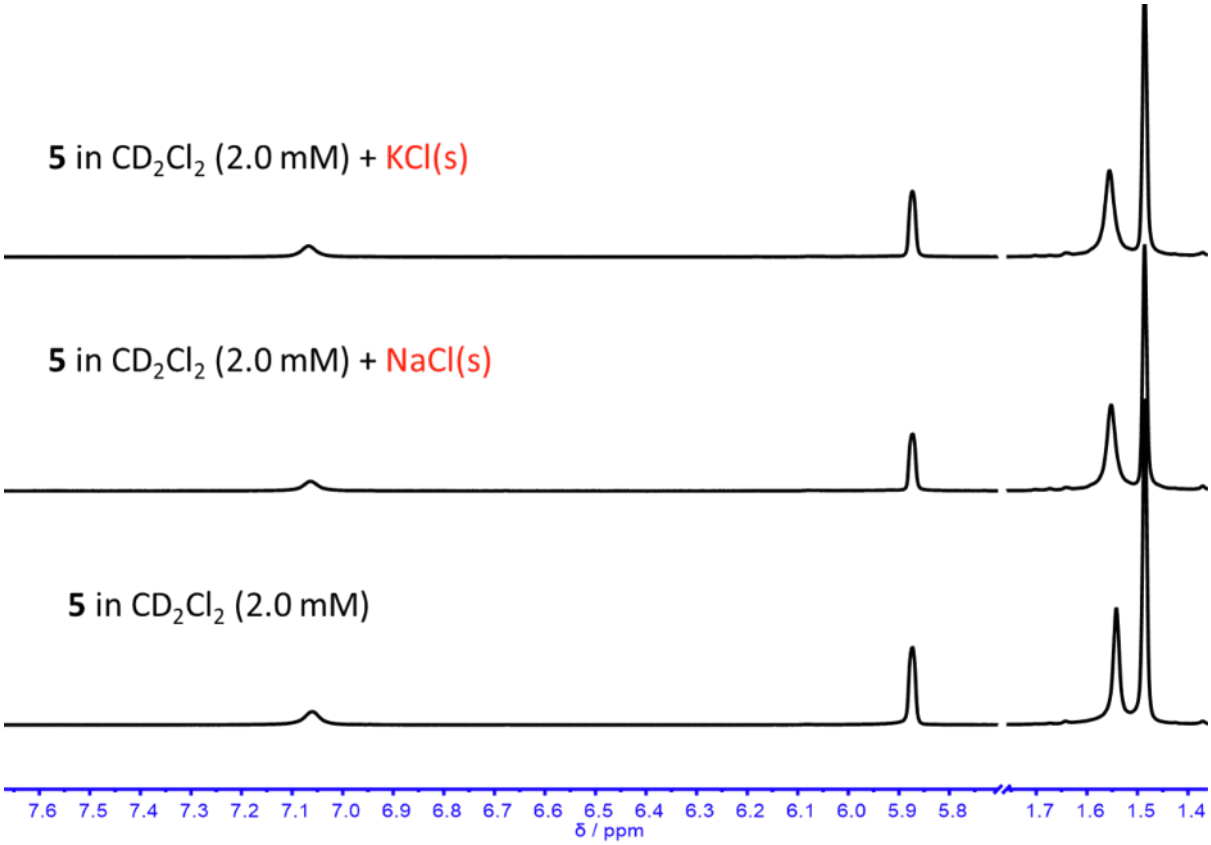

Figure S6. Partial ^{1}H NMR spectra of a 2.0 mM solution of free **5** recorded in the absence (bottom) and presence of excess NaCl (middle), and KCl (top) in CD_2Cl_2. All spectra were recorded after allowing the solid phase and the organic phase to equilibrate for 48 h. The lack of spectral change is taken as evidence that compound **5** is not able to bind either NaCl or KCl effectively.

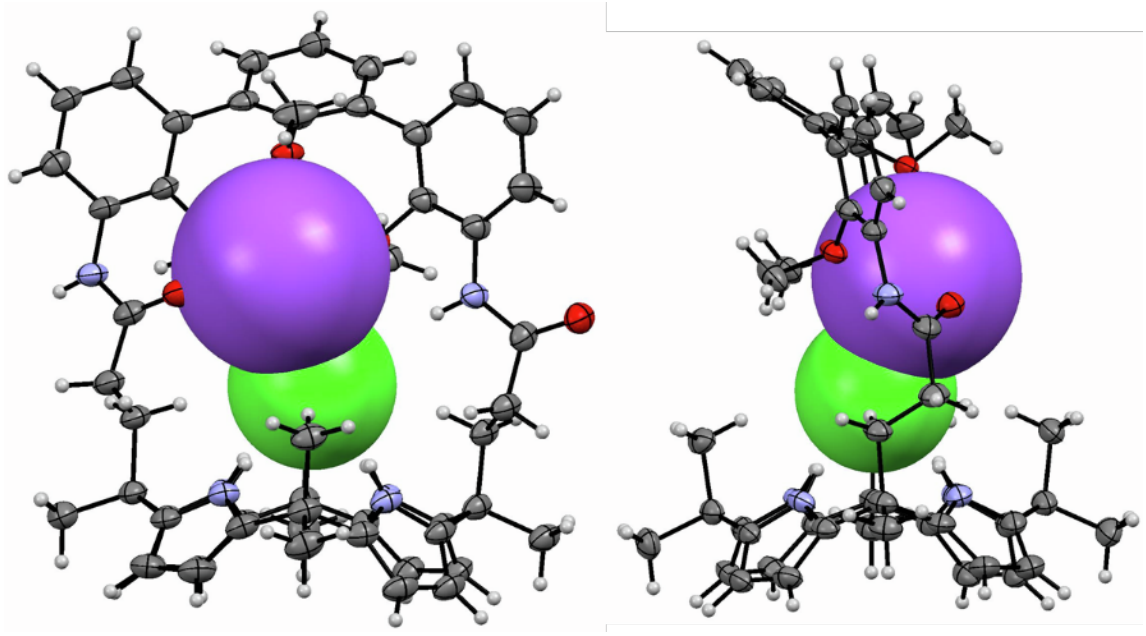

Figure S7. Front view (left) and side view (right) of the single crystal structure of complex **1**•NaCl. Displacement ellipsoids are scaled to the 50% probability level. Solvent molecules are omitted for clarity.

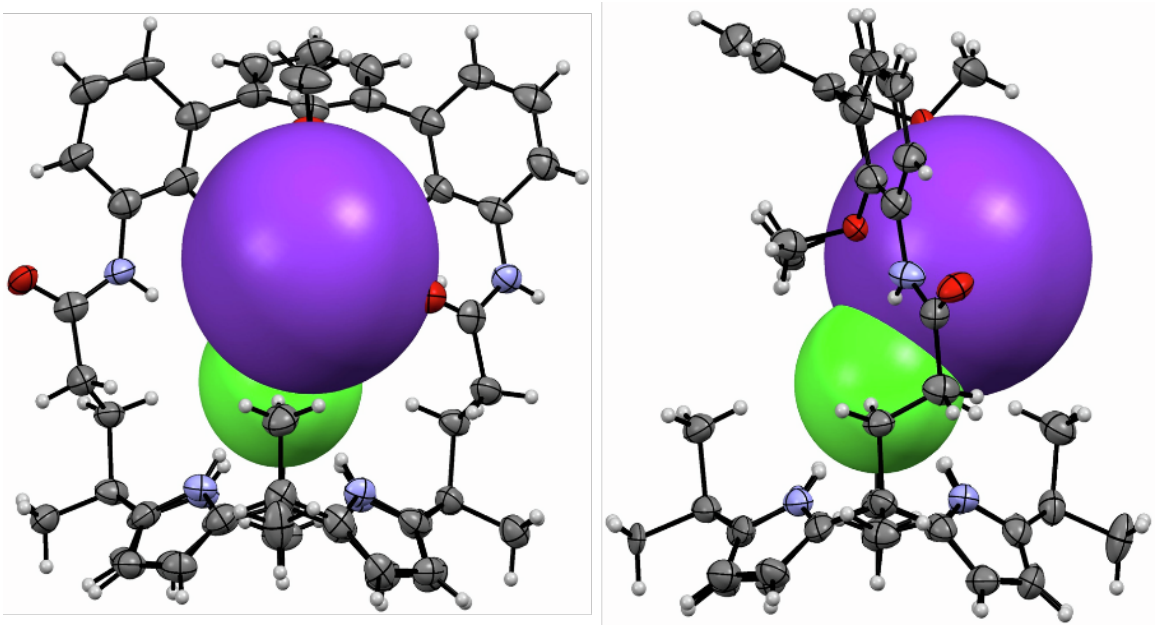

Figure S8. Front view (left) and side view (right) of the single crystal structure of complex **1**•KCl. Displacement ellipsoids are scaled to the 50% probability level. Solvent molecules are omitted for clarity.

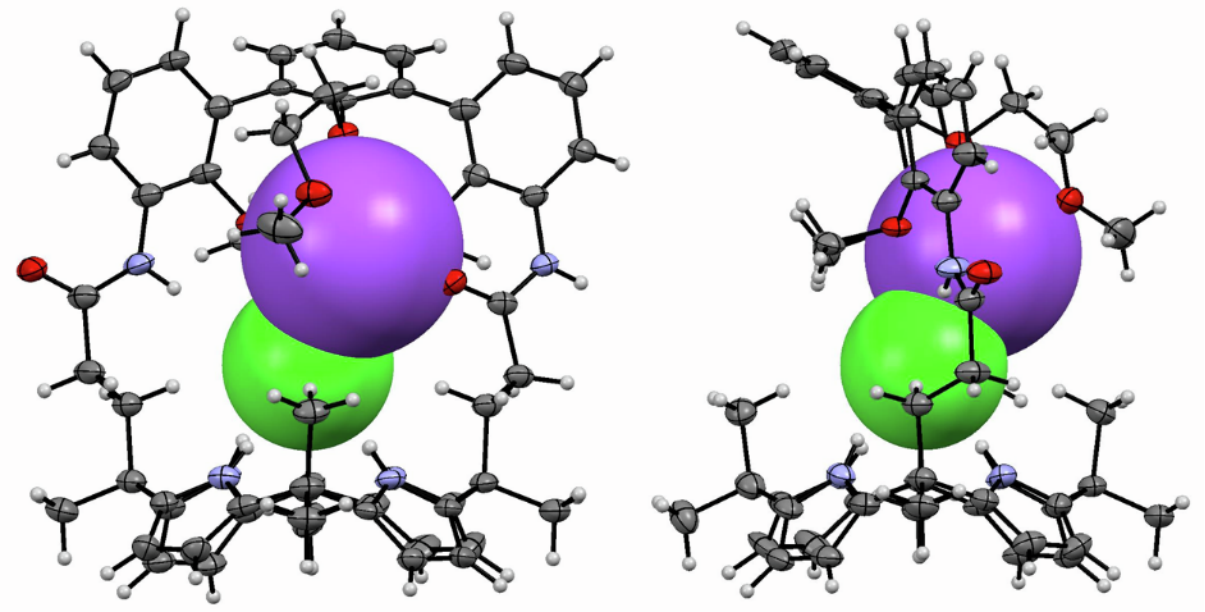

Figure S9. Front view (left) and side view (right) of the single crystal structure of complex **2**•NaCl. Displacement ellipsoids are scaled to the 50% probability level. Solvent molecules are omitted for clarity.

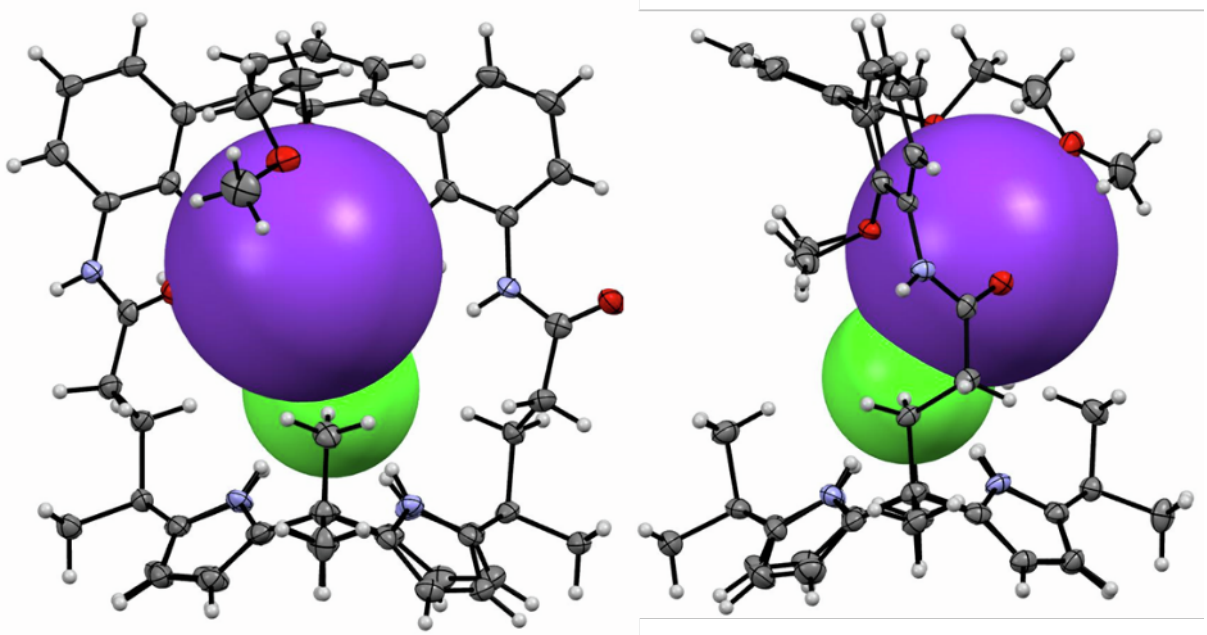

Figure S10. Front view (left) and side view (right) of the single crystal structure of complex **2**•KCl. Displacement ellipsoids are scaled to the 50% probability level. Solvent molecules are omitted for clarity.

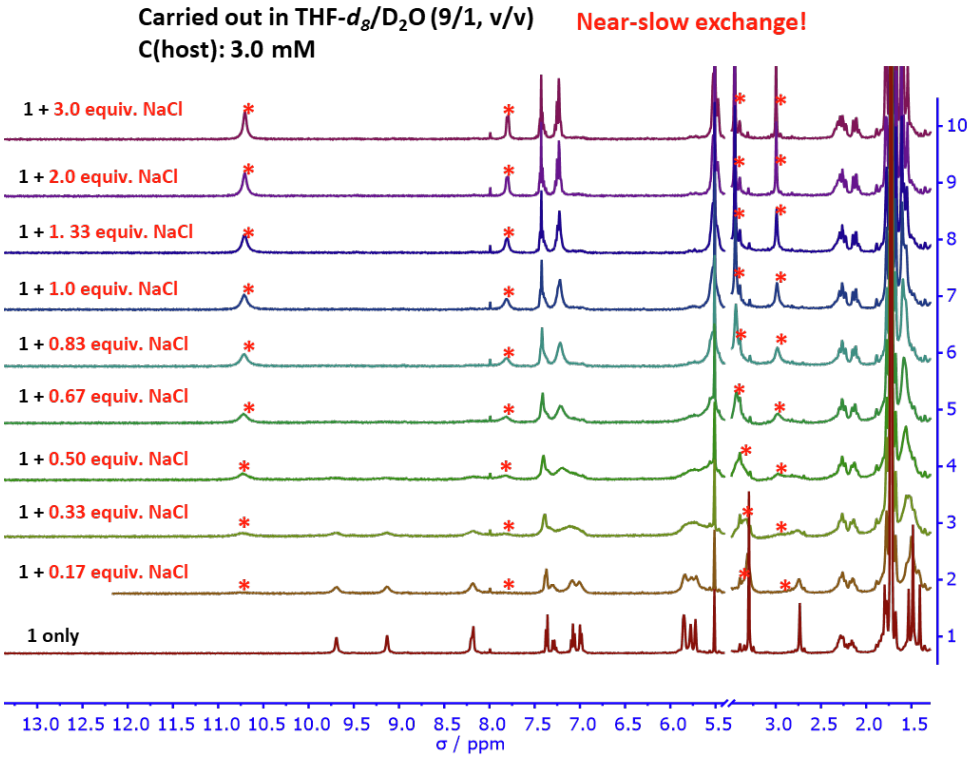

Figure S11. ^{1}H NMR spectroscopic titration of receptor **1** with NaCl in a mixed solvent consisting of THF-d_8/D_2O (9/1, v/v). The concentration of **1** was 3.0 mM.

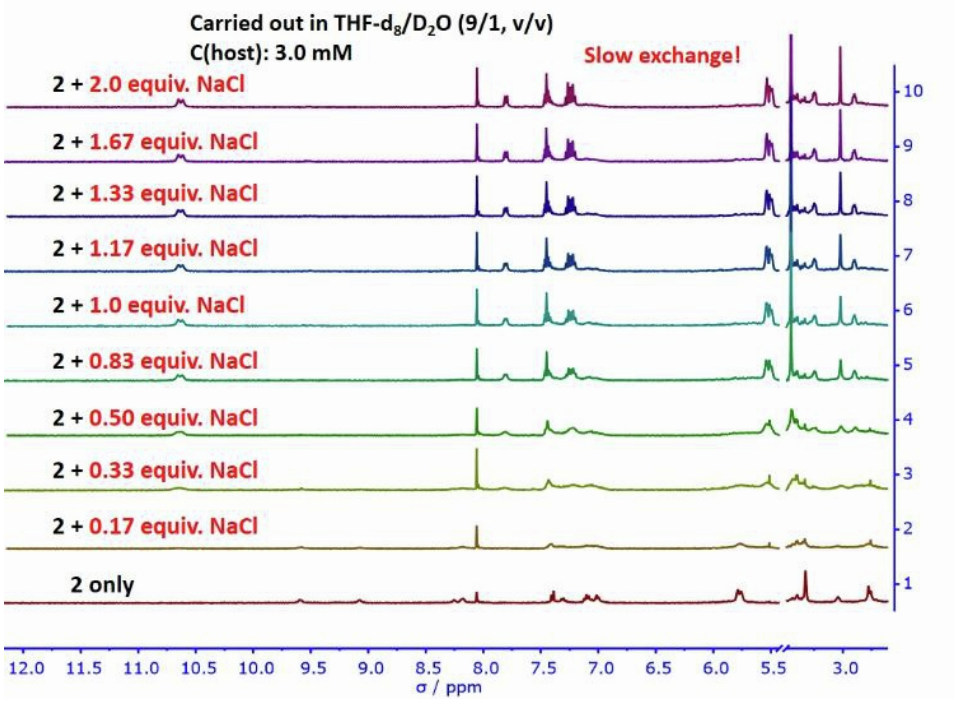

Figure S12. ^{1}H NMR spectroscopic titration of receptor **2** with NaCl in a mixed solvent consisting of THF-d_8/D_2O (9/1, v/v). The concentration of **2** was 3.0 mM.

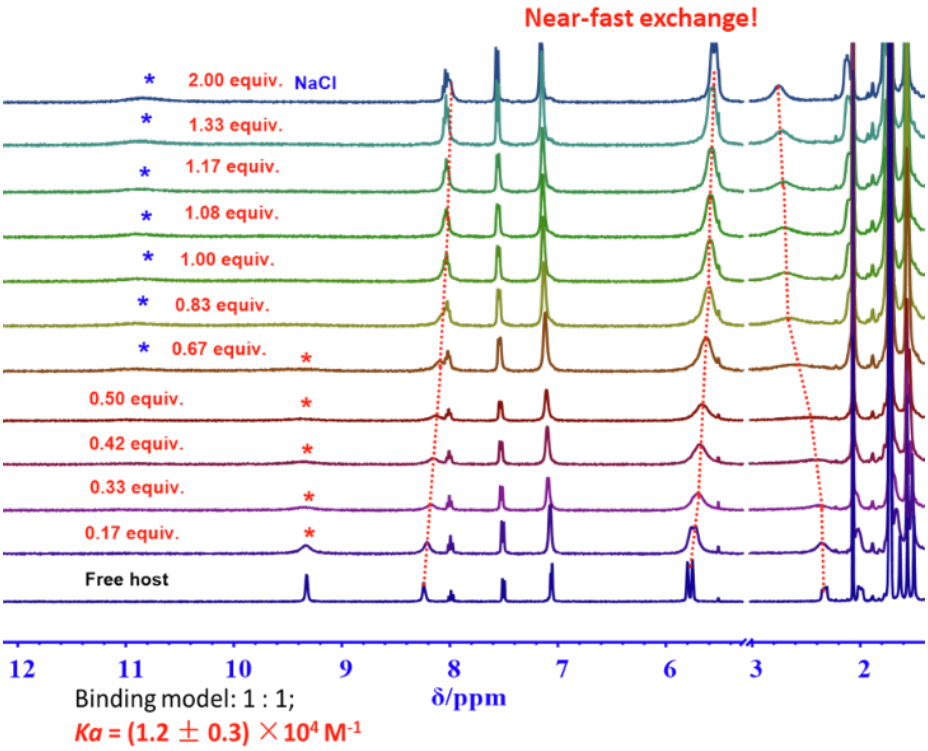

Figure S13. ^{1}H NMR spectroscopic titration of receptor **3** with NaCl in a mixed solvent consisting of THF-d_8/D_2O (9/1, v/v). The concentration of **3** was 4.0 mM.

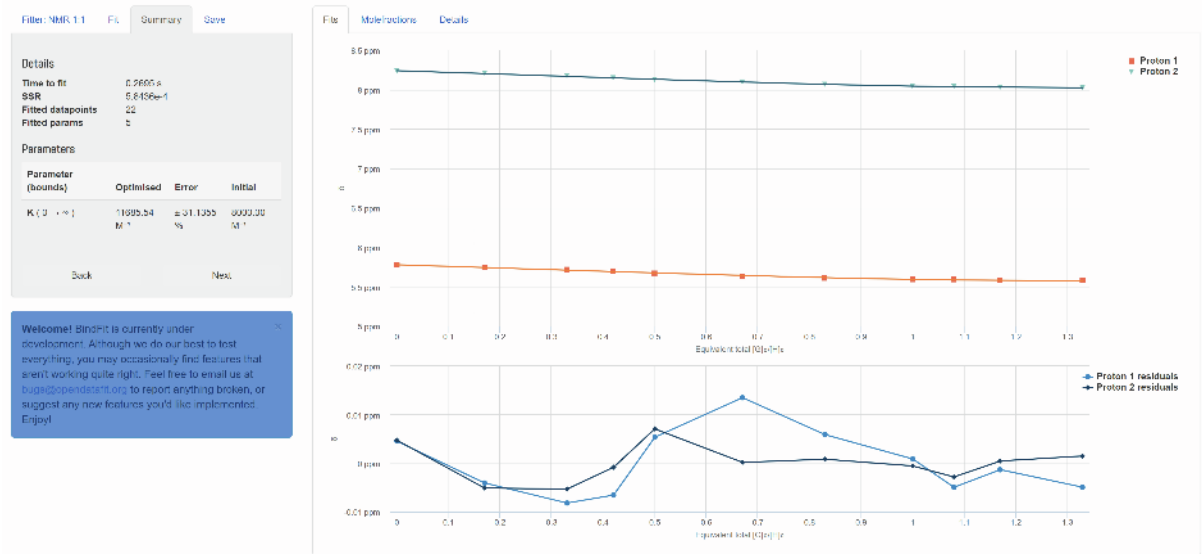

Figure S14. Nonlinear least-square analysis of the ^{1}H NMR binding data corresponding to the formation of **3**•NaCl complex. The data extracted from Figure 13 were fitted to a 1:1 binding model to give K_a = (1.2 ± 0.3) ×10^4 M^{-1}. The residual distribution is shown below the binding isotherm. All solid lines were obtained from non-linear curve-fitting to a 1:1 binding model using the www.supramolecular.org web applet.

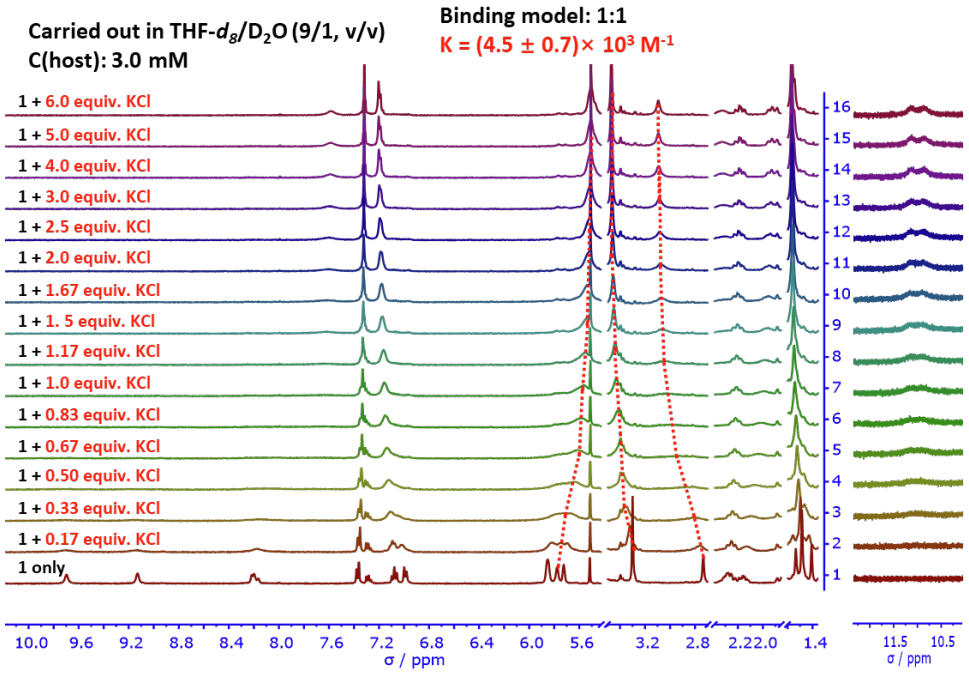

Figure S15. ^{1}H NMR spectroscopic titration of receptor **1** with KCl in a mixed solvent consisting of THF-d_8/D_2O (9/1, v/v). The concentration of **1** was 3.0 mM.

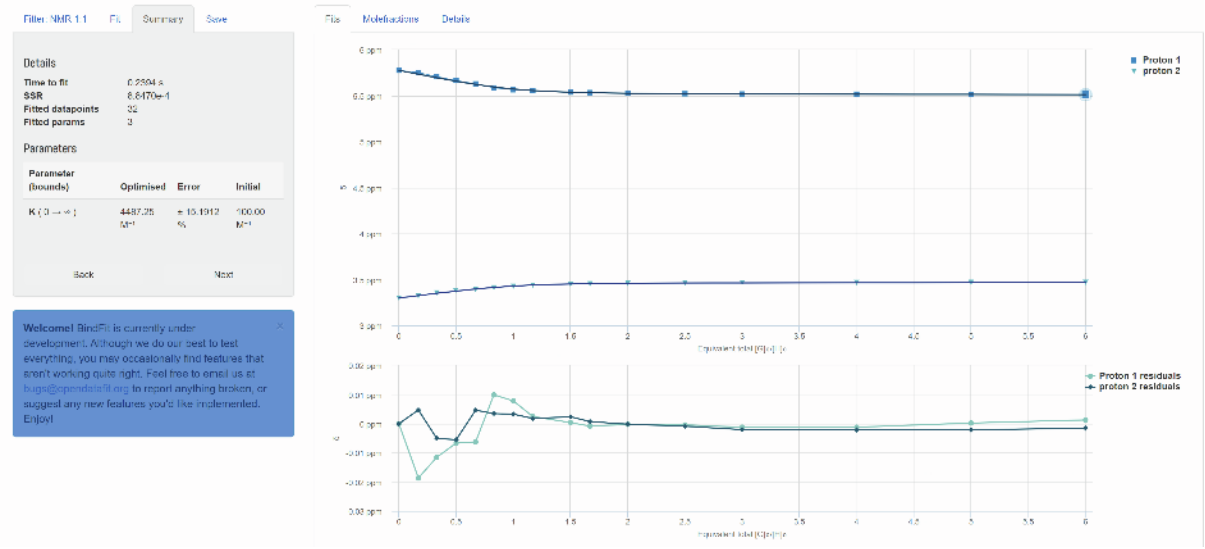

Figure S16. Nonlinear least-square analysis of the ^{1}H NMR binding data corresponding to the formation of **1**•KCl complex. The data extracted from Figure 15 were fitted to a 1:1 binding model to give K_a = (4.5 ± 0.7) ×10^3 M^{-1}. The residual distribution is shown below the binding isotherm. All solid lines were obtained from non-linear curve-fitting to a 1:1 binding model using the www.supramolecular.org web applet.

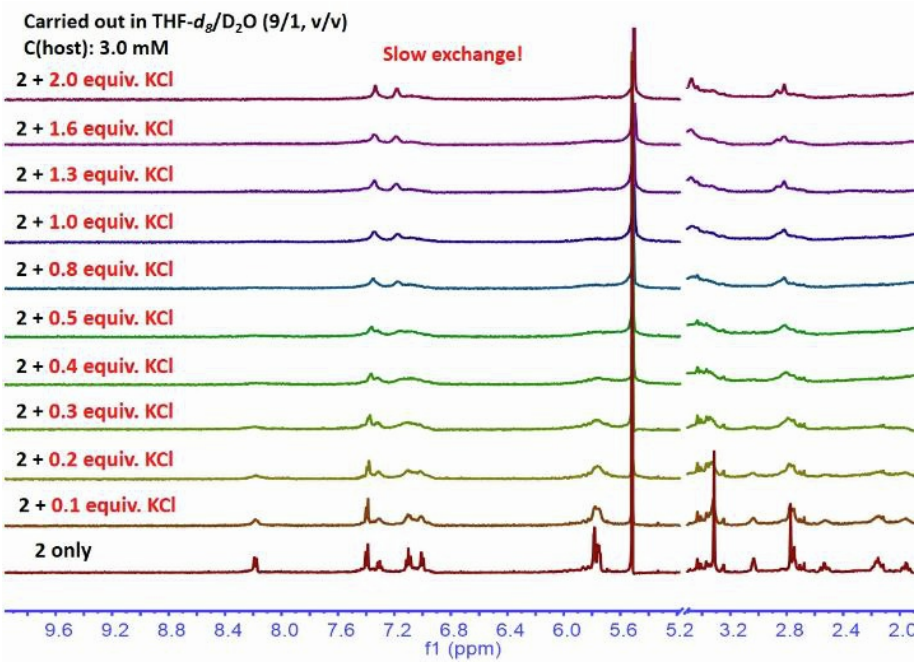

Figure S17. ^{1}H NMR spectroscopic titration of receptor **2** with KCl in a mixed solvent consisting of THF-d_8/D_2O (9/1, v/v). The concentration of **2** was 3.0 mM.

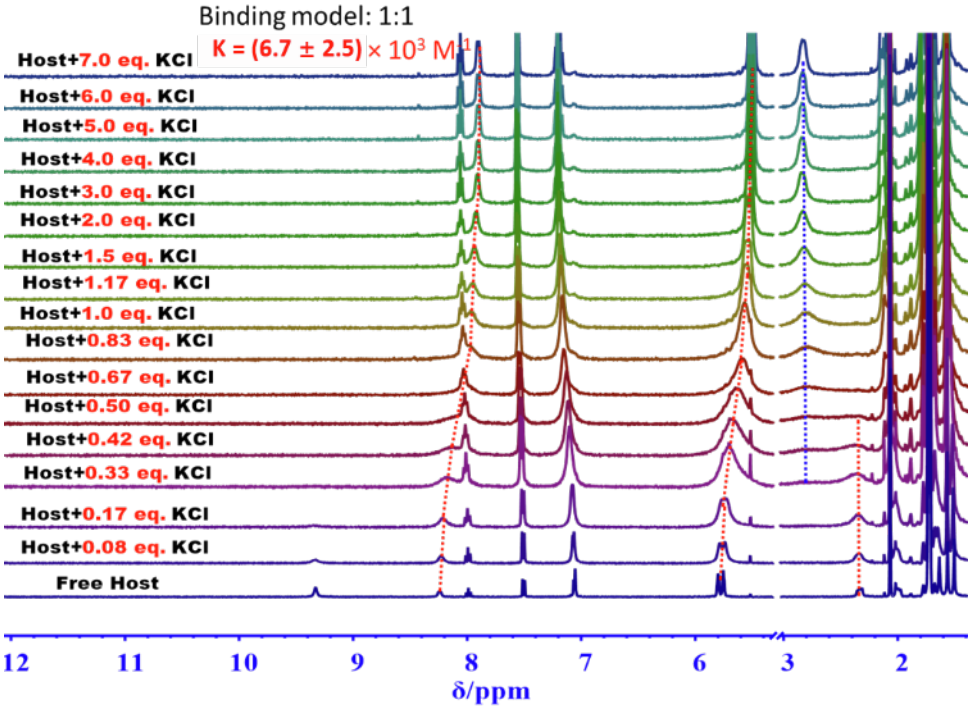

Figure S18. ^{1}H NMR spectroscopic titration of receptor **3** with KCl in a mixed solvent consisting of THF-d_8/D_2O (9/1, v/v). The concentration of **3** was 4.0 mM.

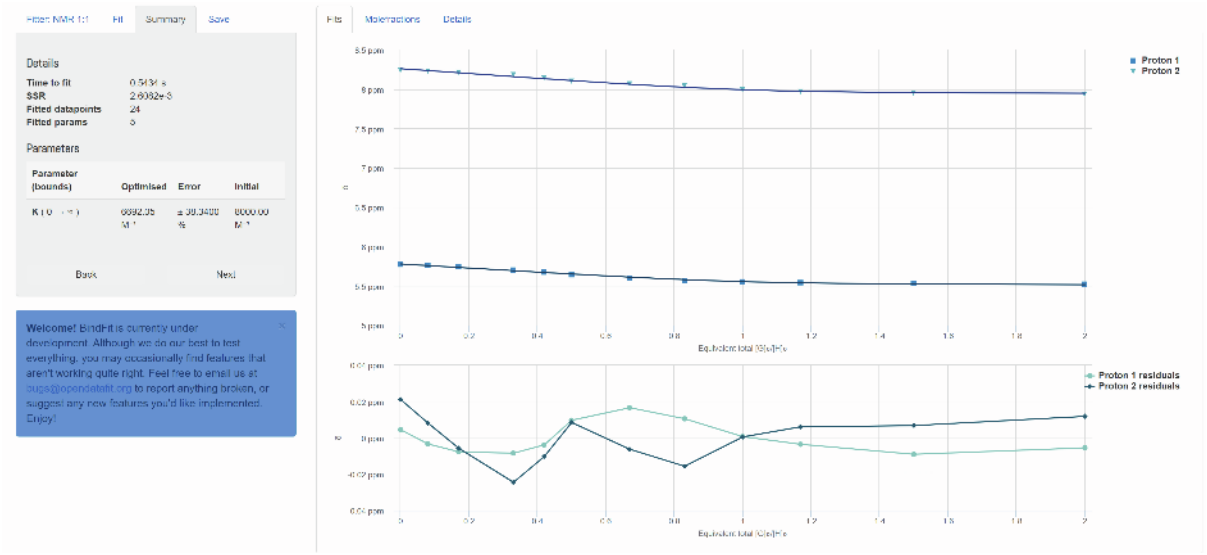

Figure S19. Nonlinear least-square analysis of the ^{1}H NMR binding data corresponding to the formation of **3**•KCl complex. The data extracted from Figure 18 were fitted to a 1:1 binding model to give $K_a = (6.7 \pm 2.5) \times 10^3$ M^{-1}. The residual distribution is shown below the binding isotherm. All solid lines were obtained from non-linear curve-fitting to a 1:1 binding model using the www.supramolecular.org web applet.

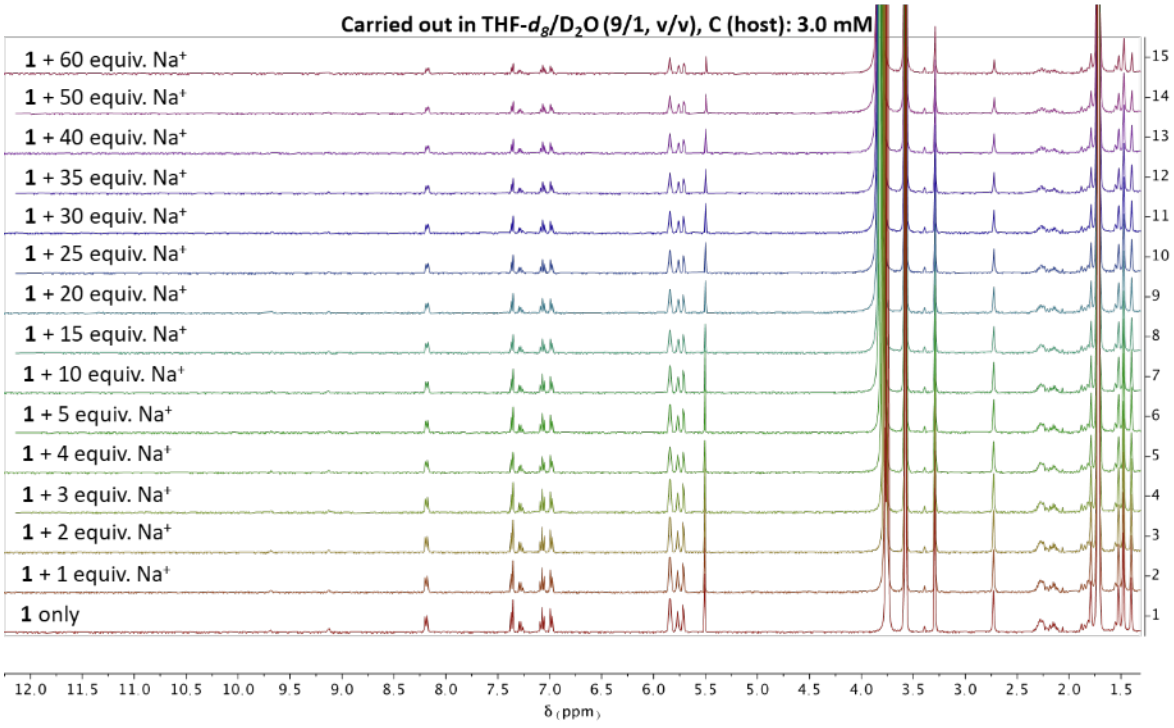

Figure S20. ^{1}H NMR spectroscopic titration of receptor **1** with Na^+ (as PF_6^- salt) in a mixed solvent consisting of THF-d_8/D_2O (9/1, v/v). The concentration of **1** was 3.0 mM. Negligible binding of single Na^+ was observed.

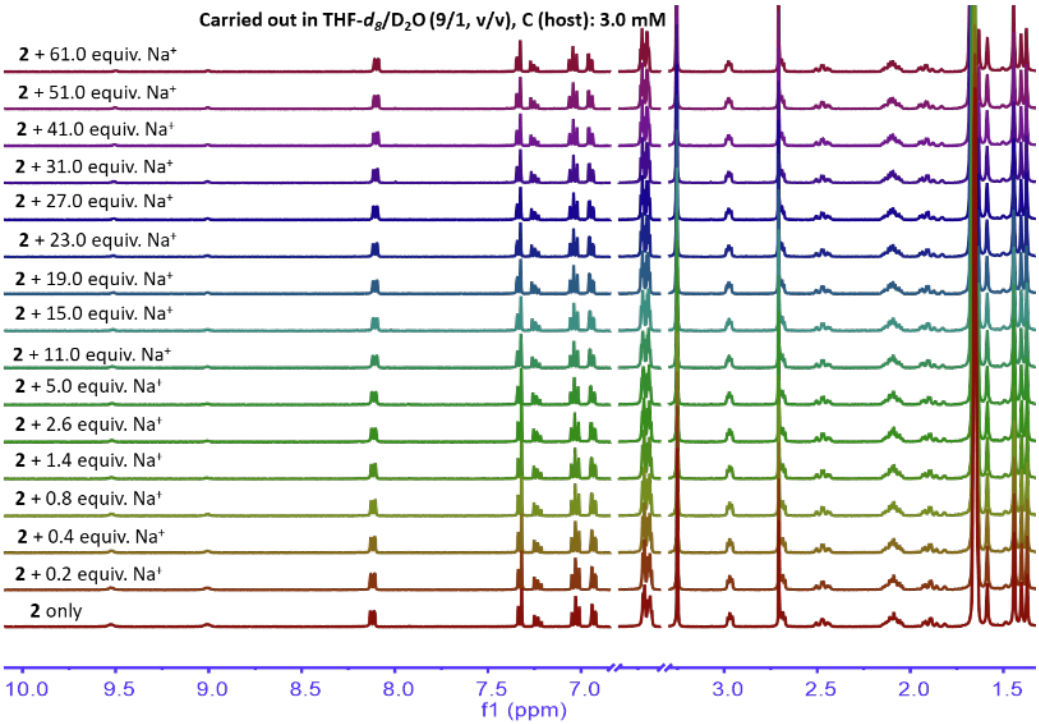

Figure S21. ^{1}H NMR spectroscopic titration of receptor **2** with Na^+ (as PF_6^- salt) in a mixed solvent consisting of THF-d_8/D_2O (9/1, v/v). The concentration of **2** was 3.0 mM. Negligible binding of single Na^+ was observed.

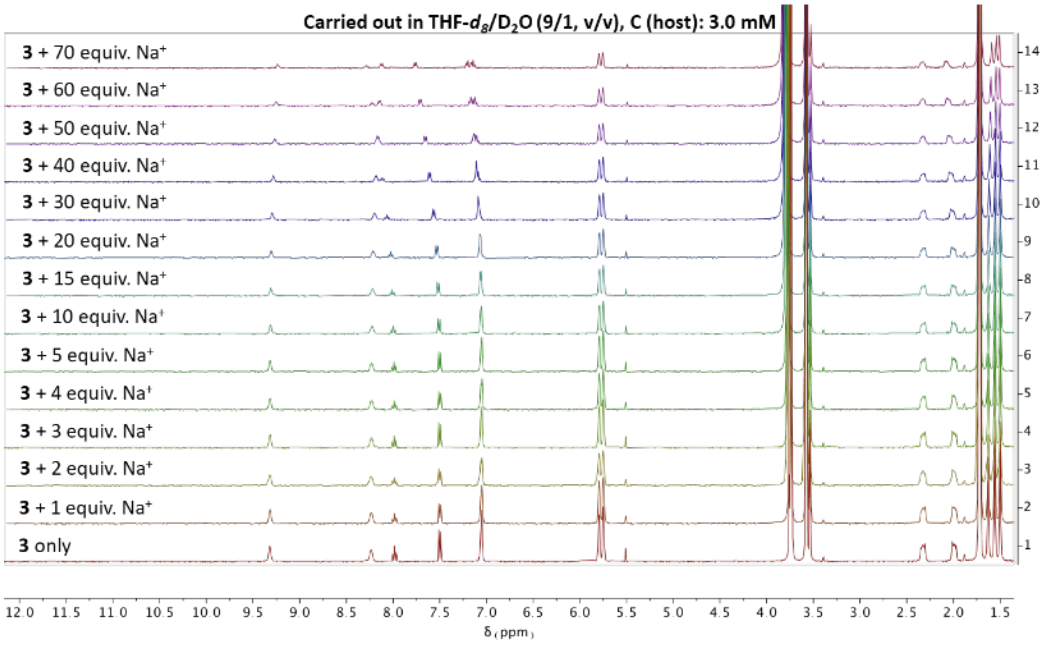

Figure S22. ^{1}H NMR spectroscopic titration of receptor **3** with Na^+ (as PF_6^- salt) in a mixed solvent consisting of THF-d_8/D_2O (9/1, v/v). The concentration of **3** was 3.0 mM. Negligible binding of single Na^+ was observed.

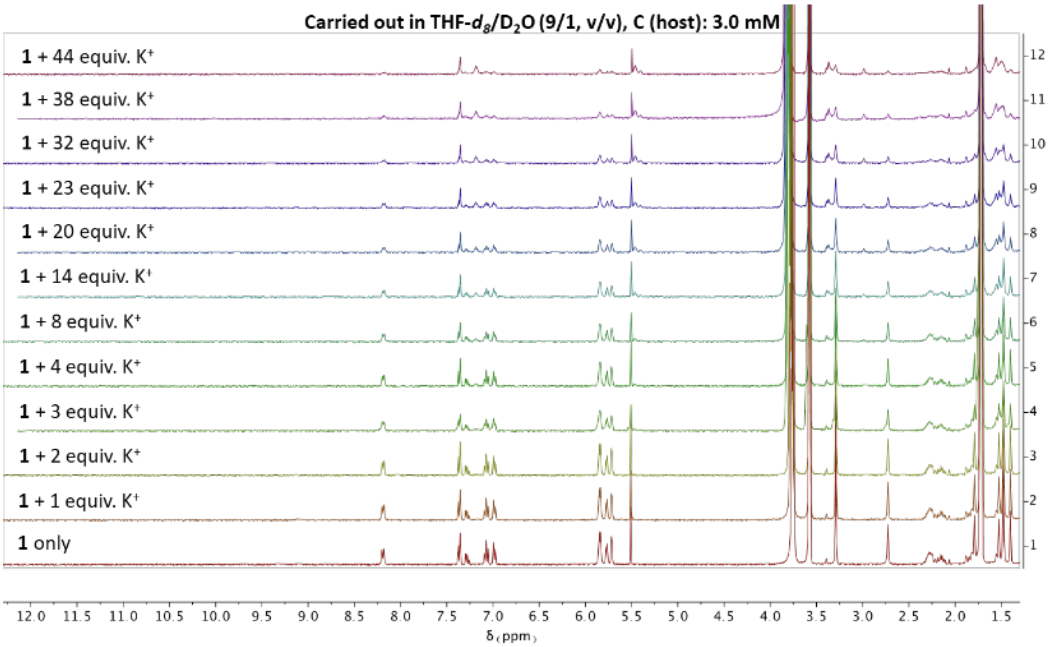

Figure S23. ^{1}H NMR spectroscopic titration of receptor **1** with K^+ (as PF_6^- salt) in a mixed solvent consisting of THF-d_8/D_2O (9/1, v/v). The concentration of **1** was 3.0 mM. Negligible binding of single K^+ was observed.

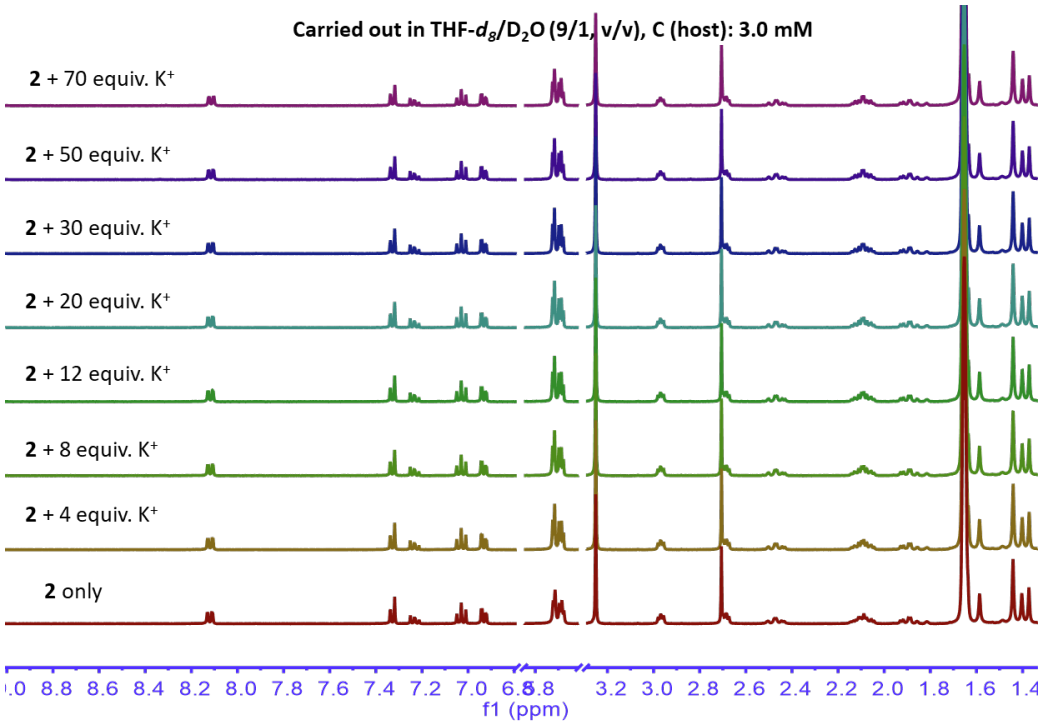

Figure S24. ^{1}H NMR spectroscopic titration of receptor **2** with K^+ (as CF_3COO^- salt) in a mixed solvent consisting of THF-d_8/D_2O (9/1, v/v). The concentration of **2** was 3.0 mM. Negligible binding of single K^+ was observed.

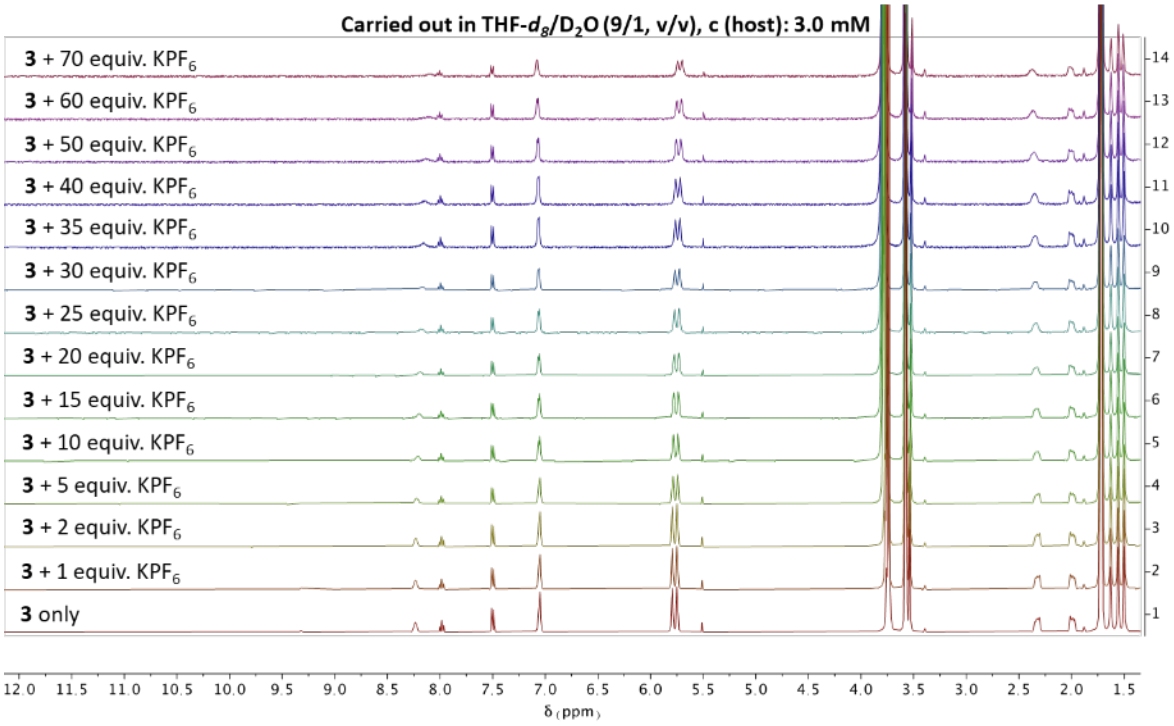

Figure S25. ^{1}H NMR spectroscopic titration of receptor **3** with K^+ (as PF_6^- salt) in a mixed solvent consisting of THF-d_8/D_2O (9/1, v/v). The concentration of **3** was 3.0 mM. Negligible binding of single K^+ was observed.

3. Theoretical calculations

All calculations were carried out with the Gaussian 16 suite[6] of programs using the X3LYP density functional[7]. A 6-31G* basis set was used for C, H, O, N, Li, Na, K and Cl. Complexation energies were corrected for basis set superposition error (BSSE) using the counterpoise correction method [8, 9]. The crystal structure parameters were used as the starting coordinates for these calculations

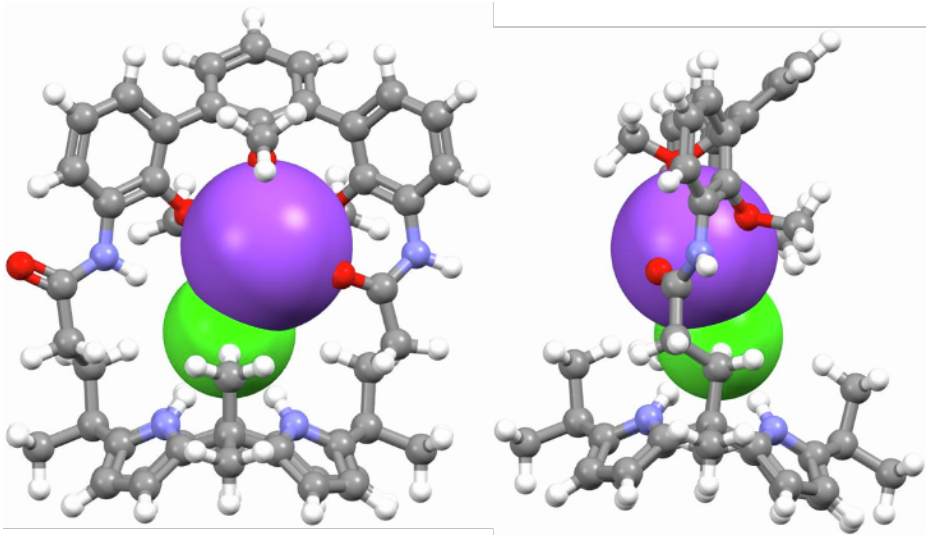

Figure S26. Front (left) and side (right) views of the DFT optimized structure of the NaCl complex of receptor **1**.

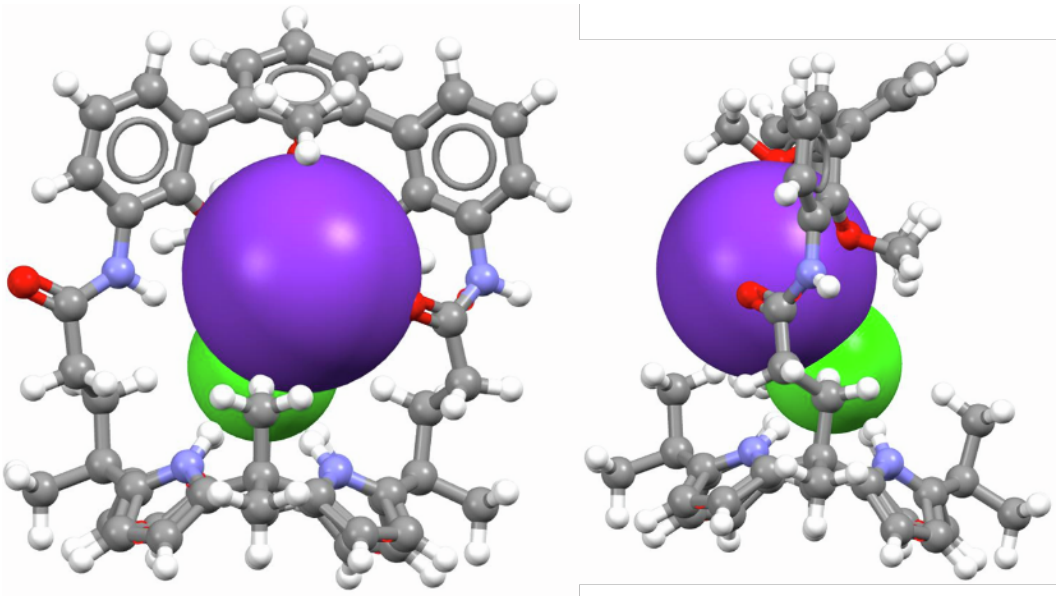

Figure S27. Front (left) and side (right) views of the DFT optimized structure of the KCl complex of receptor **1**.

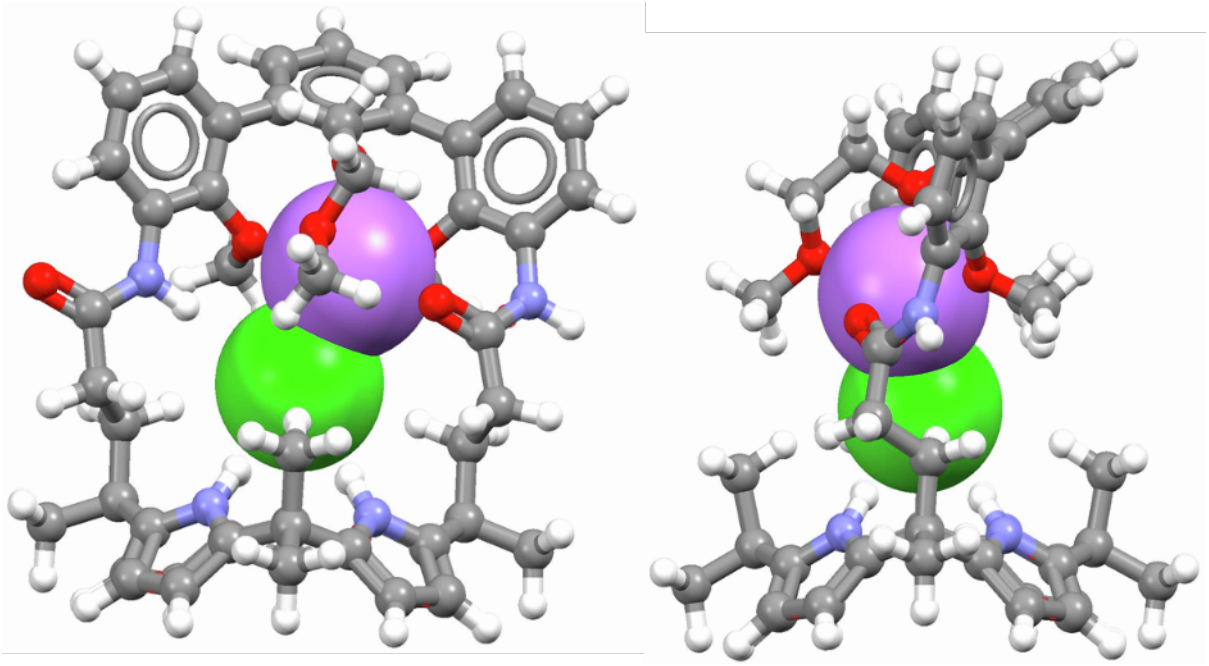

Figure S28. Front (left) and side (right) views of the DFT optimized structure of the NaCl complex of receptor **2**.

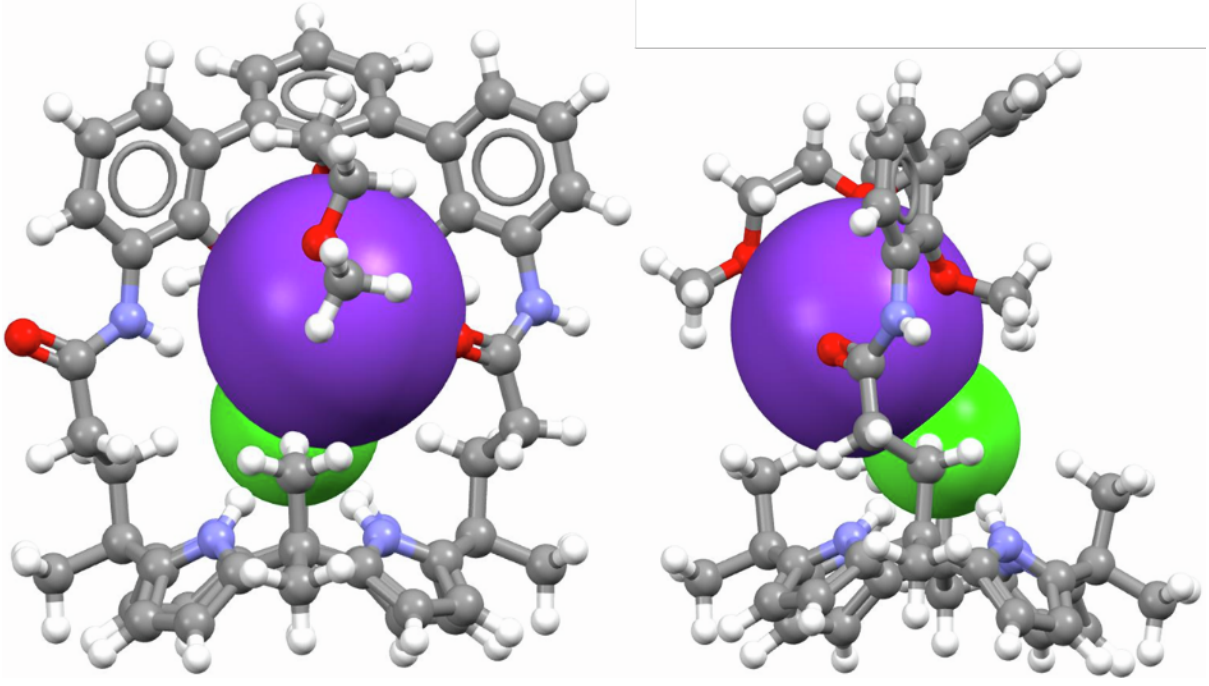

Figure S29. Front (left) and side (right) views of the DFT optimized structure of the KCl complex of receptor **2**.

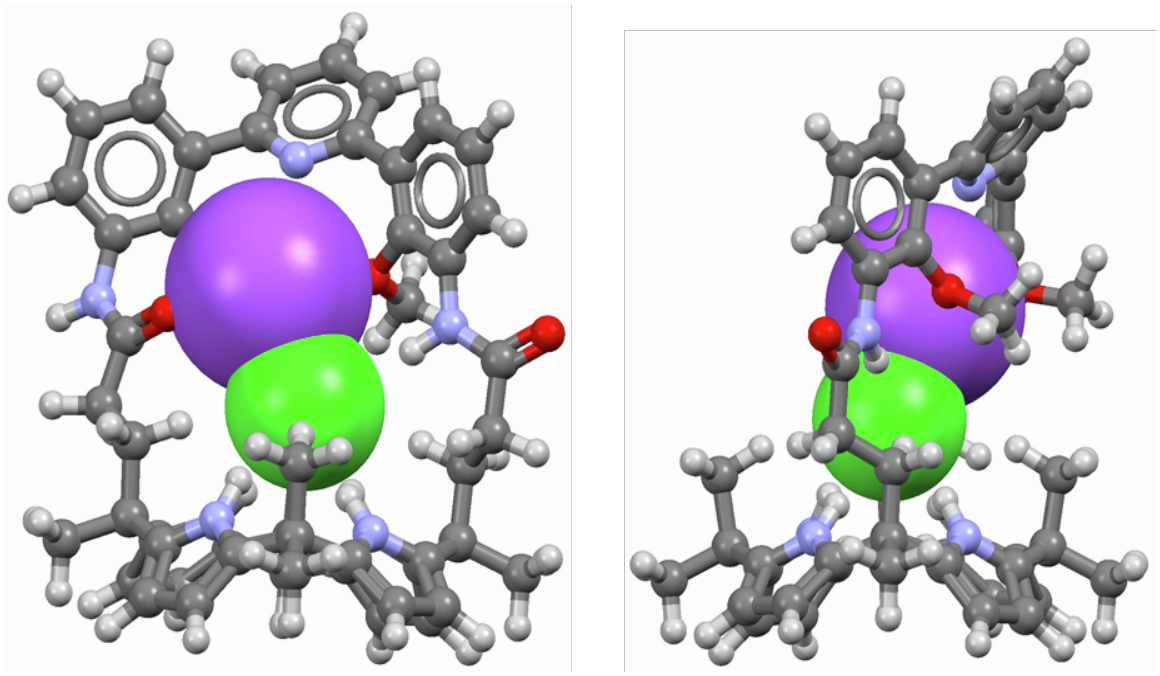

Figure S30. Front (left) and side (right) views of the DFT optimized structure of the NaCl complex of receptor **3**[1].

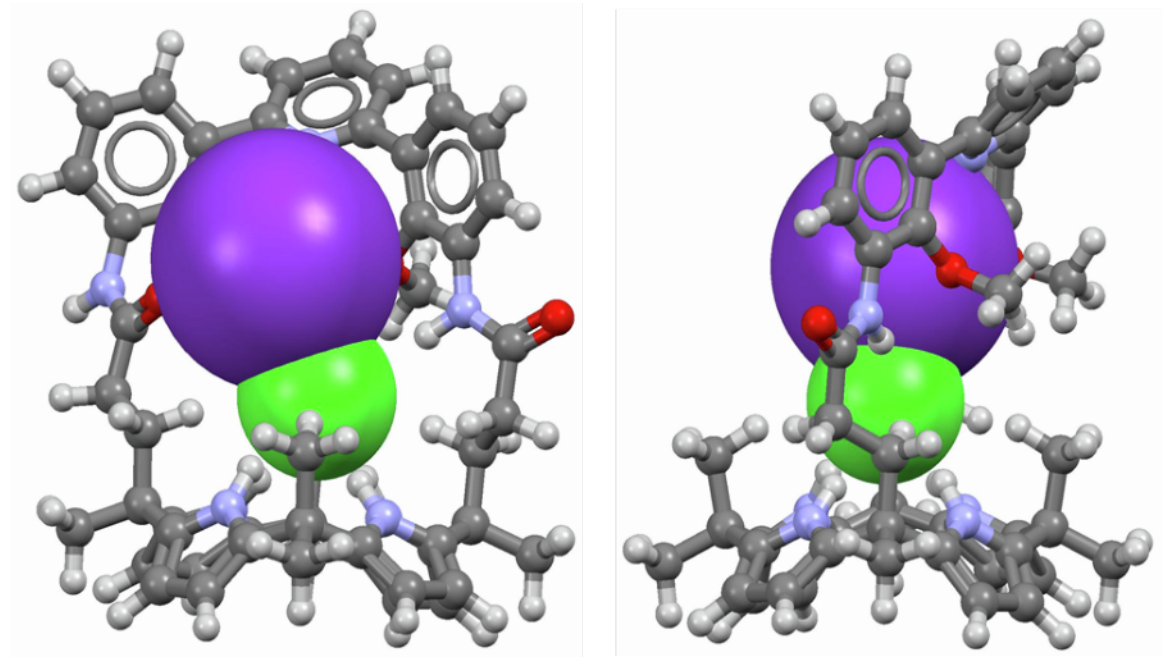

Figure S31. Front (left) and side (right) views of the DFT optimized structure of the KCl complex of receptor **3**[1].

Table S1 Comparison of the selected distances (Å) from the single-crystal structures (crysl) and the corresponding DFT calculated structures (calcd)[1].

Complexes		**1**·NaCl	**2**·NaCl	**3**·NaCl	**1**·KCl	**2**·KCl	**3**·KCl
$d_{M\cdots Cl}$[a]	crystl	2.756	2.697	2.911	3.002	3.017	3.139
	calcd	2.619	2.654	2.686	2.943	2.963	2.985
$d_{N\cdots Cl}$[b]	crystl	3.379	3.293	3.352	3.295	3.291	3.297
	calcd	3.414	3.411	3.466	3.367	3.362	3.420
$d_{O\cdots M}$[c]	crystl	2.430	2.500	2.333	2.838	2.846	2.804
	calcd	2.391	2.458	2.344	2.783	2.813	2.716

[a] The distances between the alkali metal cations and chloride. [b] The averaged distances between the pyrrole N and chloride. [c] The averaged distances between the alkali metal cations and the methoxy Os.

Table S2. Calculated Gas-Phase Binding Energy (E_{BSSE}/kcal/mol) for **1**·NaCl, **2**·NaCl, **3**·NaCl, **1**·KCl, **2**·KCl, and **3**·KCl[1].

Complexes	**1**·NaCl	**2**·NaCl	**3**·NaCl	**1**·KCl	**2**·KCl	**3**·KCl
E_{BSSE}	-206.09	-213.96	-204.51	-179.42	-186.16	-179.86

4. Ion Transport Experiments in Liposomes

Na^+/K^+ exchange experiments were conducted using unilamellar vesicles prepared using previously reported literature procedures, with a slight variation to ensure the correct solutions were used for the new assay[10]. The methods varied only by the use of either potassium and sodium chloride solutions, or potassium and sodium gluconate solutions. The use of the large, hydrophilic gluconate anion as a non-transporting control restricts the ability of K^+ or Na^+ to exchange as an ion pair and instead promotes transport as an anion-free complex. Initially, a lipid film of POPC (1-palmitoyl-2-oleoyl-*sn*-glycero-3-phosphocholine) was prepared from a chloroform solution under reduced pressure and then dried under vacuum overnight. The lipid film was rehydrated by vortexing with an internal solution of HEPES buffered potassium chloride/gluconate solution (KCl/KGlu, 300 mM) at pH 7.2. The lipid suspension was then subjected to 9 freeze-thaw cycles and left to rest at room temperature for 30 mins. Subsequently, the suspension was extruded 25 times through a 200 nm polycarbonate membrane resulting in unilamellar vesicles of an average diameter of 200 nm. The vesicles were then passed through a Sephadex® column saturated with HEPES buffered external sodium chloride/gluconate at pH 7.2, which allowed the exchange of any unencapsulated KCl/KGlu for NaCl/NaGlu, respectively. The lipid solution obtained after passing through the Sephadex® column was diluted to a standard volume with the corresponding external solution to obtain a lipid stock of known concentration.

The rate of transport properties of these compounds was found to be quite slow and solubility issues limited the ability to conduct experiments at higher transporter loadings. As a consequence, the experiments were run for 1800 seconds to allow the cation exchange to progress towards completion. Solubility issues also required the injection of each transporter in a higher volume of DMSO (100 µl of DMSO into a 5 ml vesicle suspension leading to a final DMSO content of 2 vol%) compared with the standard condition used in other recent publications (0.2 vol% DMSO), to ensure that an appreciable amount of transporter reached the membrane. For each measurement, the lipid stock solution was diluted with the external buffered solution to a standard volume (5.0 mL), to give a lipid concentration of 1.0 mM, in a 10 ml vial. Following this, a potassium ion-sensitive electrode (potassium ionplus® sure-flow® plastic membrane combination ISE) is submerged in the solution ready for the beginning of the experiment. The experiment was begun, and after 30 seconds transporter was added as a DMSO solution (100 µL) to give a known mol% concentration of transporter in solution. K^+ efflux into the external solution was monitored and recorded by the electrode for 30 minutes, before detergent was added (50 µL) to lyse the vesicles. A final 100% potassium efflux reading was recorded at 35 minutes.

Efflux plots were obtained at a number of mol% concentrations (with respect to lipid concentration) for each compound, repeated in duplicate or triplicate and averaged to obtain an efflux curve. The efflux percentage at 1800 s was plotted as a function of transporter

concentration. These data points were then fitted, using Origin Pro, to the Hill Equation:

$$y = y0 + (y1 - y0)\frac{x^n}{k^n + x^n}$$

Where y is the percentage efflux at 1800 s and x is the transporter concentration with respect to lipid (mol%). The value for y0 is obtained from a blank DMSO run, while y1 is the maximum efflux when the curve is fitted. The remaining parameters, n and k, are the Hill coefficient and the $EC_{50,1800s}$ value (the concentration required to achieve 50% efflux after 1800 s), respectively. The maximum rate of transport was calculated using an exponential decay curve for the KCl/NaCl exchange assay for compound **1**. In all other cases the maximum rate was calculated by fitting the efflux to a Boltzmann sigmoidal curve. In all calculations, the first 4 results were omitted due to lag from the electrode.

Table S3. Summary of Transmembrane Transport Rates of Transporters **1**-**4** Obtained from the K^+ ISE Assay.

	$EC_{50,\ 1800s}$[a]	n (Hill coefficient)[b]	K^+/Na^+ (%s^{-1}) with Cl^-	K^+/Na^+ (%s^{-1})	F_{en}[e]
1	0.39	1.70	1.75[c]	0.023[d]	76
2	1.05	1.90	0.046[d]	0.031[d]	1.5
3	0.86	1.70	0.086[d]	0.034[d]	2.6
4	5.75	4.00	0.021[d]	0.018[d]	1.2

a) Concentration of receptor (mol% receptor to lipid) required to achieve 50% potassium efflux at 1800 s during the Na^+/K^+ exchange experiment, using NaCl and KCl as the medium. b) Hill coefficient for the Na^+/K^+ experiment. c) Maximum rate (at 5 mol% receptor to lipid) calculated by fitting the efflux plot to an exponential decay curve using Origin 2019. d) Maximum rate (at 5 mol% receptor to lipid) calculated by fitting the efflux plot to a Boltzmann sigmoidal curve in Origin 2019. e) The ratio of maximum rates was calculated *via* division of the maximum rate in the NaCl/KCl exchange assay by the maximum rate achieved in the corresponding NaGlu/KGlu exchange assay.

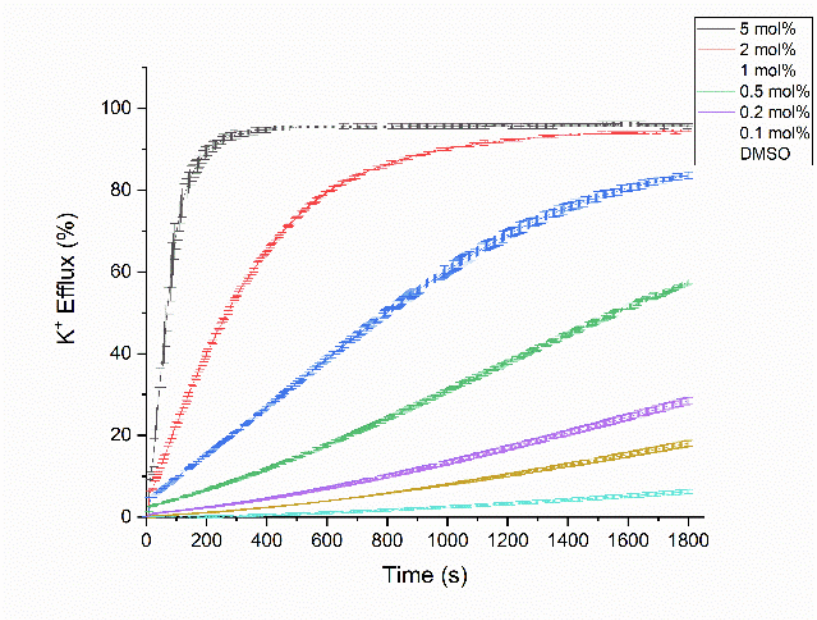

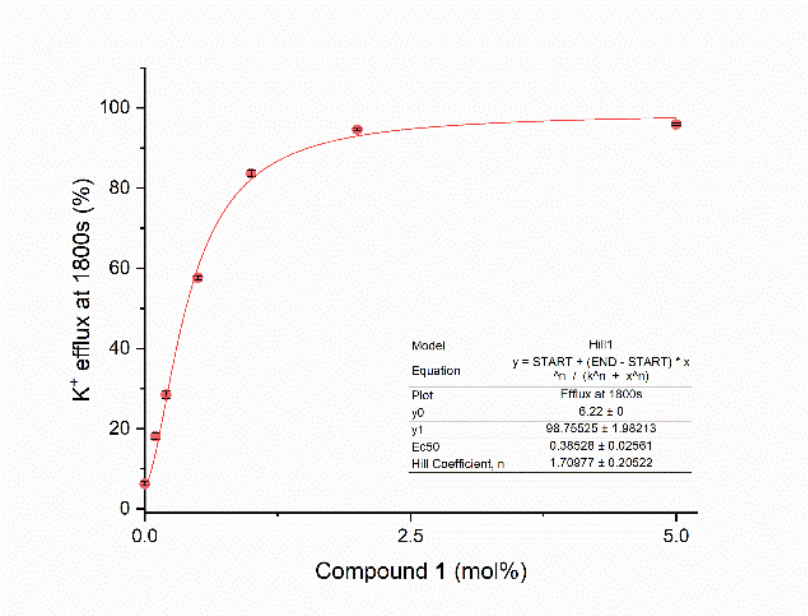

Figure S32. Top) K^+/Na^+ antiport plots using NaCl and KCl as the medium for compound **1** at various compound-to-lipid molar ratios. The experiment is started by the addition of the compound in DMSO solution (100 µL) and ended after 1800 s by adding detergent to lyse the vesicles. Bottom) Hill plot analysis for compound **1** for K^+ efflux at 1800 s as a function of the compound-to-lipid molar ratio. Error bars (black) represent the standard deviation of two repeats.

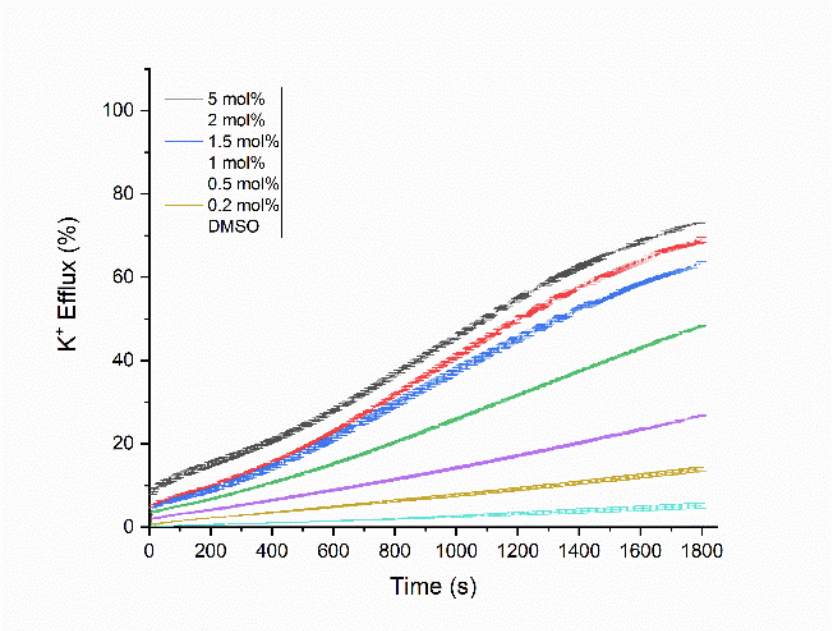

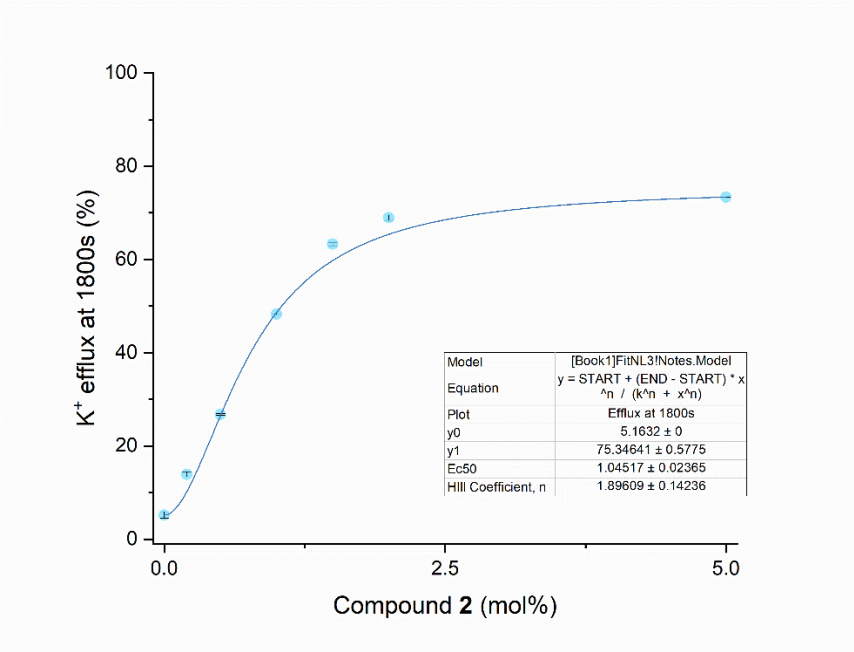

Figure S33. Top) K^+/Na^+ antiport plots using NaCl and KCl as the medium for compound **2** at various compound-to-lipid molar ratios. The experiment is started upon adding the compound as a DMSO solution (100 μL) and is terminated after 1800 s by adding detergent to lyse the vesicles. Bottom) Hill plot analysis for compound **2** and K^+ efflux at 1800 s as a function of the compound-to-lipid molar ratio. Error bars (black) represent the standard deviation of two repeats.

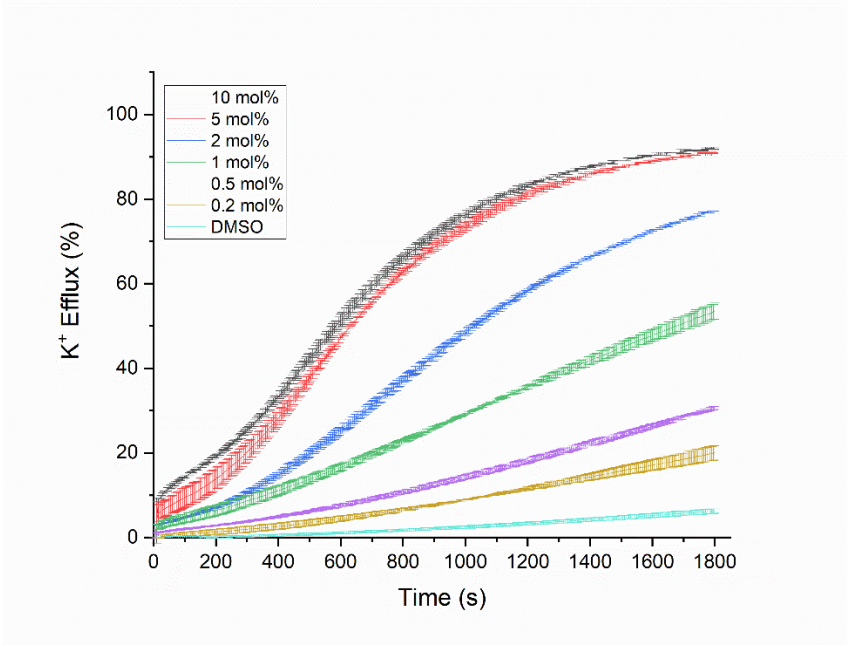

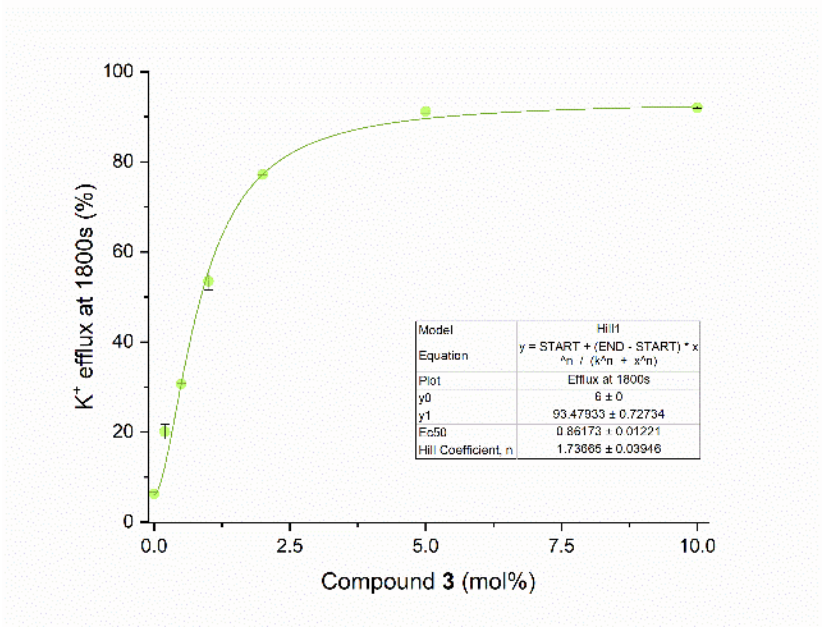

Figure S34. Top) The K^+/Na^+ antiport plots using NaCl and KCl as the medium for compound **3** at various compound-to-lipid molar ratios. The experiment is commenced by adding the compound as a DMSO solution (100 μL) and terminated after 1800 s by adding detergent to lyse the vesicles. Bottom) Hill plot analysis for compound **3** and K^+ efflux at 1800 s as a function of the compound-to-lipid molar ratio. Error bars (black) represent the standard deviation of two repeats.

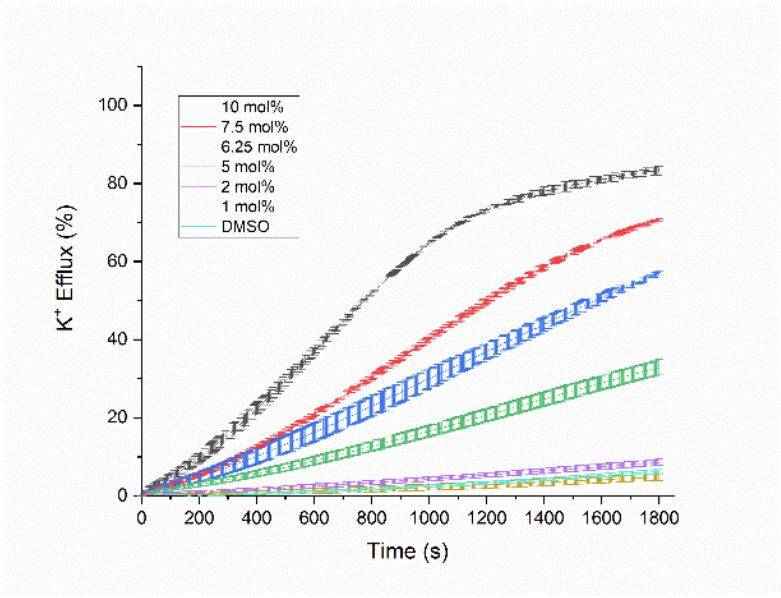

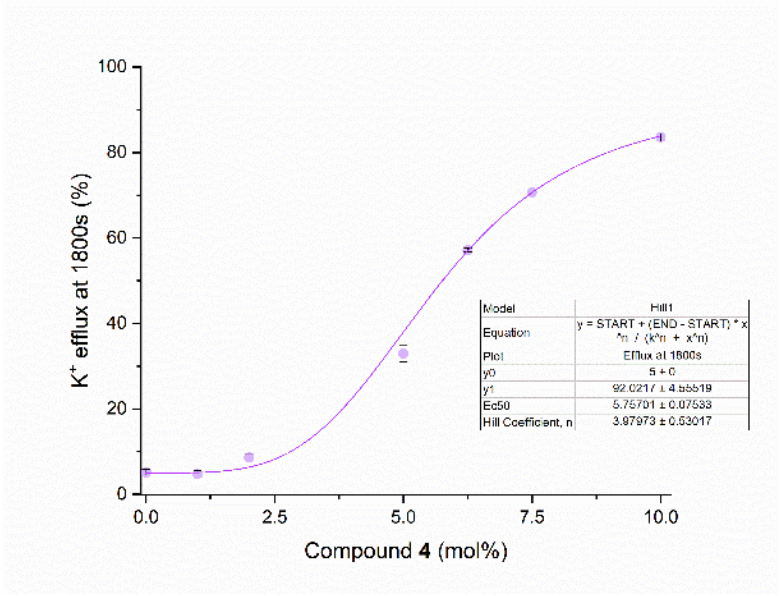

Figure S35. Top) K^+/Na^+ antiport plots using NaCl and KCl as the medium for compound **4** at various compound-to-lipid molar ratios. The experiment is started by adding the compound as a DMSO solution (100 µL) and terminated after 1800 s by adding detergent to lyse the vesicles. Bottom) Hill plot analysis for compound **4** and K^+ efflux at 1800 s as a function of the compound-to-lipid molar ratio. Error bars (black) represent the standard deviation of two repeats.

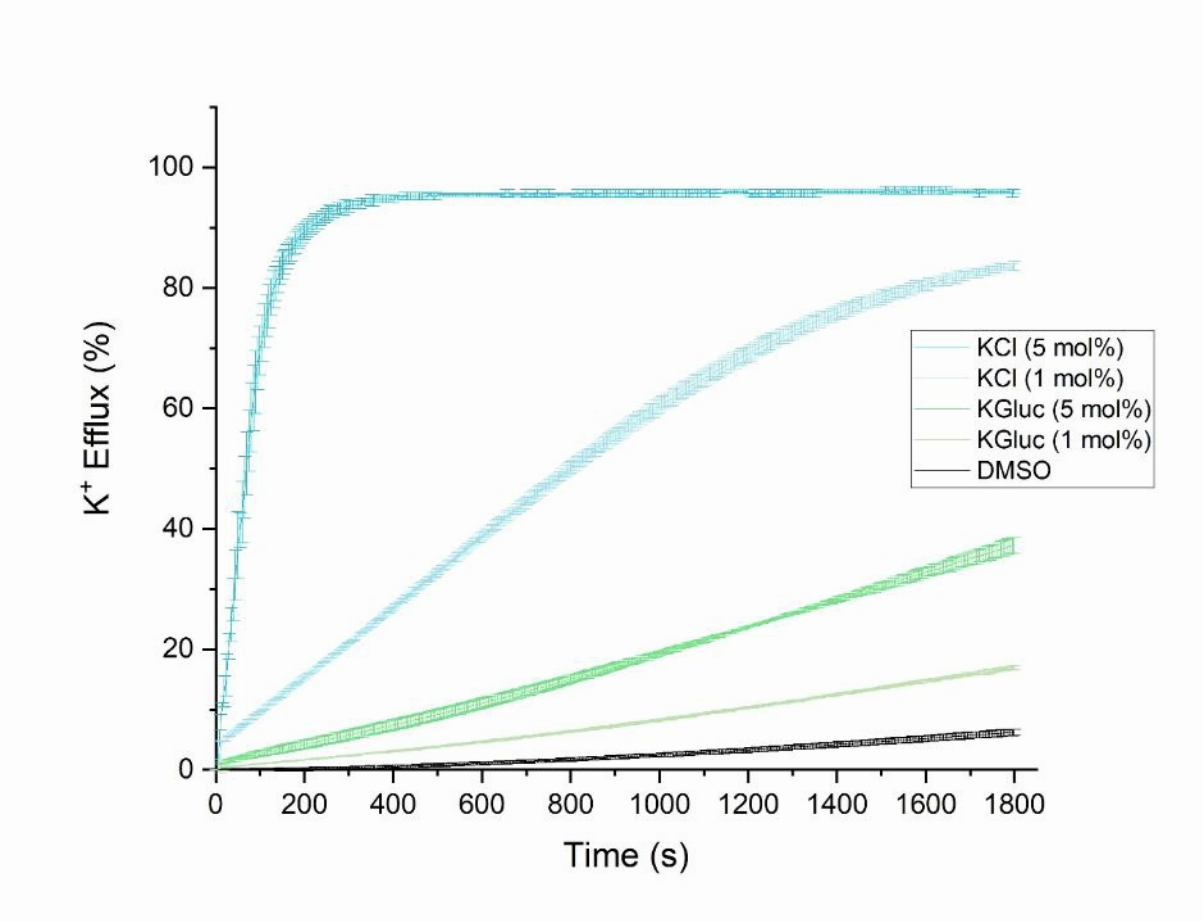

Figure S36. A comparison of the K^+/Na^+ antiport plots for compound **1** at two different compound-to-lipid molar ratios. The experiments were run in either KCl/NaCl solutions (blue) or KGlu/NaGlu solutions (green). A blank DMSO run is also included. The experiment is started by adding the compound as a DMSO solution (100 μL) and terminated after 1800 s by adding detergent to lyse the vesicles.

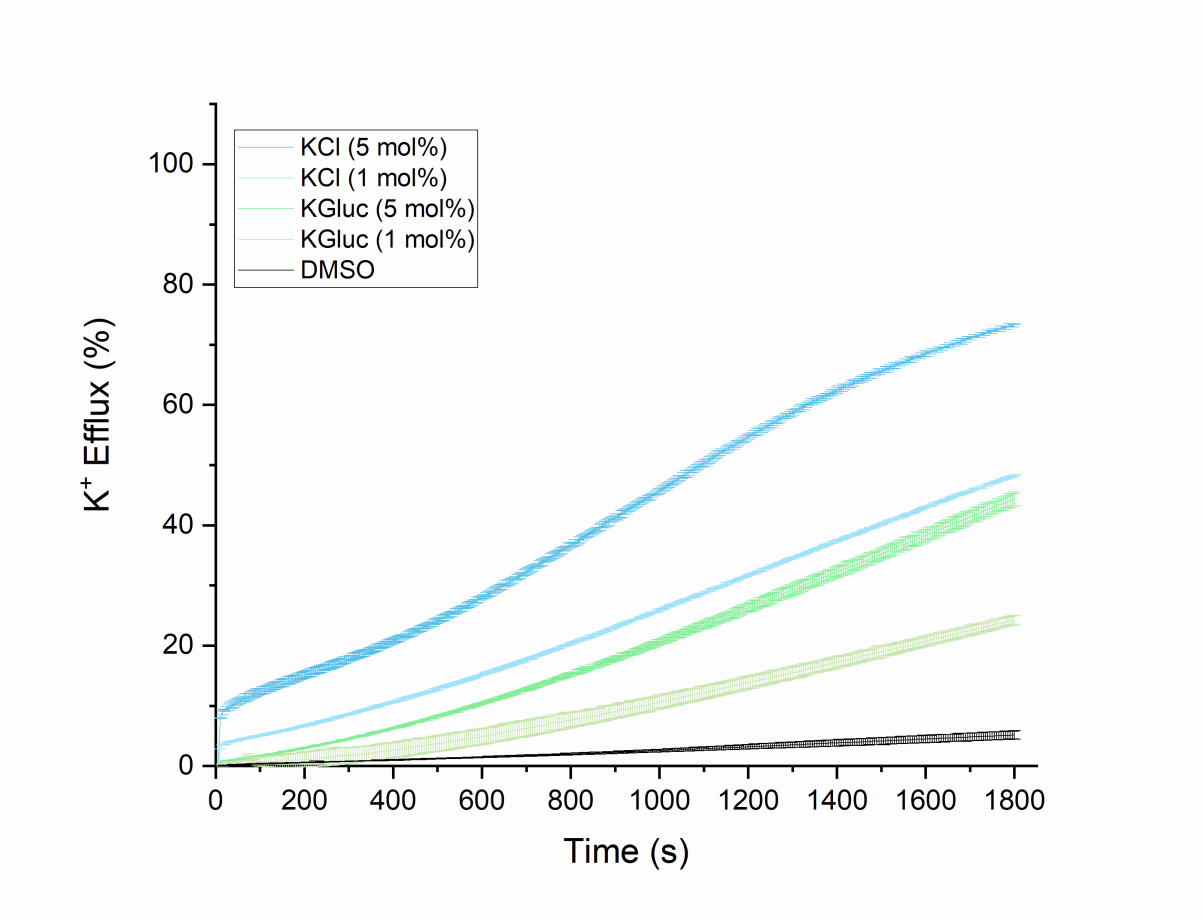

Figure S37. A comparison of the K^+/Na^+ antiport plots for compound **2** at two different compound-to-lipid molar ratios. The experiments were run in either KCl/NaCl solutions (blue) or KGlu/NaGlu solutions (green). A blank DMSO run is also included. The experiment is started by the addition of the compound in DMSO solution (100 µL) and ended after 1800 s by adding detergent to lyse the vesicles.

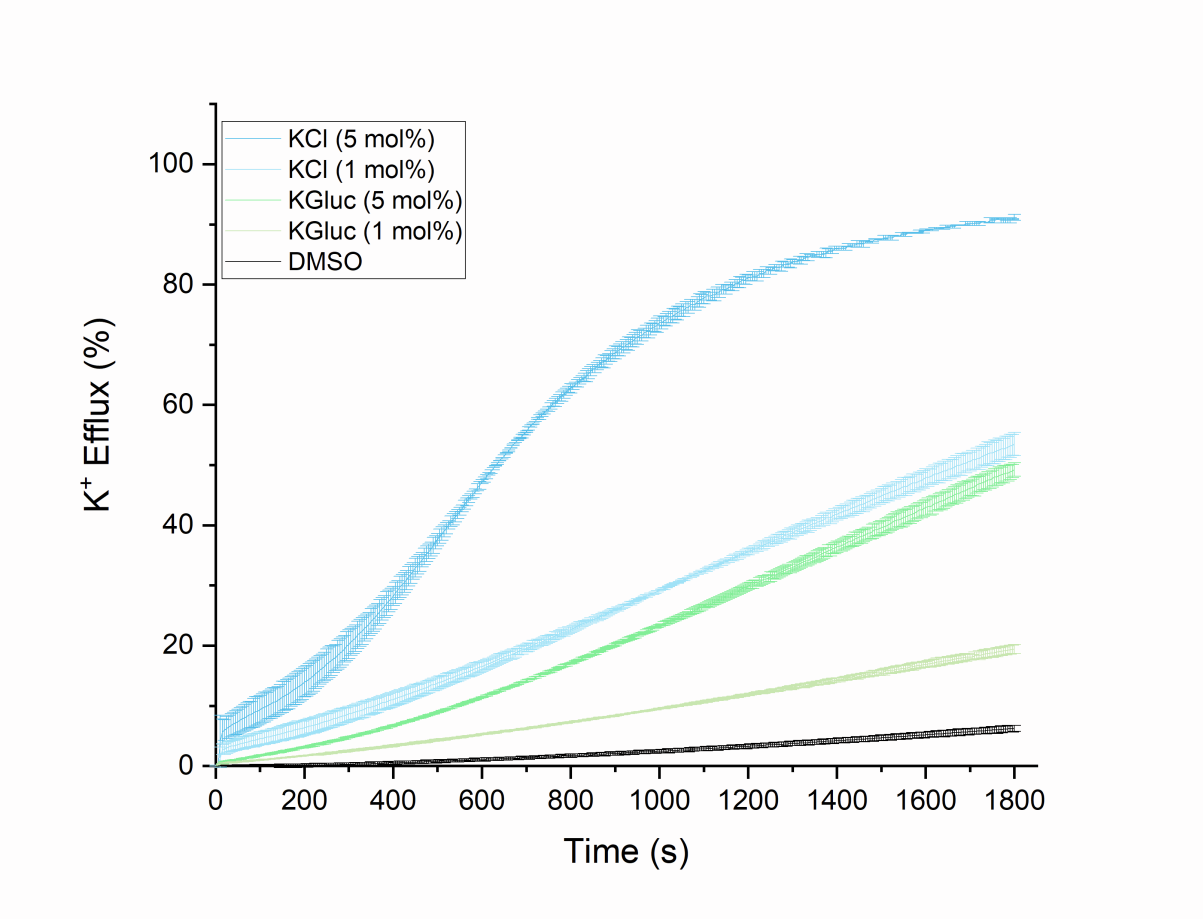

Figure S38. A comparison of the K^+/Na^+ antiport plots for compound **3** at two different compound-to-lipid molar ratios. The experiments were run in either KCl/NaCl solutions (blue) or KGlu/NaGlu solutions (green). A blank DMSO run is also included. The experiment is started by adding the compound as a DMSO solution (100 μL) and terminated after 1800 s by adding detergent to lyse the vesicles.

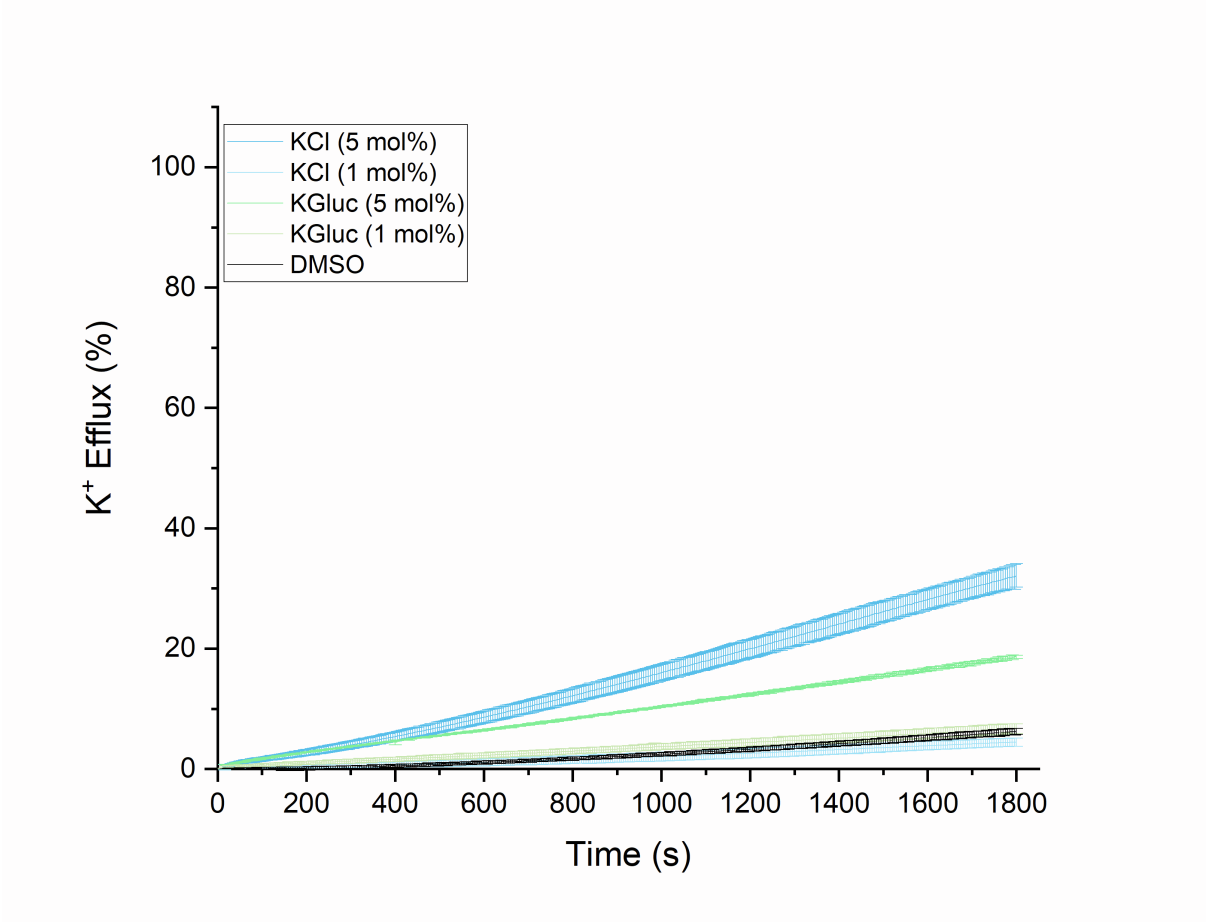

Figure S39. A comparison of the K^+/Na^+ antiport plots for compound **4** at two different compound-to-lipid molar ratios. The experiments were run in either KCl/NaCl solutions (blue) or KGlu/NaGlu solutions (green). A blank DMSO run is also included. The experiment is started by adding the compound as a DMSO solution (100 μL) and terminated after 1800 s by adding detergent to lyse the vesicles.

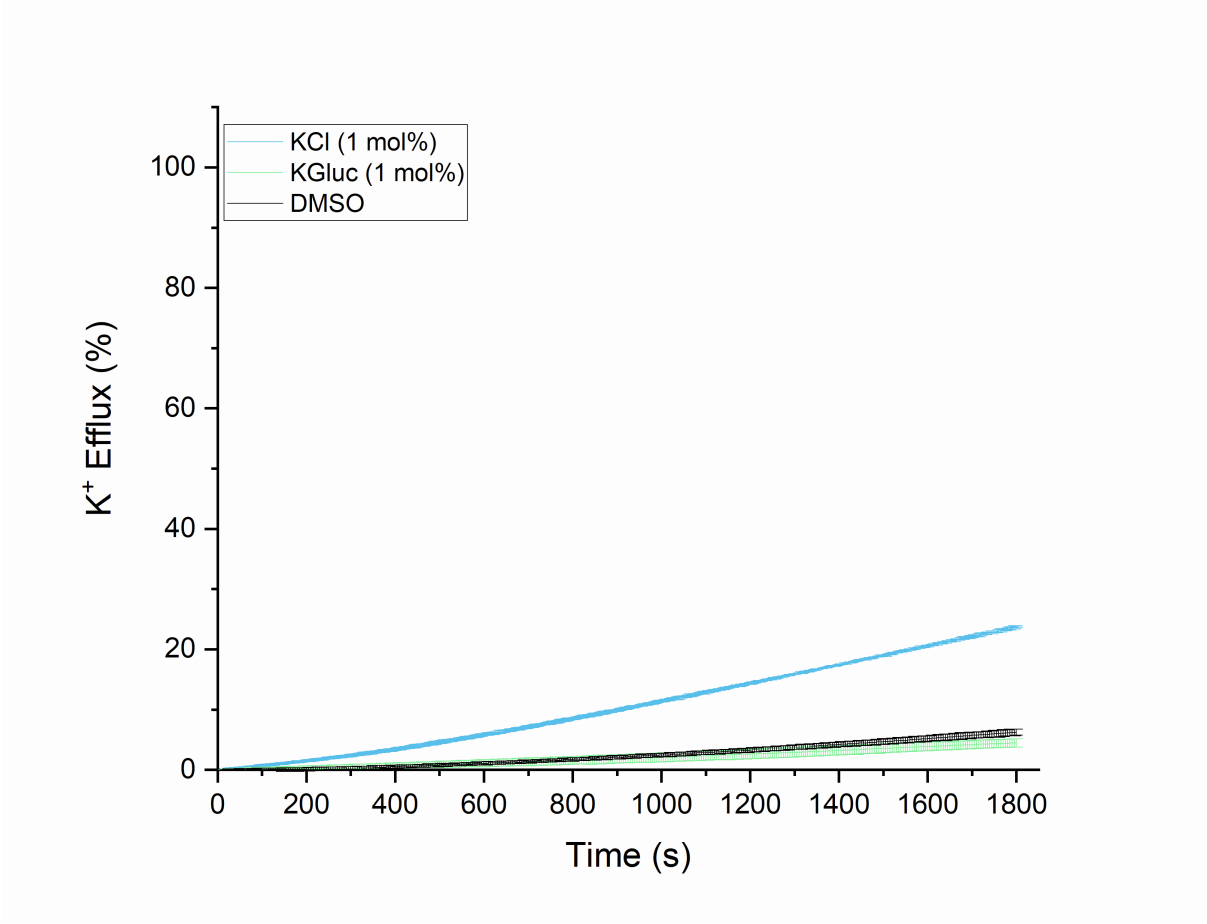

Figure S40. The K^+/Na^+ antiport plots for compound **5** at a compound-to-lipid molar ratio of 1 mol%. The experiments were run in either KCl/NaCl solutions (black and red) or KGlu/NaGlu solutions (blue). A blank DMSO run is also included. The experiment is started by adding the compound as a DMSO solution (100 µL) and terminated after 1800 s by adding detergent to lyse the vesicles. Experiments at higher molar ratios could not be carried out due to solubility issues.

The cationophore coupled ISE assay allows elucidation of the transport mechanism employed by the compound by assessing the effect on transport rate when transport is coupled to a series of ionophores. This helps determine whether receptor-mediated ion transport occurs in an electrogenic uniport mechanism, H^+ coupled electroneutral fashion, or in a nonspecific manner. Monensin facilitates the M^+/H^+ antiport ($M^+ = Na^+, K^+$), so the transporter acts only as a H^+/Cl^- symporter when coupling to monensin to facilitate overall MCl transport. An accelerated rate of chloride efflux by monensin indicates $H^+ > M^+$ selectivity (MCl symport is rate-limiting without the present of monensin). Valinomycin (K^+ assays only) facilitates the efflux of K^+ out of the vesicle, so the transporter acts as an electrogenic Cl^- carrier when coupling to valinomycin. An accelerated rate of chloride efflux by valinomycin indicates a $Cl^- >$ KCl selectivity (electroneutral KCl symport is rate-limiting without the presence of valinomycin). To assess the selectivity of this class of transporters, ISE assay tests were performed with both ionophores and compared to the independent run of each compound at the same compound to lipid molar ratio. Selectivity for either metal ion was also assessed by comparing the rate of chloride efflux with each cation present in solution.

Unilamellar vesicles were prepared using previously reported literature procedures. Initially, a lipid film of POPC (1-palmitoyl-2-oleoyl-*sn*-glycero-3-phosphocholine) was prepared from a chloroform solution under reduced pressure and then dried under vacuum overnight. The lipid film was rehydrated by vortexing with an internal solution of HEPES buffered sodium/potassium chloride solution (MCl, 300 mM) at pH 7.2. The lipid suspension was then subjected to 9 freeze-thaw cycles and left to rest at room temperature for 30 mins. Subsequently, the suspension was extruded 25 times through a 200 nm polycarbonate membrane resulting in unilamellar vesicles of an average diameter of 200 nm. The vesicles were then passed through a Sephadex® column saturated with the HEPES buffered external sodium/potassium gluconate solution (MGlu, 300 mM) at pH 7.2, which allowed the exchange of any unencapsulated MCl for MGlu. The lipid solution obtained after Sephadex® was diluted to a standard volume with the corresponding external solution to obtain a lipid stock of known concentration.

For each measurement, the lipid stock solution was diluted with the external buffered solution to a standard volume (5.0 mL), to give a lipid concentration of 1.0 mM, in a 10 ml vial. Following this, a chloride ion-sensitive electrode is submerged in the solution ready for the beginning of the experiment. In cases where an ionophore was used (monensin, valinomycin), it was added as a DMSO solution (10 μL) prior to the addition of the transporter. The experiment was begun, and after 30 seconds transporter was added as a DMSO solution (20 μL) to give a known mol% concentration of transporter in solution. Cl^- efflux into the external solution was monitored and recorded by the electrode for 30 minutes, before detergent was added (50 μL) to lyse the vesicles. A final 100% chloride efflux reading was recorded at 35 minutes. Efflux plots at a loading of 2 mol% compound to lipid ratio were obtained and repeated in duplicate to obtain an efflux curve.

It was found that all the hemispherand-strapped calixpyrroles can facilitate a certain degree of Cl^- uniport (electrogenic, when coupling with valinomycin), Cl^-/H^+ symport (or functionally equivalent Cl^-/OH^- antiport) (electroneutral, when coupling with monensin), and M^+/Cl^- cotransport. The increased rate in the presence of valinomycin and monensin demonstrates that those hemispherand-strapped calixpyrroles are better chloride carriers than M^+/Cl^- cotransporters and that the cotransport of NaCl and KCl is rate limited by the cation flux. The results imply a selectivity for Na^+ over K^+ for this class of compounds. The rate of NaCl cotransport mediated by compounds **1** and **2** are faster than the cotransport of KCl, indicating their selectivity for Na^+ over K^+. Rate of transport for compound **4** was slow in both cases.

Table S4. Summary of Transmembrane Transport Rates[a] of Transporters **1-3** Inferred from Cl-ISE Assays.

	Cl^- uniport (%s^{-1}) with Vln	Cl^-/H^+ (Na^+) (%s^{-1}) with Mon	Cl^-/H^+ (K^+) (%s^{-1}) with Mon	Na^+/Cl^- (%s^{-1})	K^+/Cl^- (%s^{-1})
1	0.113	0.086	0.077	0.063	0.020
2	0.129	0.150	0.093	0.145	0.066
3	0.306	0.138	0.131	0.023	0.032

[a] Maximum rate (at 5 mol% receptor to lipid) calculated by fitting the efflux plot to a Boltzmann sigmoidal curve. Vln and Mon refer to valinomycin and monensin, respectively.

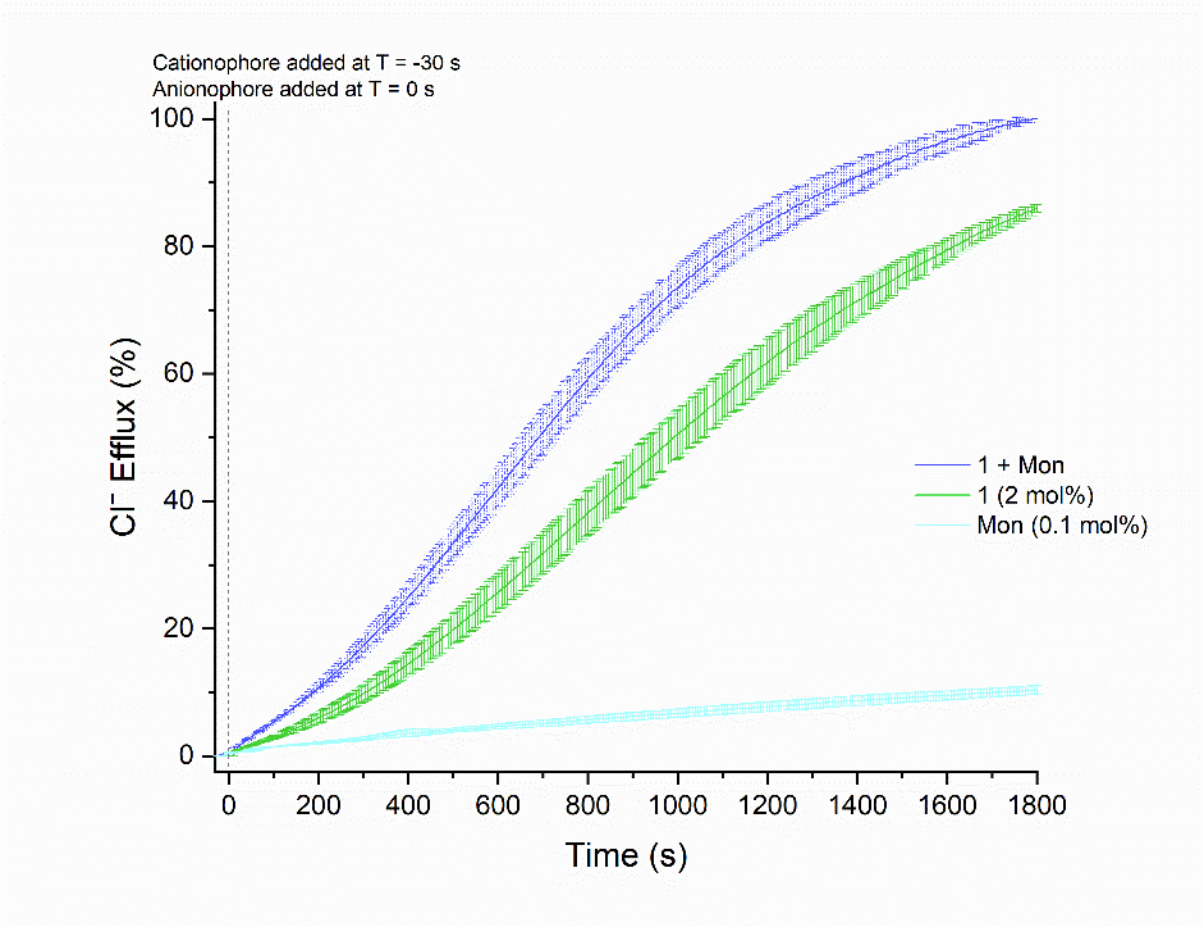

Figure S41. NaCl symport plots for compound **1** at 2 mol% loading with respect to lipid. The experiment is started by adding the compound as a DMSO solution (20 μL) and terminated after 1800 s by adding detergent to lyse the vesicles. The monensin concentration is given as the ionophore to lipid molar ratio. Errors bars represent the standard deviation of two repeats.

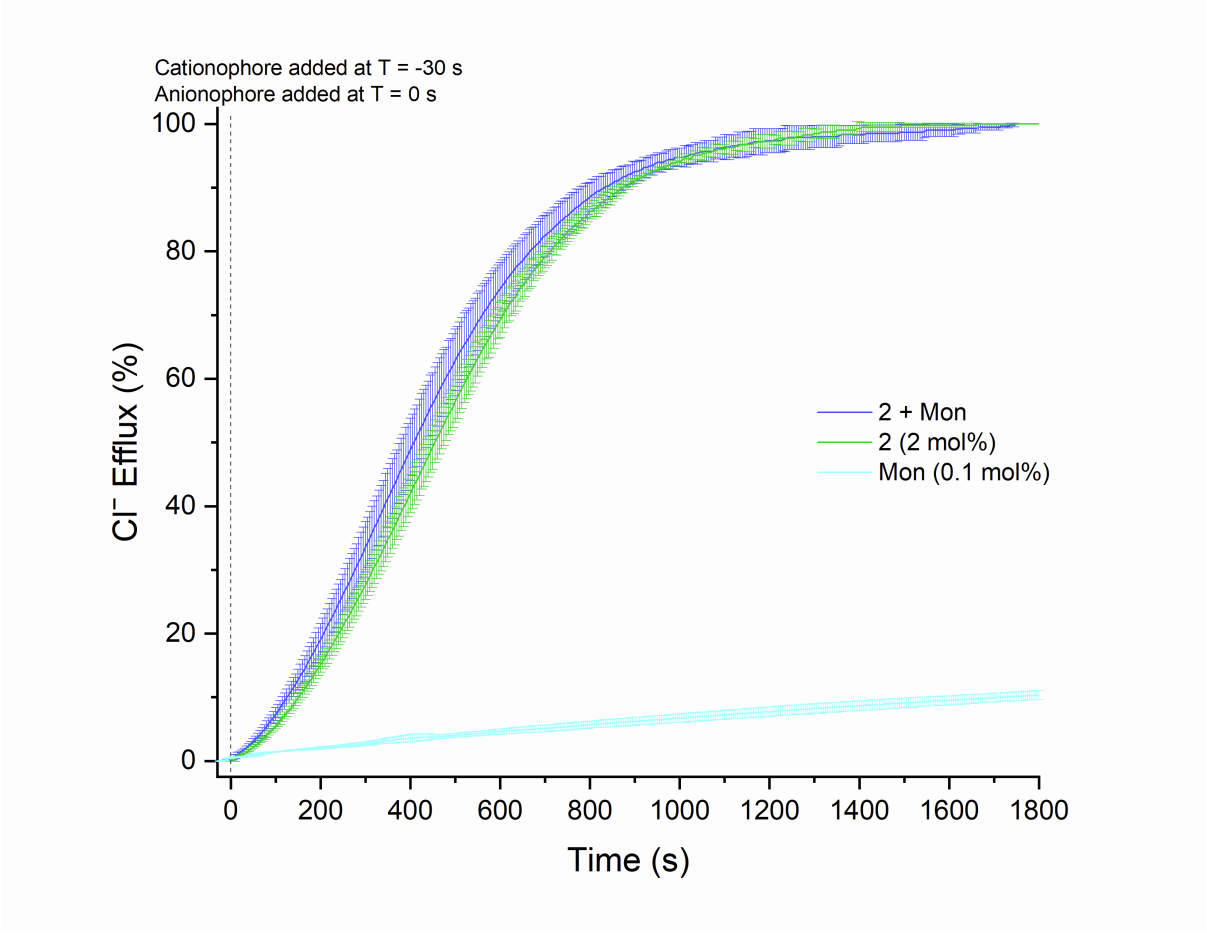

Figure S42. NaCl symport plots for compound **2** at 2 mol% loading with respect to lipid. The experiment is started by adding the compound as a DMSO solution (20 μL) and terminated after 1800 s by adding detergent to lyse the vesicles. The monensin concentration is given as the ionophore to lipid molar ratio. Errors bars represent the standard deviation of two repeats.

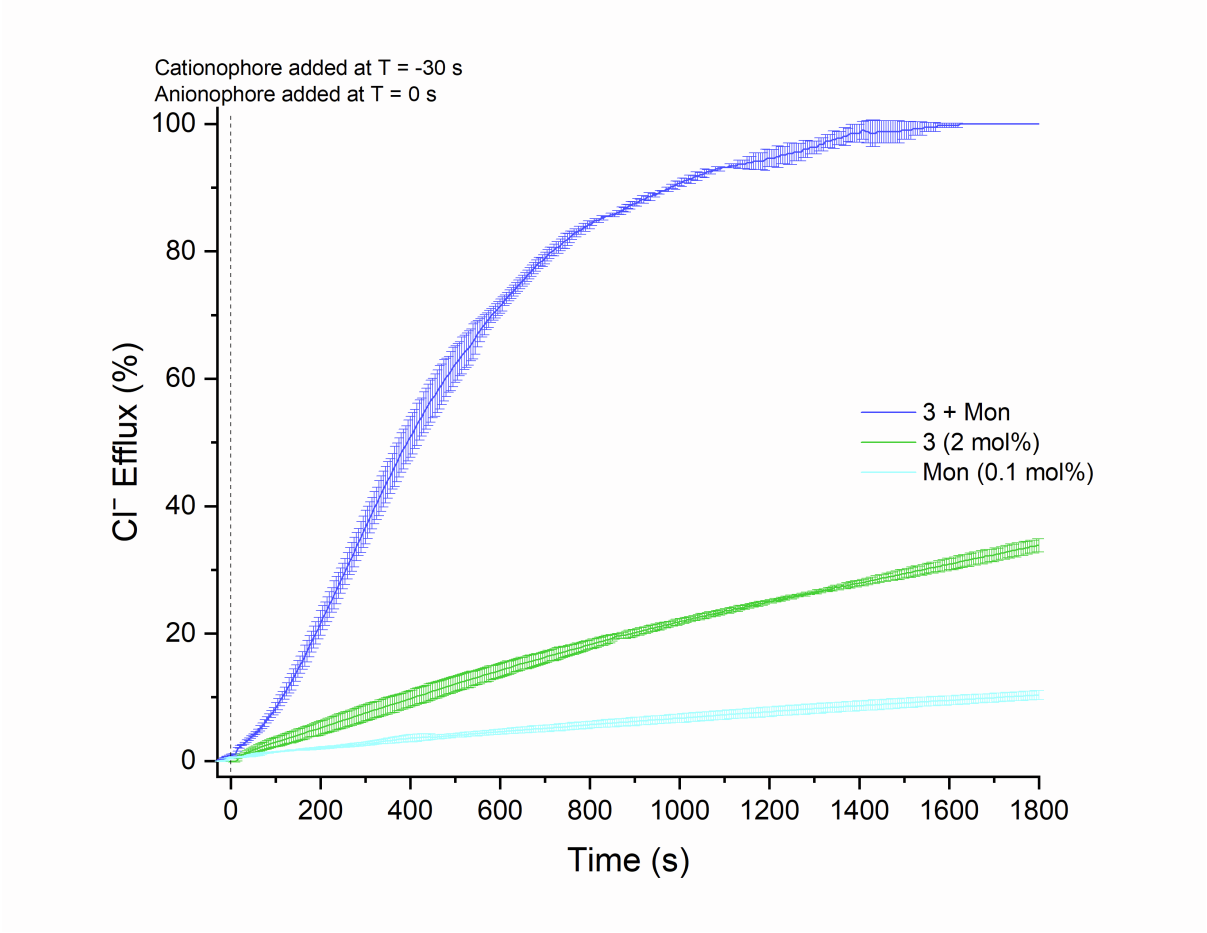

Figure S43. NaCl symport plots for compound **3** at 2 mol% loading with respect to lipid. The experiment is started by adding the compound as a DMSO solution (20 μL) and ended after 1800 s by adding detergent to lyse the vesicles. The monensin concentration is given as the ionophore to lipid molar ratio. Errors bars represent the standard deviation of two repeats.

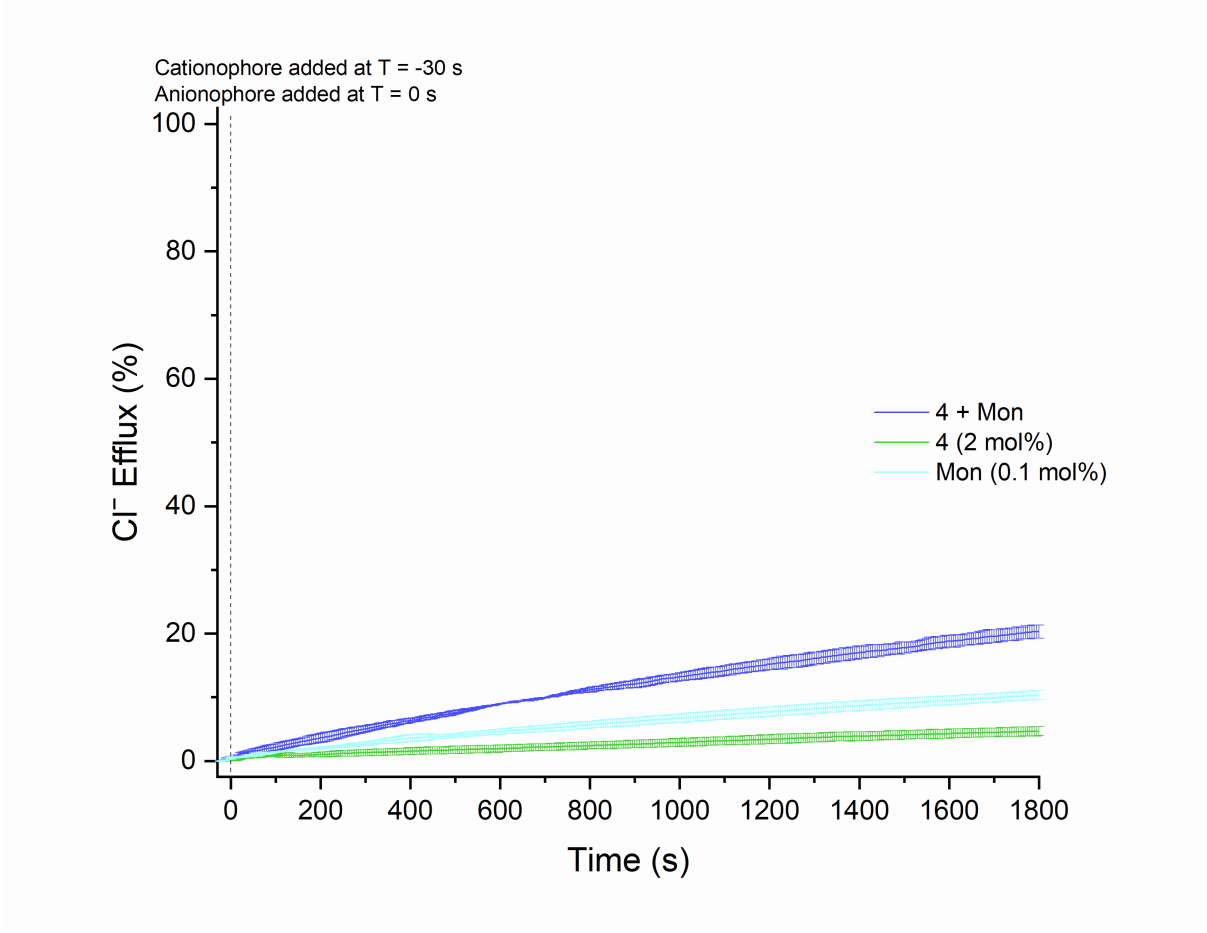

Figure S44. NaCl symport plots for compound **4** at 2 mol% loading with respect to lipid. The experiment is started by adding the compound as a DMSO solution (20 μL) and terminated after 1800 s by adding detergent to lyse the vesicles. The monensin concentration is given as the ionophore to lipid molar ratio. Errors bars represent the standard deviation of two repeats.

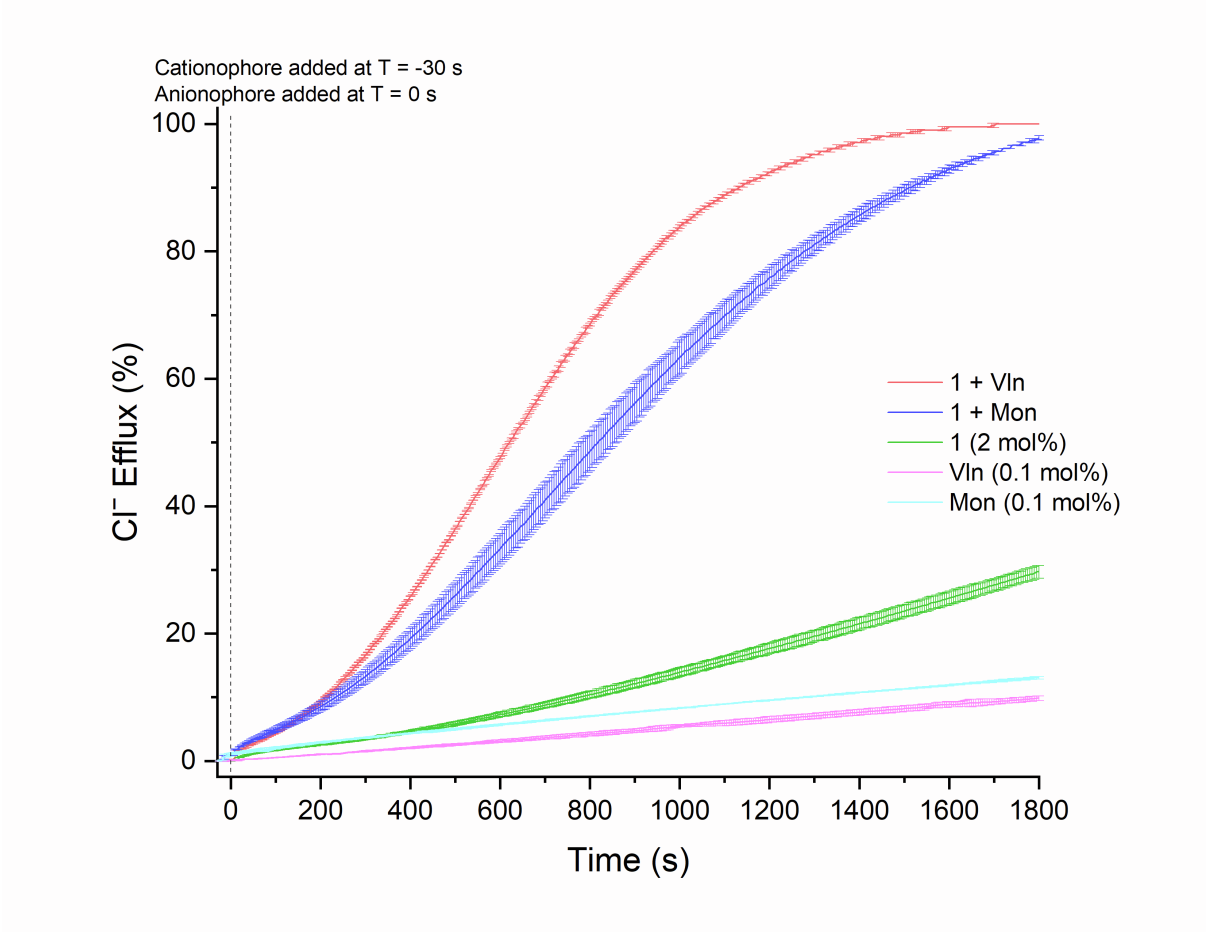

Figure S45. KCl symport plots for compound **1** at 2 mol% loading with respect to lipid. The experiment is started by adding the compound as a DMSO solution (20 µL) and terminated after 1800 s by adding detergent to lyse the vesicles. The ionophore concentration is shown as the ionophore to lipid molar ratio. Errors bars represent the standard deviation of two repeats.

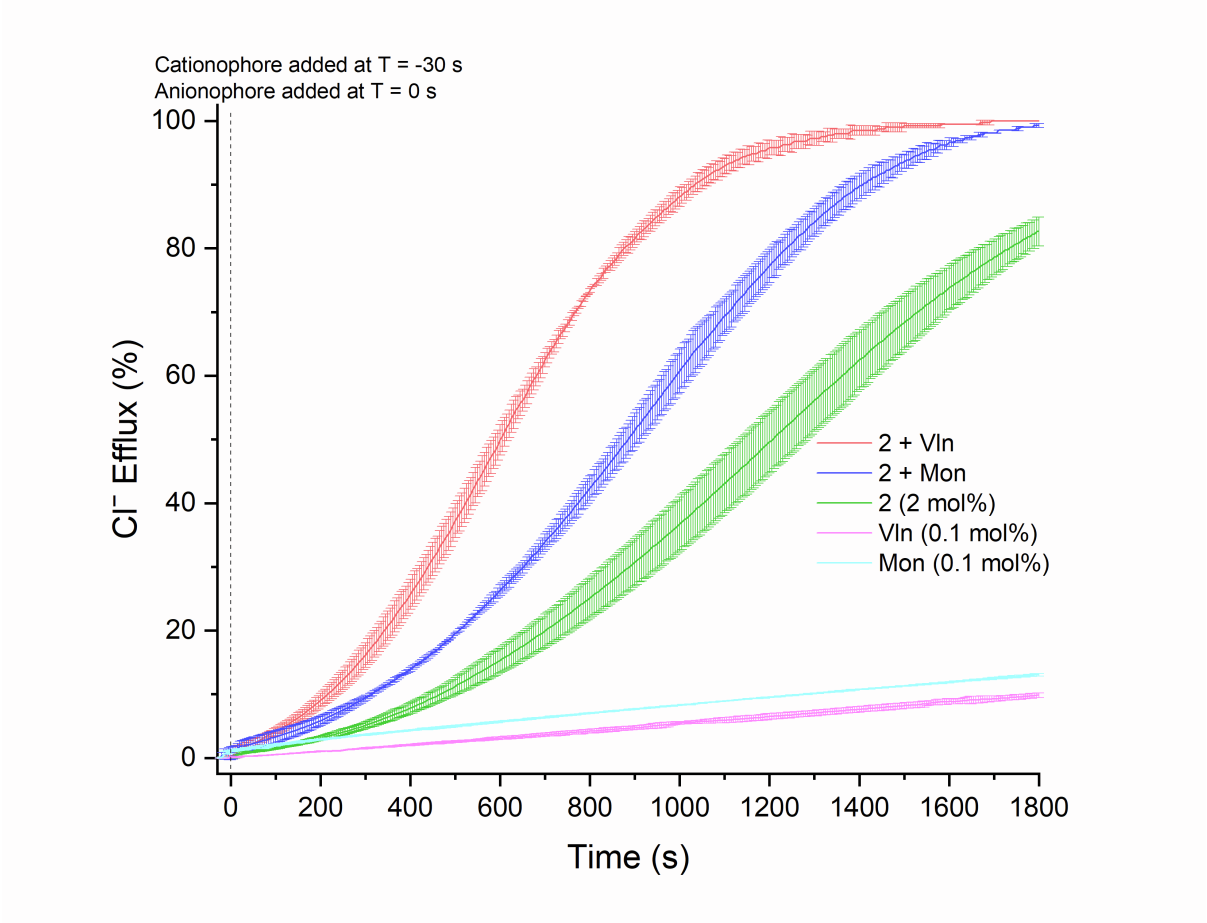

Figure S46. KCl symport plots for compound **2** at 2 mol% loading with respect to lipid. The experiment is started by adding the compound as a DMSO solution (20 µL) and terminated after 1800 s by adding detergent to lyse the vesicles. The ionophore concentration is shown as the ionophore to lipid molar ratio. Errors bars represent the standard deviation of two repeats.

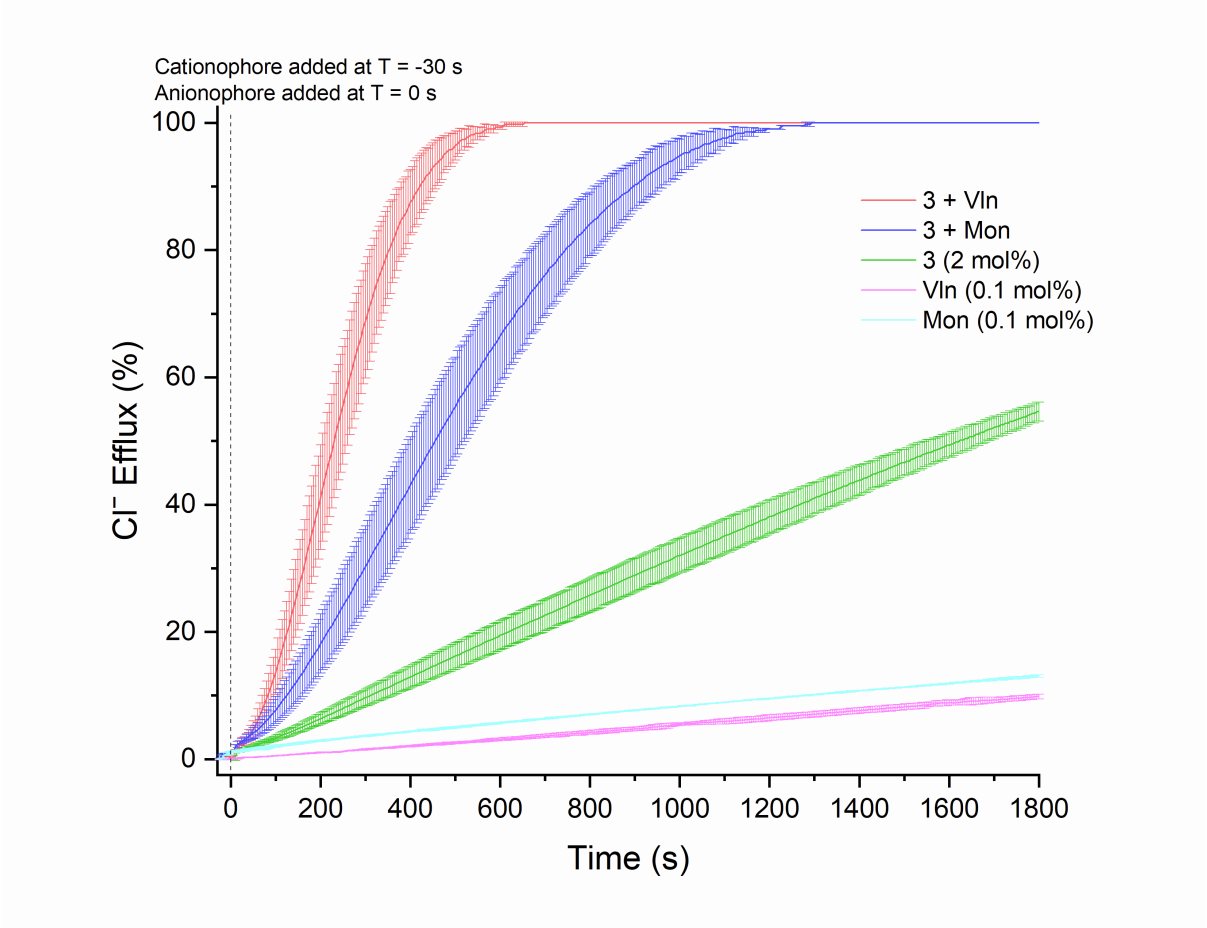

Figure S47. KCl symport plots for compound **3** at 2 mol% loading with respect to lipid. The experiment is started by adding the compound as a DMSO solution (20 μL) and ended after 1800 s by adding detergent to lyse the vesicles. The ionophore concentration is shown as the ionophore to lipid molar ratio. Errors bars represent the standard deviation of two repeats.

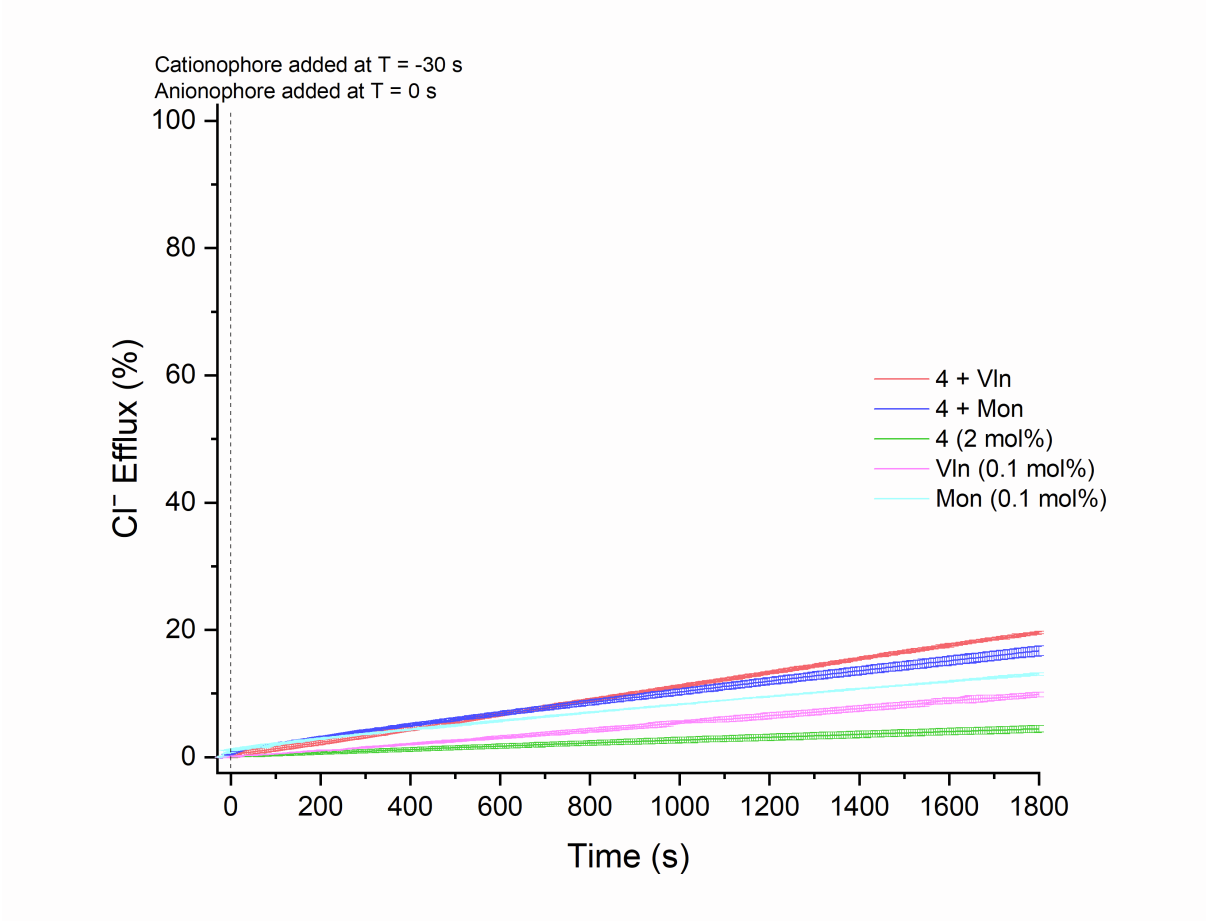

Figure S48. KCl symport plots for compound **4** at 2 mol% loading with respect to lipid. The experiment is started by adding the compound as a DMSO solution (20 μL) and ended after 1800 s by adding detergent to lyse the vesicles. The ionophore concentration is shown as the ionophore to lipid molar ratio. Errors bars represent the standard deviation of two repeats.

The cationophore coupled HPTS base pulse assay enables more information regarding the transport mechanism to be elucidated. The HPTS assay was used to assess metal cation-only transport in the absence of ion-pair coupled transport with chloride. Additional ionophores were used in these experiments, as well as an alternative source of base pulse. When the transporter is used in the absence of other ionophores in this assay the results give information about the ability of the transporter to facilitate K^+/H^+ exchange (or K^+/OH^- cotransport). In the presence of valinomycin (K^+ assays only), which facilitates the efflux of K^+ out of the vesicle, the transporter facilitates H^+ efflux to dissipate the pH gradient. An accelerated dissipation of pH gradient indicates a $H^+ > K^+$ selectivity. Carbonyl cyanide *m*-chlorophenyl hydrazone (CCCP) was used as an ionophore in the metal cation assays and as a proton carrier. An accelerated dissipation in this assay indicates that H^+ efflux is the rate-limiting step and that the transport displays $H^+ < K^+$ selectivity. The tetrabutylammonium cation (TBA^+) is membrane permeable, and therefore acts similarly to the valinomycin coupled assay. The influx of TBA^+ into the vesicles maintains electroneutrality instead of metal cation efflux; therefore, the transporters act as H^+/OH^- transporters. To assess the selectivity of this class of transporters, HPTS assay tests were performed with each ionophore in conjunction with a base pulse and compared to the independent run of each compound at the same compound-to-lipid molar ratio. Furthermore, the influence of trace fatty acids in the membrane were assessed by treating the vesicles with bovine albumin serum, thereby removing these traces from the lipids before experiments with each ionophore were repeated.

Unilamellar vesicles were prepared initially by evaporating a lipid film of POPC (1-palmitoyl-2-oleoyl-*sn*-glycero-3-phosphocholine) was prepared from a chloroform solution under reduced pressure and then dried under vacuum overnight. The lipid film was rehydrated by vortexing with an internal solution of HEPES (10 mM) buffered sodium/potassium gluconate solution (MGlu, 100 mM) containing HPTS (1 mM) at pH 7.0. The lipid suspension was then subjected to 9 freeze-thaw cycles and left to rest at room temperature for 30 mins. Subsequently, the suspension was extruded 25 times through a 200 nm polycarbonate membrane resulting in unilamellar vesicles of an average diameter of 200 nm. The vesicles were then passed through a Sephadex® column saturated with the HEPES buffered, HPTS-free external sodium/potassium gluconate solution (MGlu, 100 mM) at pH 7.0, which allowed the removal of any uncaptured HPTS. The lipid solution obtained after Sephadex® was diluted to a standard volume with the corresponding external solution to obtain a lipid stock of known concentration. BSA treatment of vesicles was achieved by adding 1 mol% (with respect to lipid) of BSA to the lipid stock solution and leaving to stir for 30 minutes.

For each measurement, the lipid stock solution was diluted with the external buffered solution to a standard volume (2.5 mL) to give a lipid concentration of 0.1 mM. Following this, the cuvette was placed in a Cary Eclipse Fluorescence Spectrometer to begin the experiment. In cases where an ionophore was used (monensin, valinomycin, CCCP), it was added as a DMSO solution (5 μL) prior to the addition of the transporter. Each transporter was added as a DMSO

solution (5 uL, 10 mol% with respect to lipid). The experiment was initiated by adding NaOH (25 μL, 0.5 M) to generate a pH gradient across the membrane. After 600 s, monensin (0.1 mol% with respect to lipid) was added to achieve 100% efflux and a final reading was taken after an additional 120 s for calibration. The fractional fluorescence intensity (I_f) was calculated using:

$$\boldsymbol{I(f) = \frac{R(t) - R(0)}{R(m) - R(0)}}$$

where R_f is the fluorescence ratio at time t, R_0 is the ratio at time 0 and R_m is the ratio at the end of the experiment following the addition of monensin. Efflux plots at a 10 mol% compound to lipid ratio loading level were obtained and repeated in duplicate to obtain an efflux curve.

The results indicate that coupling to valinomycin or the use of TBAOH as the base pulse results in an increase in the rate of pH dissipation. By contrast, the addition of CCCP results in no comparable increase in rate. We thus conclude that in this experiment, the rate of H^+/M^+ antiport is rate limited by the influx of metal cations into the vesicles. For all the compounds tested, prior treatment of the vesicles with BSA led to a decrease in rate. This is consistent with the notion that metal cation influx in the absence of chloride can still be partially attributed to an ion-pair symport mechanism, this time facilitated by the trace fatty acid present in the membrane.

Table S5. Summary of Transmembrane Transport Rates[a] of Transporters **1-4** Derived from the HPTS Assay.

		H^+ efflux or OH^- influx (10^{-2} %s^{-1})			K^+/H^+	K^+	Na^+/H^+	Na^+
		with Vln	TBAOH (K^+)	TBAOH (Na^+)	(10^{-2} %s^{-1})	(10^{-2} %s^{-1}) with CCCP	(10^{-2} %s^{-1})	(10^{-2} %s^{-1}) with CCCP
1	BSA	0.52	0.67	1.05	0.10	0.12	0.15	0.18
		4.64	4.23	5.00	0.31	0.32	0.73	0.76
2	BSA	0.09	0.12	0.23	0.07	0.08	0.10	0.12
		0.93	0.99	1.29	0.32	0.30	0.66	0.71
3	BSA	0.62	0.84	3.03	0.19[c]	0.29[c]	0.57[b,c]	0.64[b,c]
		2.94	4.70	9.82	0.09	0.08	0.21[b]	0.31[b]
4	BSA	0.05	0.06	0.20	--	--	0.44[b,c]	0.35[b,c]
		0.48	1.13	1.09	0.05	0.06	0.08	0.06

a) Initial rate derived from single exponential fit. b) Initial rate derived from double exponential fit. c) Early plateau kinetics; therefore, the initial rate must be interpreted with caution. Vln refers to valinomycin.

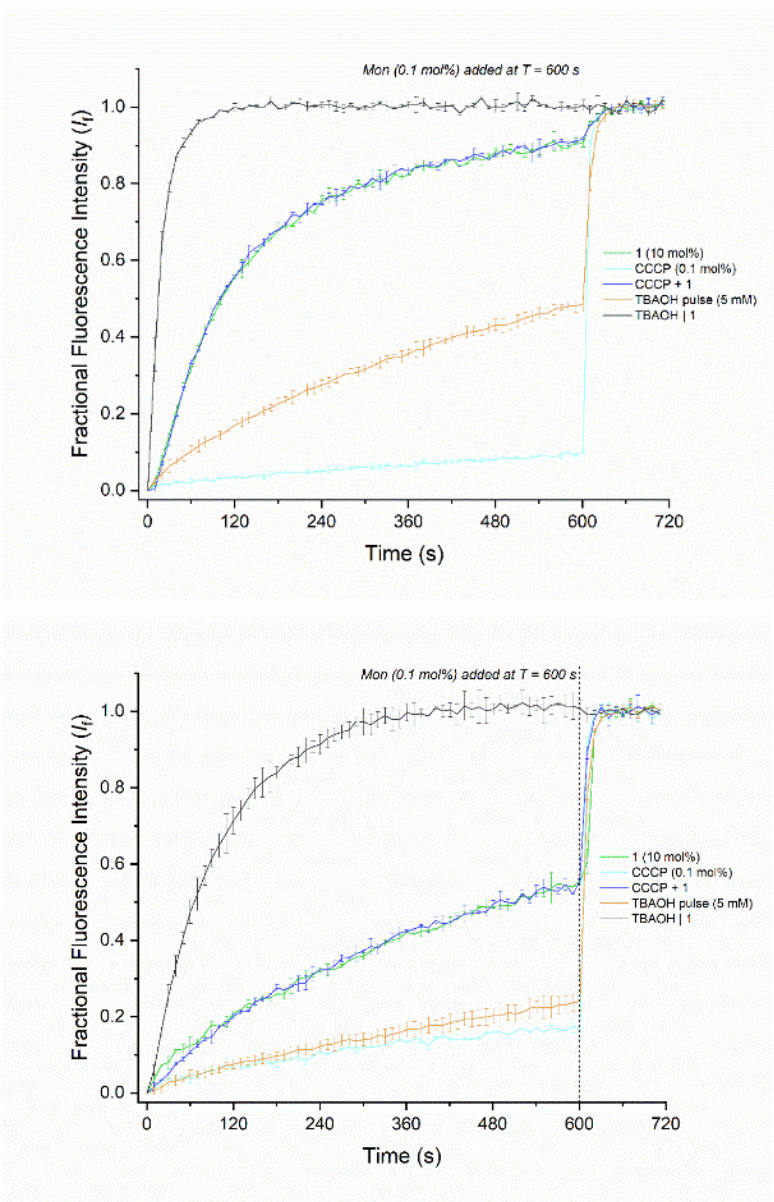

Figure S49. Top) HPTS NaGlu plots for compound **1** at 10 mol% loading with respect to lipid. The experiment is started by adding a NaOH base pulse (25 µL, 0.5 M), unless stated otherwise, and ended after 600 s by adding monensin (0.1 mol%) to facilitate complete pH gradient dissipation. The CCCP concentration is shown as ionophore to lipid molar ratio. Errors bars represent the standard deviation of two repeats. Bottom) HPTS NaGlu plots for compound **1** at 10 mol% loading in 'fatty acid free conditions' with BSA treated vesicles. Experimental conditions are otherwise the same.

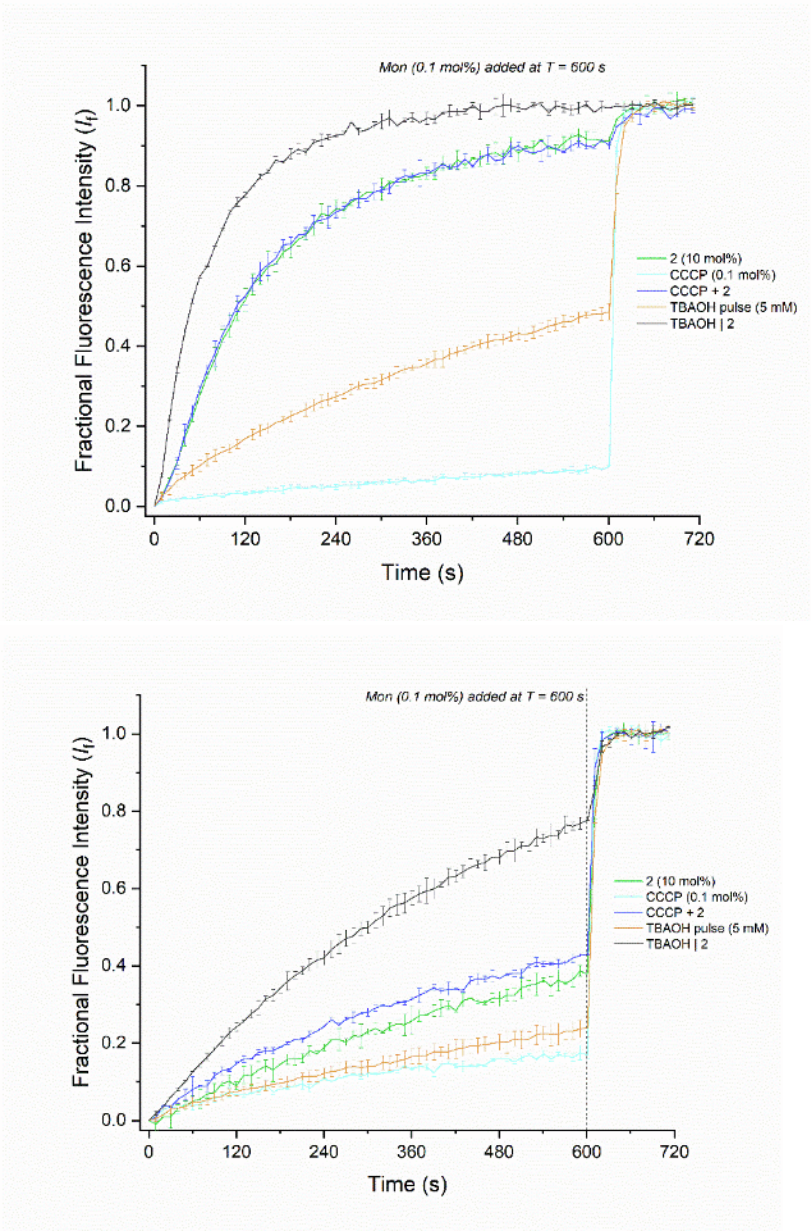

Figure S50. Top) HPTS NaGlu plots for compound **2** at 10 mol% loading with respect to lipid. The experiment is started by adding a NaOH base pulse (25 μL, 0.5 M), unless stated otherwise, and ended after 600 s by adding monensin (0.1 mol%) to facilitate complete pH gradient dissipation. The CCCP concentration is shown as ionophore to lipid molar ratio. Errors bars represent the standard deviation of two repeats. Bottom) HPTS NaGlu plots for compound **2** at 10 mol% loading in 'fatty acid free conditions' with BSA treated vesicles. Experimental conditions are otherwise the same.

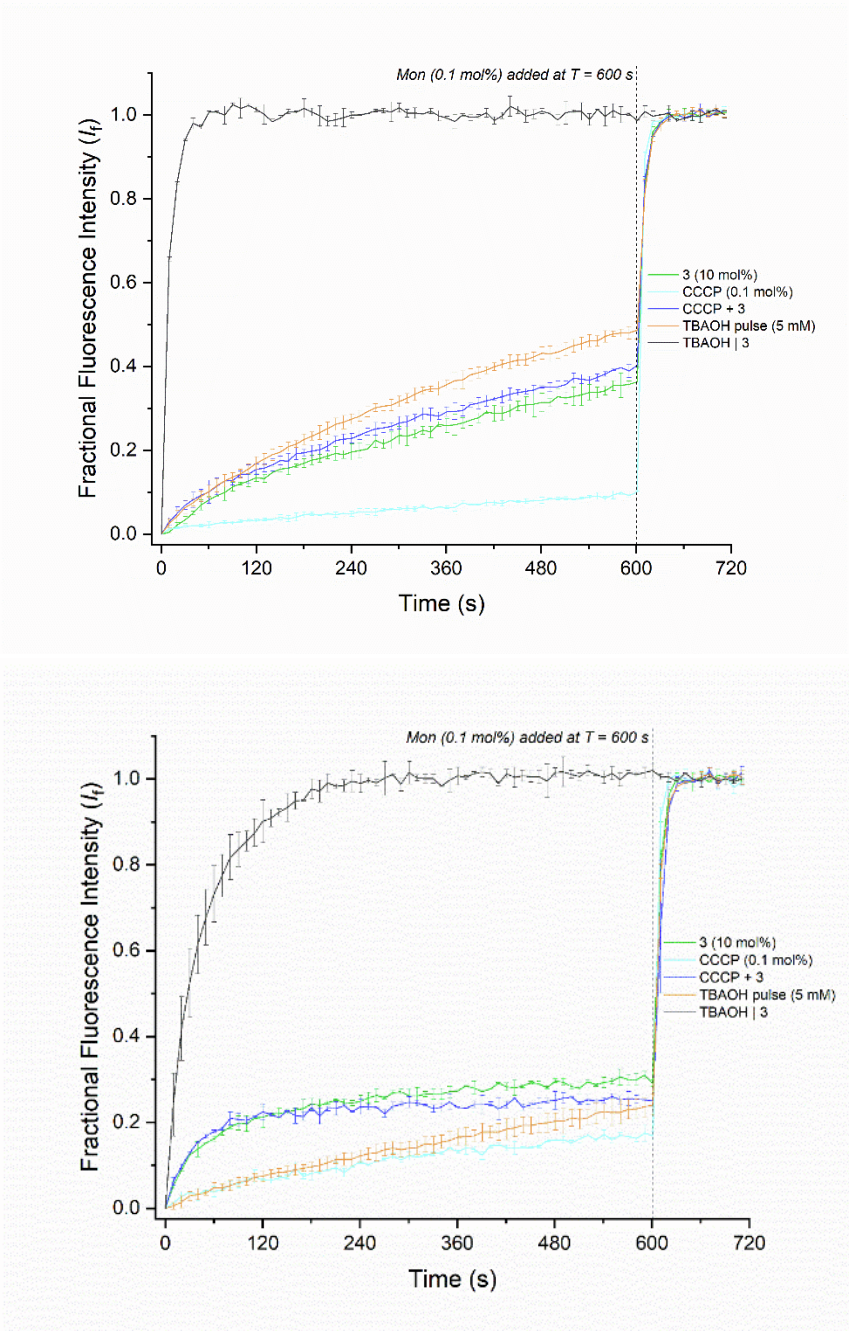

Figure S51. Top) HPTS NaGlu plots for compound **3** at 10 mol% loading with respect to lipid. The experiment is started by adding a NaOH base pulse (25 µL, 0.5 M), unless stated otherwise, and ended after 600 s by adding monensin (0.1 mol%) to facilitate complete pH gradient dissipation. The CCCP concentration is shown as ionophore to lipid molar ratio. Errors bars represent the standard deviation of two repeats. Bottom) HPTS NaGlu plots for compound **3** at 10 mol% loading in 'fatty acid free conditions' with BSA treated vesicles. Experimental conditions are otherwise the same.

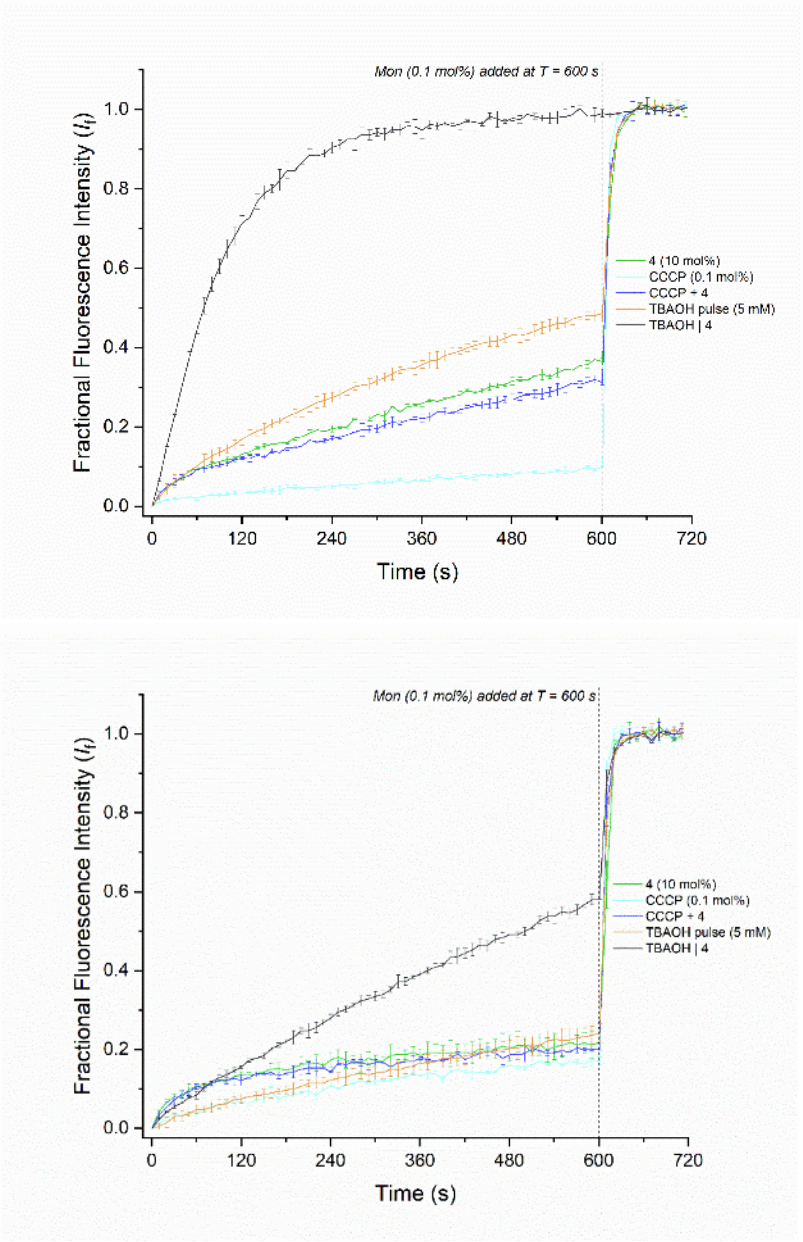

Figure S52. Top) HPTS NaGlu plots for compound **4** at 10 mol% loading with respect to lipid. The experiment is started by adding a NaOH base pulse (25 µL, 0.5 M), unless stated otherwise, and ended after 600 s by adding monensin (0.1 mol%) to facilitate complete pH gradient dissipation. The CCCP concentration is shown as ionophore to lipid molar ratio. Errors bars represent the standard deviation of two repeats. Bottom) HPTS NaGlu plots for compound **4** at 10 mol% loading in 'fatty acid free conditions' with BSA treated vesicles. Experimental conditions are otherwise the same.

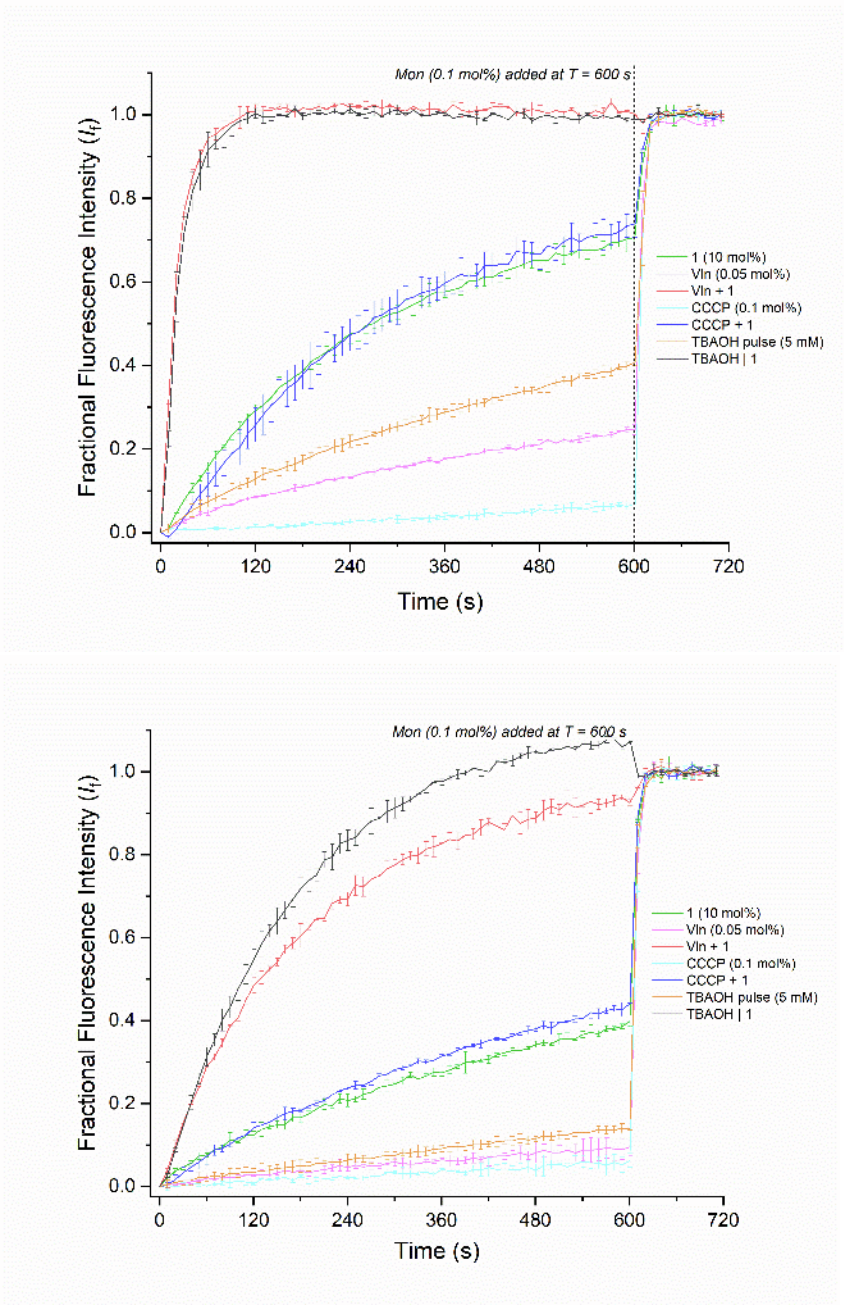

Figure S53. Top) HPTS KGlu plots for compound **1** at 10 mol% loading with respect to lipid. The experiment is started by adding a NaOH base pulse (25 µL, 0.5 M), unless stated otherwise, and ended after 600 s by adding monensin (0.1 mol%) to facilitate complete pH gradient dissipation. The CCCP concentration is shown as ionophore to lipid molar ratio. Errors bars represent the standard deviation of two repeats. Bottom) HPTS KGlu plots for compound **1** at 10 mol% loading in 'fatty acid free conditions' with BSA treated vesicles. Experimental conditions are otherwise the same.

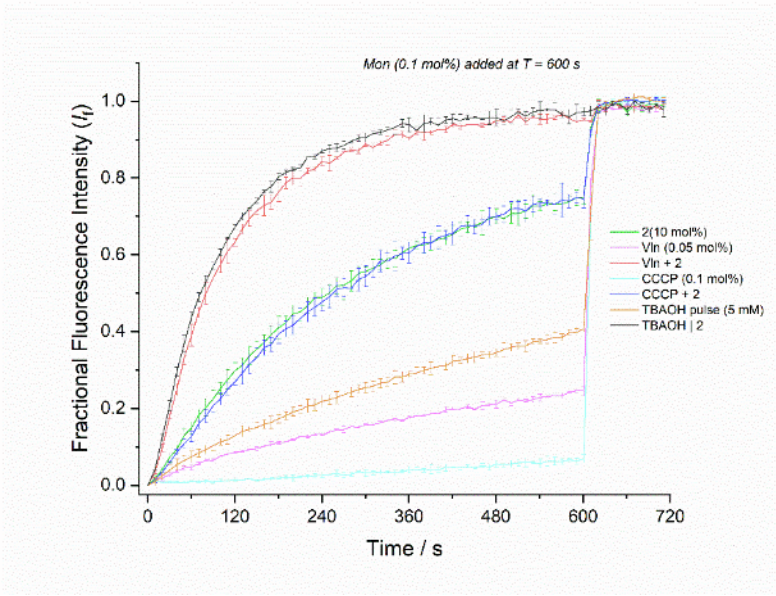

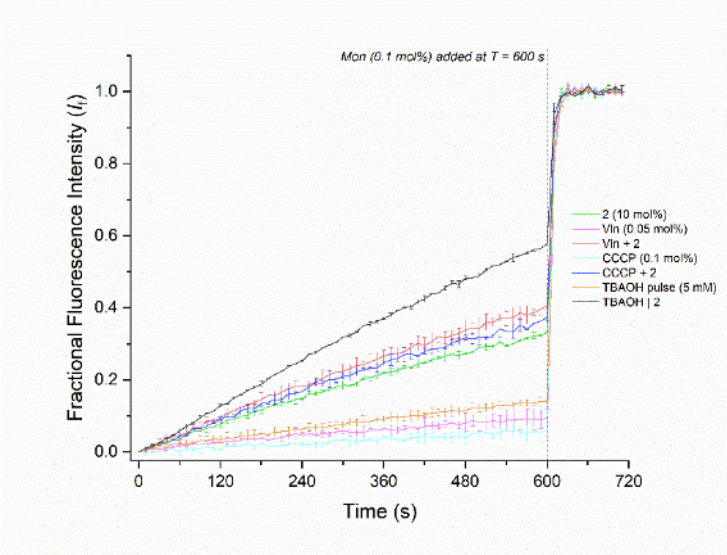

Figure S54. Top) HPTS KGlu plots for compound **2** at 10 mol% loading with respect to lipid. The experiment is started by adding a NaOH base pulse (25 μL, 0.5 M), unless stated otherwise, and ended after 600 s by adding monensin (0.1 mol%) to facilitate complete pH gradient dissipation. The CCCP concentration is shown as ionophore to lipid molar ratio. Errors bars represent the standard deviation of two repeats. Bottom) HPTS KGlu plots for compound **2** at 10 mol% loading in 'fatty acid free conditions' with BSA treated vesicles. Experimental conditions are otherwise the same.

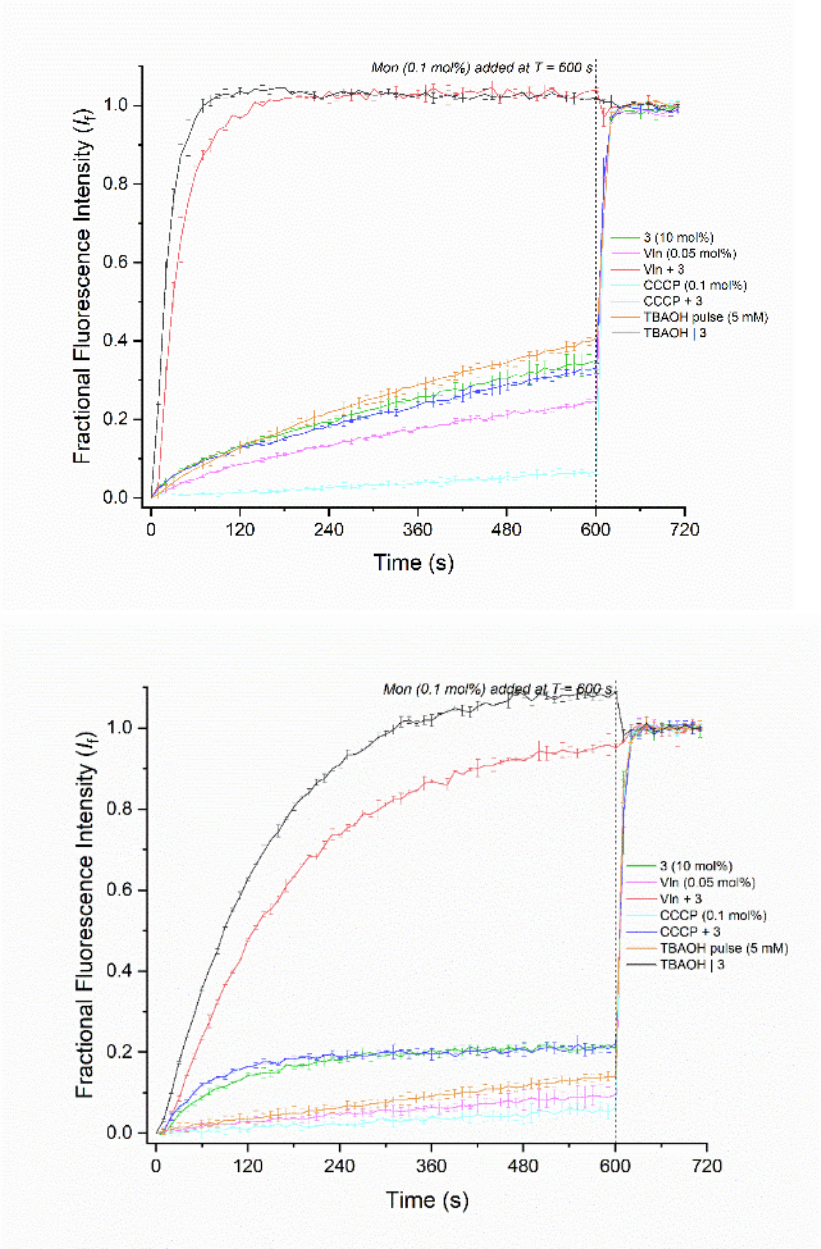

Figure S55. Top) HPTS KGlu plots for compound **3** at 10 mol% loading with respect to lipid. The experiment is started by adding a NaOH base pulse (25 µL, 0.5 M), unless stated otherwise, and ended after 600 s by adding monensin (0.1 mol%) to facilitate complete pH gradient dissipation. CCCP concentration is shown as ionophore to lipid molar ratio. Errors bars represent the standard deviation of two repeats. Bottom) HPTS KGlu plots for compound **3** at 10 mol% loading in 'fatty acid free conditions' with BSA treated vesicles. Experimental conditions are otherwise the same.

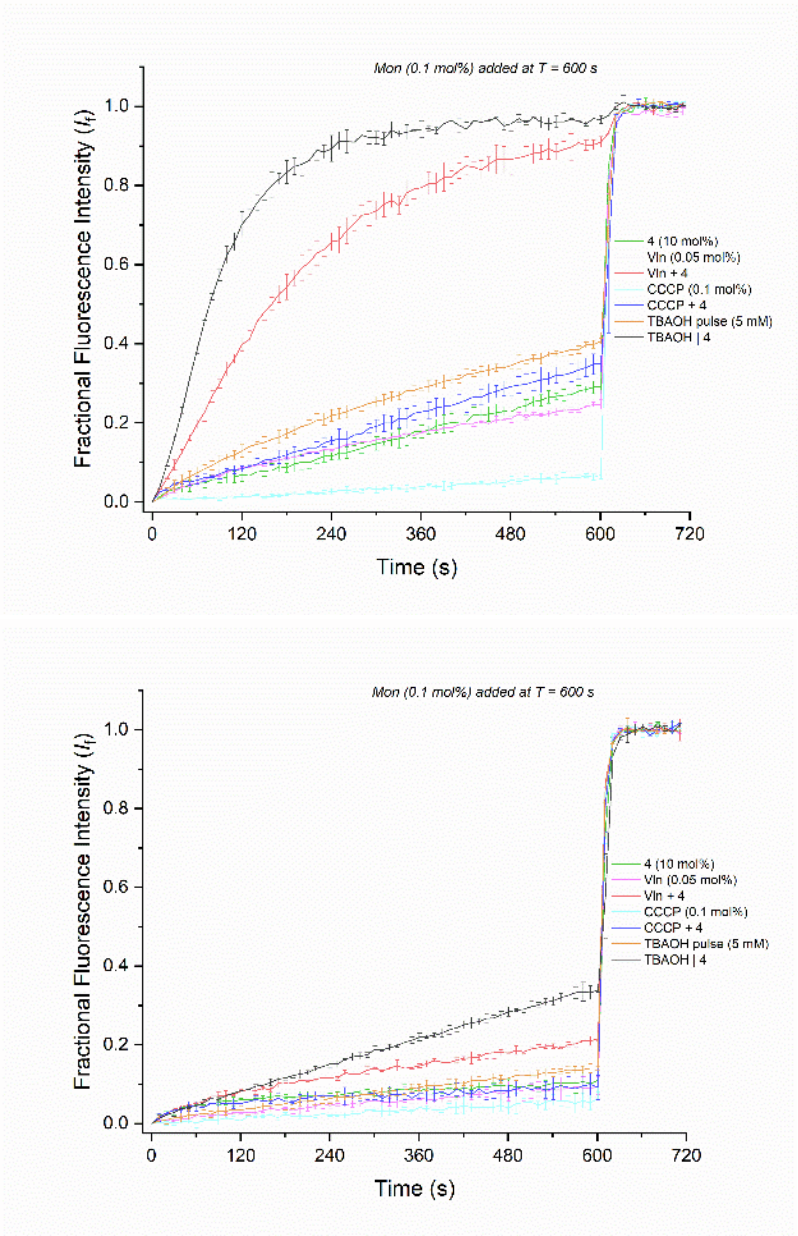

Figure S56. Top) HPTS KGlu plots for compound **4** at 10 mol% loading with respect to lipid. The experiment is started by adding a NaOH base pulse (25 µL, 0.5 M), unless stated otherwise, and ended after 600 s by adding monensin (0.1 mol%) to facilitate complete pH gradient dissipation. The CCCP concentration is shown as ionophore to lipid molar ratio. Errors bars represent the standard deviation of two repeats. Bottom) HPTS KGlu plots for compound **4** at 10 mol% loading in 'fatty acid free conditions' with BSA treated vesicles. Experimental conditions are otherwise the same.

5. Biological Studies

Cell culture and transfection. HeLa (cervical cancer cells), A549 (lung carcinoma epithelial cells), PLC/PRF/5 (hepatoma cells), HCT116 (colorectal carcinoma cells), HepG2 (hepatocellular carcinoma cells), MRC-5 (fetal lung fibroblast cells), C2C12 (myoblast cells) and MEF (embryonic fibroblast cells) cells were cultured in RPMI 1640 (Invitrogen), DMEM (Invitrogen), or MEM (Invitrogen) supplemented with 10% fetal bovine serum (FBS), 50 units/mL penicillin and 50 units/mL streptomycin. HeLa cells were transfected with the tandem mRFP-EGFP-LC3 plasmid (Addgene) by using Lipofectamin 2000 (Invitrogen) and stably transfected cells were selected using 600 μg/mL G418 (Tocris) over 3 weeks. Cells were maintained at 37 ºC under a humidified atmosphere of 5% CO_2.

Determination of changes in Cl^- concentrations. HeLa and A549 cells were detached from the culture dish by treating with 2% trypsin-EDTA solutions in Dulbecco's phosphate-buffered saline (DPBS). After washing the cells with DPBS, the number of live cells stained with 0.5% trypan blue was counted using a hemacytometer. The suspended cells (5 x 10^3 cells) in culture media were seeded in triplicate onto 96-well plates. After 24 hours, the cells were washed with fresh culture media. One of 96-wells containing cells was treated with propidium iodide (PI) to detect dead cells. For the most part, no dead cells were observed. The treated cells were incubated with the indicated concentrations of each test compound (**1**-**5**) in culture media for 2 hours at 37 ºC. After washing with PBS, cells were incubated with 5 mM MQAE for 30 min. After washing, the fluorescence intensity of MQAE in cells was measured using a microplate reader (λ_{ex} = 350 nm, λ_{em} = 460 nm).

Determination of changes in Na^+ concentrations. HeLa and A549 cells cultured by above procedures were treated with 10 μM SBFI-AM (ThermoFisher Scientific) in culture media for 2 hours at 37 ºC. After washing with PBS to remove the remaining SBFI-AM, the cells were incubated with the indicated concentrations of each test compound (**1**-**5**) in culture media for 2 hours at 37 ºC. The SBFI-AM fluorescence was measured using a microplate reader (λ_{ex} = 340 nm, λ_{em} = 500 nm).

Determination of changes in K^+ concentrations. HeLa and A549 cells cultured in accord with the above procedures were treated with 10 μM PBFI-AM (ThermoFisher Scientific) in culture media for 1.5 hour at 37 ºC. After washing with PBS to remove the remaining PBFI-AM, solutions of HEPES buffer were added to the cells. The cells were incubated with each test compound for 2 hours at 37 ºC. The PBFI fluorescence was measured using a microplate reader (λ_{ex} = 340 nm, λ_{em} = 500 nm).

Determination of changes in Ca^{2+} concentrations. HeLa and A549 cells cultured in accord with the above procedures were treated with 10 μM Fluo-4 NW (ThermoFisher Scientific) in culture media for 1 hour at 37 ºC. After washing with PBS to remove the remaining Fluo-4 NW, solutions of HEPES buffer were added to each well. Cells were incubated with each test

compound (**1-5**) for 2 hours at 37 ºC. Fluo-4 fluorescence was measured using a microplate reader (λ_{ex} = 485 nm, λ_{em} = 538 nm).

Measurement of changes of cytosolic pH. HeLa cells were seeded onto 96-well plates and treated with each test compound (**1-5**) for indicated time followed by incubation with 100 nM BCECF-AM for 30 min at 37 ºC. After washing the cells with HEPES-buffered solutions, the BCECF fluorescence was measured by using a microplate reader (λ_{ex} = 490/440 nm, λ_{em} = 530 nm).

Measurement of cell death. Cancer cells cultured by above procedures were incubated with various concentrations of each test compound (**1-5**) in culture media. MTT assays were performed using standard procedures. The absorbance at 570 nm was measured by means of a microplate reader.

Sodium and chloride depletion study. HEPES-buffered solutions were prepared with the following compositions: 120 mM NaCl, 5 mM KCl, 1 mM $MgCl_2$, 1 mM $CaCl_2$, 10 mM D-glucose, 10 mM HEPES (pH 7.4), and 25 mM $NaHCO_3$. To prepare Cl^-–free HEPES-buffered solutions, Cl^- ions in the buffer solutions were replaced with equimolar concentrations of gluconate salts. The cells were used to detect changes in intracellular potassium and sodium ion concentrations after treatment with the indicated concentration of each test compound (**1-5**) by using PBFI-AM and SBFI-AM, respectively, in accord with the procedures detailed above.

Flow cytometry. For analysis of apoptosis, HeLa cells were incubated with 1, 2, or 3 for 24 hours at 37 ºC. Untreated cells were used as a negative control. After washing with PBS twice, the cells were trypsinized with 0.5 mL of trypsin-EDTA (0.05% trypsin, 0.02% EDTA, Sigma-Aldrich) for 5-10 min at 37 ºC and collected by centrifugation. The cells were stained with the FITC-annexin V apoptosis detection kit with propidium iodide (PI) according to the manufacturer's protocol. Flow cytometry was performed using a BD FACSVerse™ instrument.

Determination of cell size by flow cytometry. HeLa cells were incubated with 1, 2, or 3 for 24 hours at 37 ºC. Untreated cells were used as a negative control. Cell size was measured using a flow cytometer by exciting with a 488-nm argon laser and determining the distribution on a forward scatter versus side scatter dot plot. Light scattered in the forward direction is proportional to cell size, and light scattered at a 90º angle (side scatter) is proportional to cell density.

Cell imaging using JC-1. HeLa cells were incubated with **1**, **2**, or **3** for 18 hours at 37 ºC. Untreated cells were used as a negative control. Treated cells were washed with DPBS for three times and incubated with 2.5 μg/mL of JC-1 in culture media for 15 min at 37 ºC. Cell images were obtained by means of confocal fluorescence microscopy. The red and green fluorescence features were recorded by monitoring the emission at 600 nm and 535 nm, respectively.

DNA fragmentation assays. HeLa cells were incubated with **1**, **2**, or **3** for 24 hours at 37 ºC. The cells were lysed in a buffer containing 10 mM Tris, 1 mM EDTA, and 0.2% Triton X-100 at pH 8.0. Samples were incubated with 100 µg/mL Rnase A for 0.5 h at 37 ºC and then 100 µg/mL proteinase K for 10 min at 56 ºC. The DNA was precipitated by adding 0.5 M NaCl-isopropyl alcohol. It was then washed with 70% ethanol. Samples were loaded on a 1.5% agarose gel and were subjected to electrophoresis at 100 V for 30 min in TBE (Tris/Borate/EDTA) buffer (0.5X). The resulting DNA was stained with RedSafe™ Nucleic Acid Staining Solution (Intron, Korea) and analyzed using a G:BOX Chemi Fluorescent & Chemiluminescent Imaging System (Syngene).

Measurements of changes in cell size by confocal microscopy. HeLa cells were incubated with Hoechest 33342 dye for 10 min. After washing with DPBS to remove the remaining Hoechest 33342 stain, the cells were treated with the compound under study in culture media. Changes in cell size were monitored over a 1.5 hour period following initial incubation by means of confocal microscopy (Zeiss LSM 800). Cell images were analyzed to determine the changes in cell size, if any, by drawing a region of interest (ROI) around the cell boundaries using the ImageJ software.

Isolation of cytosolic and mitochondrial fractions. HeLa cells were incubated with each substance for 18 hours. Mitochondrial and cytosol fractions of the cells were prepared using a mitochondrial/cytosol fractionation kit (Biovision). Cells were harvested by centrifugation at 600 × g for 5 min and washed twice with cold PBS buffer. The cells were re-suspended in 250 µL extraction buffer containing the protease inhibitor mixture (Biovision) and dithiothreitol. After allowing to incubate on ice for 30 min, the cells were homogenized on ice and centrifuged at 700 × g for 10 min at 4 °C, and the supernatant collected. This supernatant was centrifuged again at 10,000 × g for 30 min at 4 °C. The resulting supernatant was harvested and used as the cytosolic fractions. The pellets were re-suspended and used as the mitochondrial fractions.

Western blot analysis. Proteins were separated by 6–12% SDS-PAGE. Rabbit caspase-3 (H277) polyclonal (1:1000, sc-7272, Santa Cruz Bio Technology), rabbit cleaved caspase-3 (Asp175) polyclonal (1:1000, #9661, Cell Signaling Technology), rabbit PARP polyclonal (1:1000, #9542, Cell Signaling Technology), mouse cytochrome c monoclonal (1:1000, k257, Biovision), rabbit anti-phospho-p38 polyclonal (1:1000, # 9211, Cell Signaling Technology), rabbit PKC polyclonal (1:1000, ab59411, Abcam), rabbit anti-LC3 monoclonal (1:2000, L8919, Sigma), mouse anti-p62 monoclonal (1:1000, sc-28359, Santa Cruz Bio Technology), rabbit Bid polyclonal (1:1000, #2002, Cell Signaling Technology), rabbit anti-IRE1 polyclonal (1:1000, ab37073, Abcam), rabbit anti-phospho-IRE1 polyclonal (1:1000, ab48187, Abcam), rabbit anti-PERK monoclonal (1:1000, #5683, Cell Signaling Technology), rabbit anti-phospho-PERK monoclonal (1:1000, #3719, Cell Signaling Technology), rabbit anti-JNK polyclonal (1:1000, MBS840351, Biocompare), mouse anti-phospho-JNK monoclonal (1:1000, sc-6254, Santa Cruz Bio Technology), and mouse anti-β-actin monoclonal (1:1000, sc-47778,

Santa Cruz Bio Technology) antibodies were used as primary antibodies. Horseradish peroxidase-conjugated goat anti-rabbit IgG (1:2000, sc-2357, Santa Cruz Bio Technology) and goat anti-mouse IgG (1:2000, sc-516102, Santa Cruz Bio Technology) were used as the secondary antibodies. The blots were developed by using a West-ZOL® plus Western Blot Detection System (Intron Biotechnology Inc., South Korea). Protein bands were analyzed using a G:BOX Chemi Fluorescent & Chemiluminescent Imaging System.

Measurement of the level of ROS. HeLa cells were incubated with the indicated concentrations of each substance over an 8 hour period. The cells were incubated with 10 μM PF1 for 1 hour. The fluorescence intensity of PF1 was measured by using a microplate reader (λ_{ex} = 485 nm, λ_{em} = 535 nm).

Measurement of caspase activity. HeLa cells were incubated with various concentrations of each compound under sudy for 18 hours at 37 °C. The cells were lysed in a buffer containing 50 mM HEPES at pH 7.4, 5 mM CHAPS, and 5 mM DTT. Cell lysates were placed into the appropriate wells of 96-well plate. Assay buffer containing 20 mM HEPES at pH 7.4, 0.01% CHAPS, 5 mM DTT and 2 mM EDTA was added to each of the wells. A caspase inhibitor Ac-DEVD-CHO (20 μM) was added to the appropriate wells. Caspase activity was determined by adding 200 μM Ac-DEVD-pNA (Sigma-Aldrich, USA) to each of the wells. The enzyme-catalyzed release of pNA was monitored at 405 nm using a microplate reader.

Measurement of lysosomal Cl^- concentrations. HeLa cells were incubated with various concentrations of each substance for 4 hours at 37 °C. The cells were incubated with 1 mM MQAE-MP for 30 min. The cells were imaged by means of confocal fluorescence microscopy. Cell images were analyzed using the ZEN 2011 software.

Fluorescence cell imaging. HeLa cells, stably expressing mRFP-EGFP-LC3, were incubated with the indicated concentrations of **1**, **2**, **3**, **4**, **5**, torin-1 or bafilomycin A1. The cells were fixed in 3% formaldehyde for 10 min at 37 °C. The cells were imaged by using confocal fluorescence microscopy. Cell images were analyzed by means of the ZEN 2011 software.

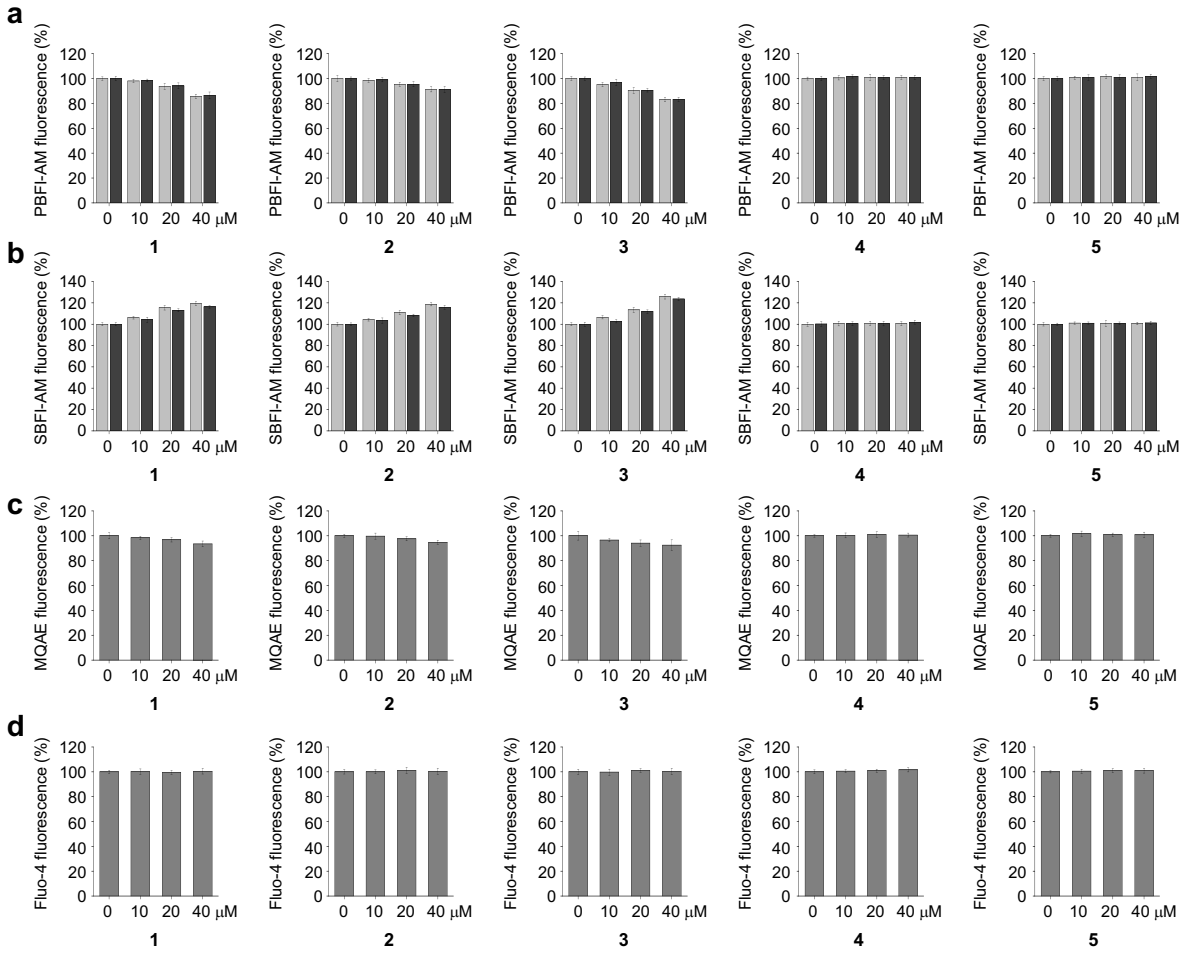

Figure S57. Effects of synthetic transporters on ion concentrations in A549 cells. (a) A549 cells pretreated with 10 μM PBFI-AM were incubated with various concentrations of the indicated compound in the absence (grey bars) and presence (black bars) of 20 μM 4-aminopyridine for 2 hours. The PBFI fluorescence was measured to examine changes in intracellular potassium ion concentrations (mean ± s.d., n = 3). (b) A549 cells pretreated with 10 μM SBFI-AM were incubated for 2 hours with various concentrations of the indicated compounds in the absence (grey bars) and presence (black bars) of 1 mM amiloride. SBFI-AM fluorescence was measured to determine changes in intracellular sodium ion concentrations (mean ± s.d., n = 3). (c) A549 cells were treated for 2 hours with various concentrations of indicated substances. The treated cells were further incubated with 5 mM MQAE and MQAE fluorescence was measured to determine changes in the intracellular chloride ion concentrations (mean ± s.d., n = 3). (d) A549 cells pretreated with 10 μM Fluo-4-NW were incubated with various concentrations of the indicated compounds for 2 hours. The Fluo-4 fluorescence was used to monitor changes in intracellular calcium ion concentrations (mean ± s.d., n = 3).

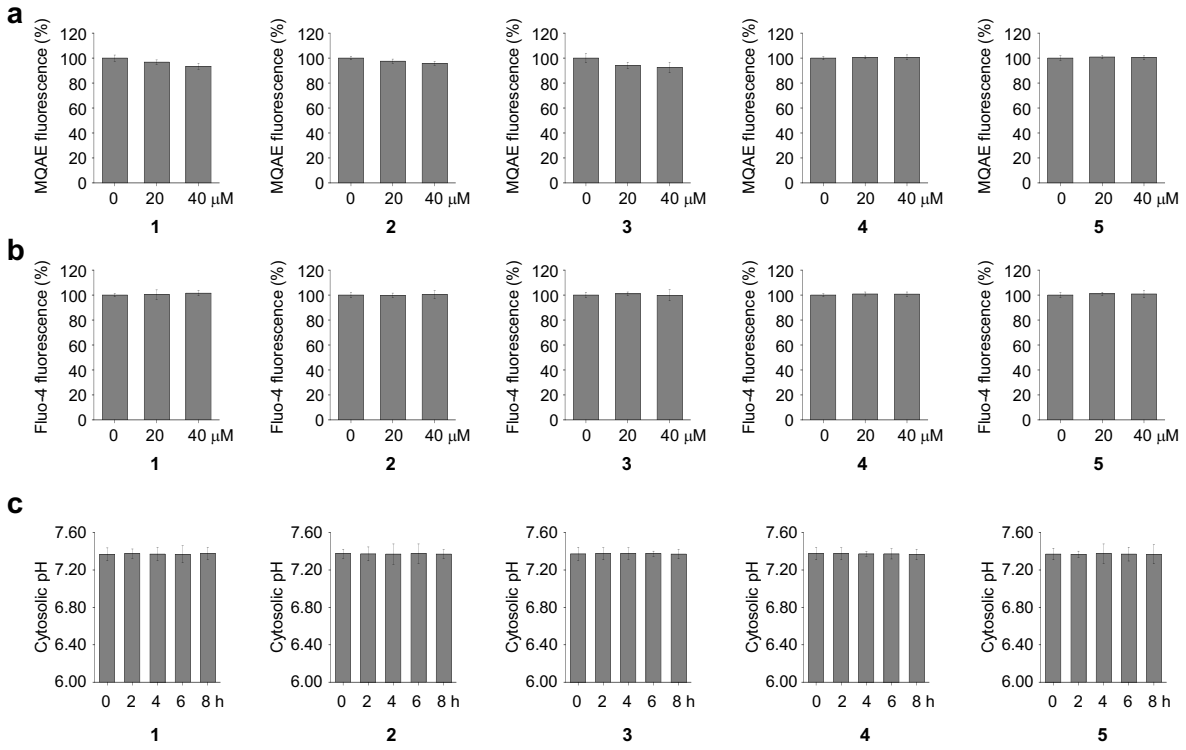

Figure S58. Effects of synthetic transporters on ion concentrations in HeLa cells. (a) HeLa cells were treated for 2 hours with various concentrations of the indicated compounds. The treated cells were further incubated with 5 mM MQAE and the MQAE fluorescence was measured to determine changes in the intracellular chloride ion concentrations (mean ± s.d., n = 3). (b) HeLa cells pretreated with 10 μM Fluo-4-NW were incubated with various concentrations of the indicated compounds for 2 hours. The Fluo-4 fluorescence was measured to examine changes in intracellular calcium ion concentrations (mean ± s.d., n = 3). (c) HeLa cells were incubated with 20 μM **1**, 40 μM **2**, 20 μM **3**, 40 μM **4**, and 40 μM **5** for indicated times. The cytosolic pH was measured using a pH-sensitive fluorescent probe BCECF-AM (mean ± s.d., n = 3).

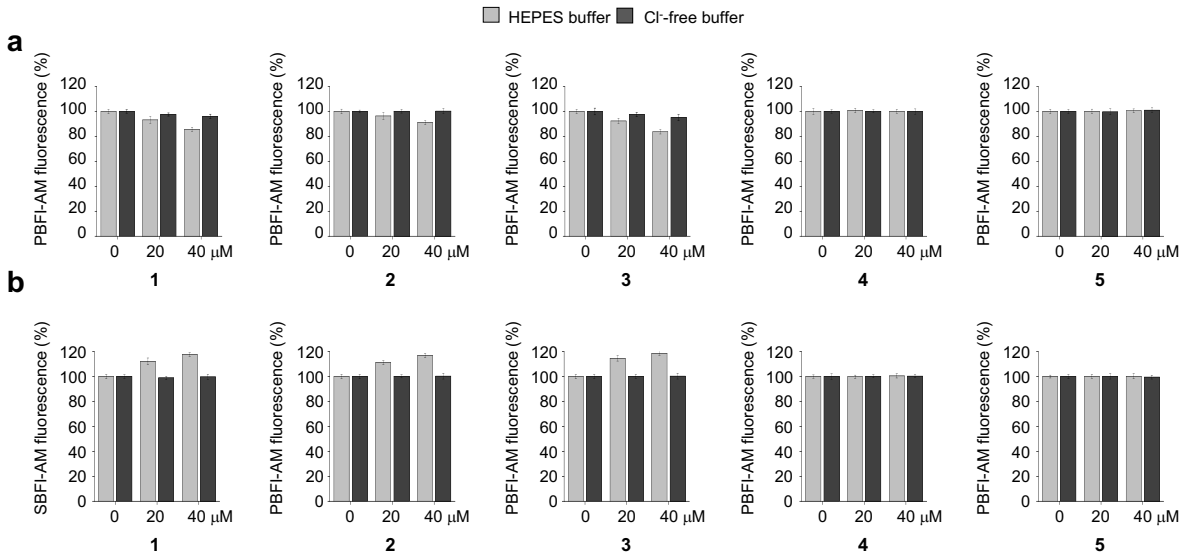

Figure S59. Synthetic transporters do not change intracellular potassium or sodium ion concentrations in Cl^--free solutions. HeLa cells pretreated with (a) 10 μM PBFI-AM and (b) 10 μM SBFI-AM for 1.5 hour were incubated with various concentrations of indicated the compounds in HEPES buffer (gray bars) or Cl^- -free solutions (black bars) for 2 hours. The PBFI and SBFI fluorescence was measured to examine changes in the intracellular potassium and sodium ion concentrations (mean ± s.d., n = 3).

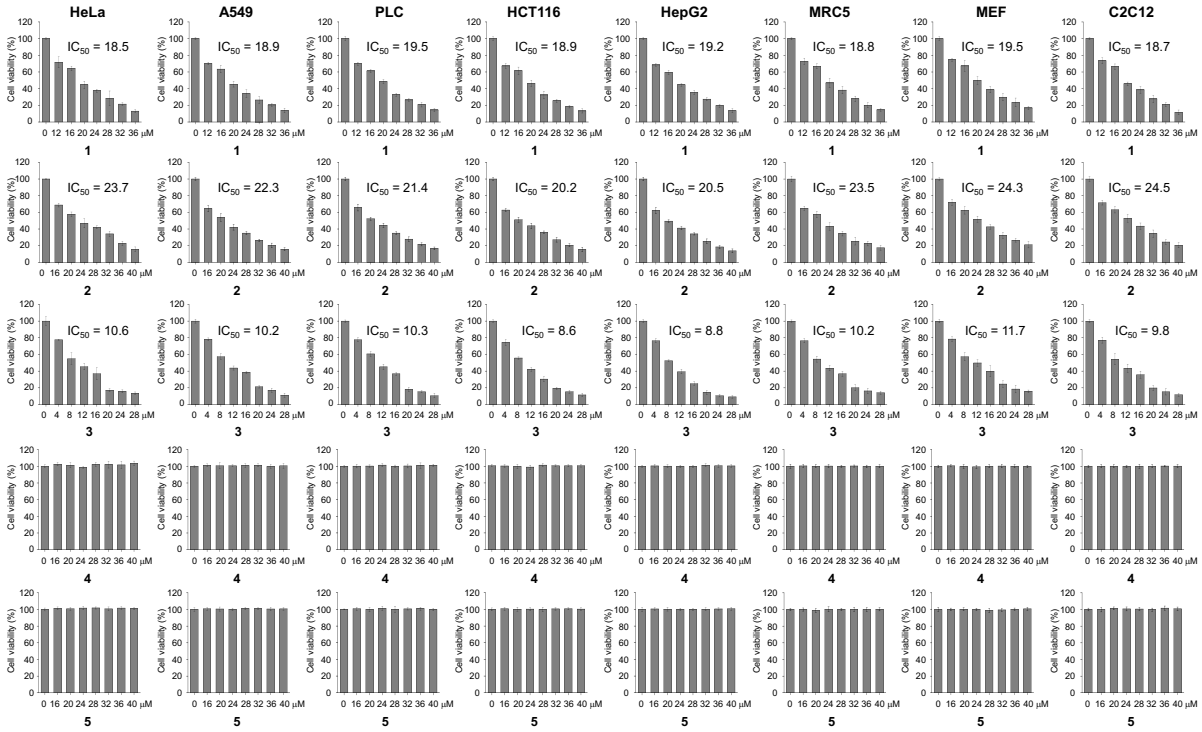

Figure S60. Cytotoxicity of compounds. HeLa, A549, PLC, HCT116 , HepG2, MRC-5, MEF, and C2C12 cells were treated with various concentrations of indicated compounds for 24 hours. Cell death was measured by means of an MTT assay (mean ± s.d., n = 3).

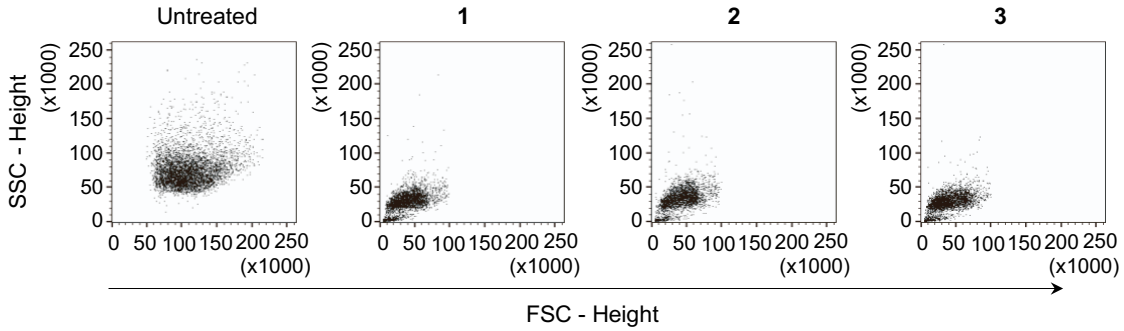

Figure S61. Synthetic transporters induce cell shrinkage. HeLa cells were treated with 20 μM **1**, 40 μM **2** or 20 μM **3** for 24 hours. Cell size was determined by means of flow cytometry (FSC: forward scatter, SSC: side scatter).

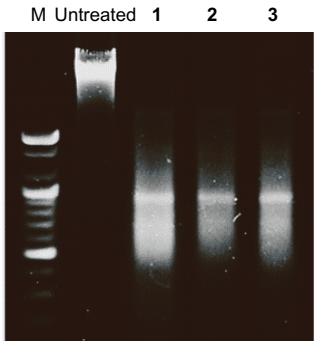

Figure S62. Synthetic transporters promote DNA fragmentation. HeLa cells were treated with 20 μM **1**, 40 μM **2** or 20 μM **3** for 24 hours. The DNA fragments were visualized by staining with nucleic acid staining solutions. Untreated cells are shown as a negative control.

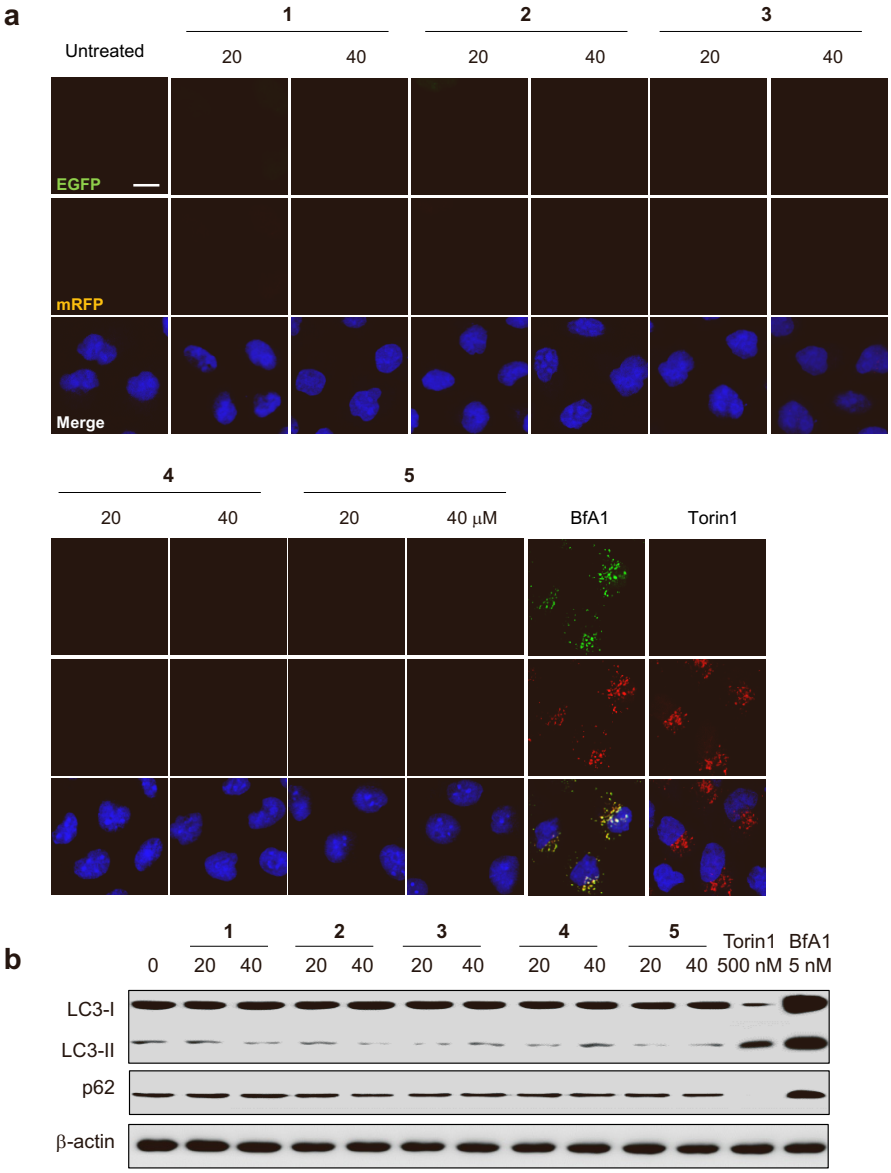

Figure S63. Synthetic transporters show no effects on autophagy. (a) HeLa cells stably expressing mRFP-EGFP-LC3 fusion protein were treated with each compound under study for 10 hours. Bafilomycin A1 (BfA1, 5 nM) and toin-1 (500 nM) were used as controls. Cell images were obtained by means of confocal fluorescence microscopy (scale bar: 10 μm). Note: The pH-sensitive fluorescence of EGFP is efficiently quenched in acidic autolysosomes. However, the pH-insensitive fluorescence of mRFP is not quenched in acidic autolysosomes. As a consequence, cells undergoing autophagy display red vesicles, but disruption of autophagy in cells exhibits yellow vesicles arising from merge of red and green fluorescence. (b) HeLa cells were treated with each substance for 10 hours. Bafilomycin A1 (BfA1, 5 nM) and toin-1 (500 nM) were used as controls. Immunoblotting was conducted by using LC3 and p62 antibody and β-actin was used as a control. Note: Typically, increased levels of LC3-II and decreased levels of p62 are observed during autophagy induction. In contrast, the levels of both LC3-II and p62 are increased when autophagic flux is disrupted.

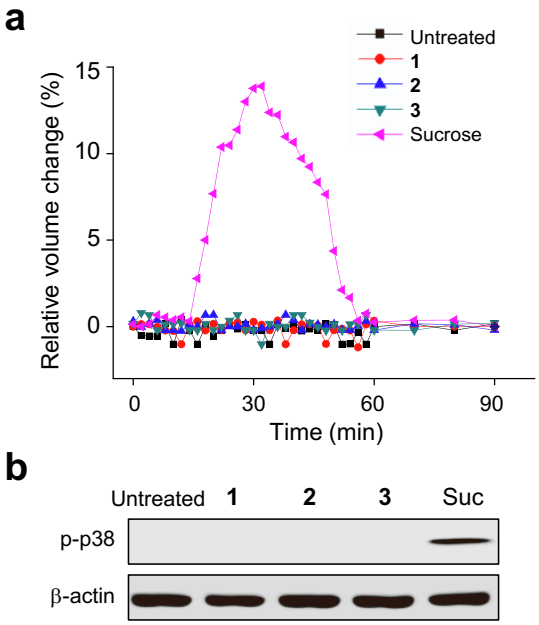

Figure S64. Synthetic transporters do not affect osmotic stress. (a) HeLa cells were individually treated with 40 μM of each compound under study or 100 mM sucrose in culture media over 1.5 hour period. Cell size was analyzed using the ImageJ software. Experiments were repeated three times, giving similar results. (b) HeLa cells were treated with 40 μM of each substance or 100 mM sucrose for 0.5 hour. Immunoblotting was conducted using the phosphor-p38 antibody.

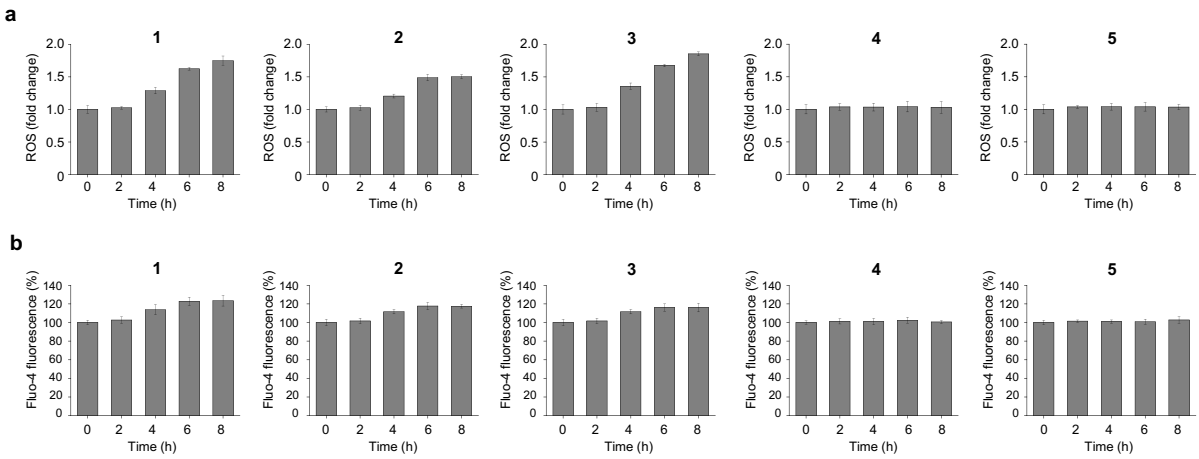

Figure S65. **Synthetic transporters induce ER stress.** (a) HeLa cells were incubated with 10 μM PF1 for 1 hour followed by incubation with 20 μM **1**, 40 μM **2**, 20 μM **3**, 40 μM **4**, and 40 μM **5** for 8 hours with 2 hour increment. The fluorescence intensity of PF1 was measured using a microplate reader (mean ± s.d., n = 3). (b) HeLa cells pretreated with 10 μM Fluo-4-NW were incubated with 20 μM **1**, 40 μM **2**, 20 μM **3**, 40 μM **4**, and 40 μM **5** for the indicated times. The Fluo-4 fluorescence was measured to examine changes in intracellular calcium ion concentrations (mean ± s.d., n = 3).

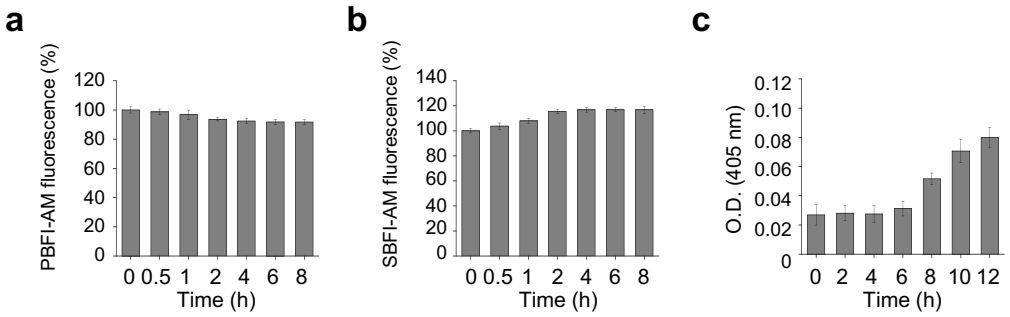

Figure S66. Potassium efflux and sodium influx precede apoptosis induced by transporter 1. (a) HeLa cells pretreated with 10 μM PBFI-AM were incubated with 20 μM of **1** for the indicated times. The PBFI fluorescence was measured to examine changes in intracellular potassium ion concentrations (mean ± s.d., n = 3). (b) HeLa cells pretreated with 10 μM SBFI-AM were incubated with 20 μM of **1** for the indicated times. SBFI-AM fluorescence was measured to determine changes in intracellular sodium ion concentrations (mean ± s.d., n = 3). (c) HeLa cells were incubated with 20 μM of **1** for the indicated times. The caspase activities of the cell lysates were determined using Ac-DEVD-pNA (200 μM) (mean ± s.d., n = 3).

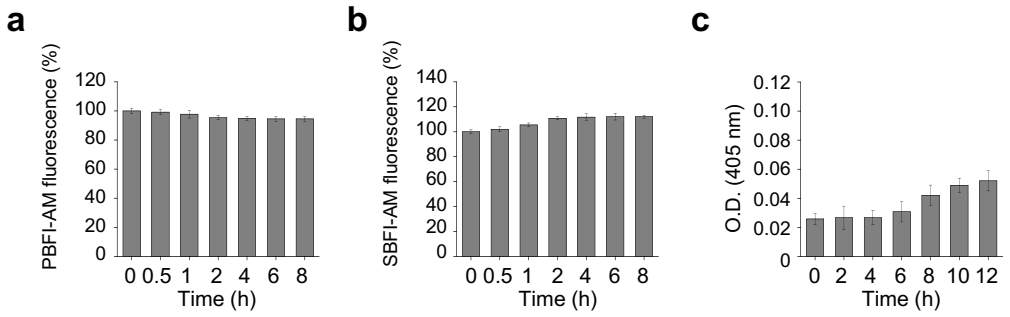

Figure S67. Potassium efflux and sodium influx precede apoptosis induced by transporter 2. (a) HeLa cells pretreated with 10 μM PBFI-AM were incubated with 20 μM of **2** for indicated times. The PBFI fluorescence was measured to examine changes in intracellular potassium ion concentrations (mean ± s.d., n = 3). (b) HeLa cells pretreated with 10 μM SBFI-AM were incubated with 20 μM of **2** for the indicated times. SBFI-AM fluorescence was measured to determine changes in intracellular sodium ion concentrations (mean ± s.d., n = 3). (c) HeLa cells were incubated with 20 μM of **2** for the indicated times. The caspase activities of cell lysates were determined using Ac-DEVD-pNA (200 μM) (mean ± s.d., n = 3).

6. X-ray Experimental

X-ray experimental for compound 1

Crystals of compound **1** grew as colorless blocks by the slow evaporation of a acetone solution of receptor **1**. A suitable crystal was selected and the data were collected on an Agilent Technologies SuperNova Dual Source diffractometer using a μ-focus Cu Kα radiation source (λ = 1.5418 Å) with collimating mirror monochromators at 100 K using an Oxford Cryostream low temperature device. Details of the crystal data, data collection and structure refinement are listed in Table S6 and in the corresponding CIF file. Data collection, unit cell refinement and data reduction were performed using Agilent Technologies CrysAlisPro V 1.171.37.31.6.[11] Using Olex2,[12] the structure was solved with the ShelXT structure solution program using direct methods and refined with the ShelXL refinement package using least squares minimization.[13, 14] Tables of positional and thermal parameters, bond lengths and angles, torsion angles and figures are in the corresponding CIF file, which may be obtained from the Cambridge Crystallographic Data Centre; CCDC deposition number: 2063566.

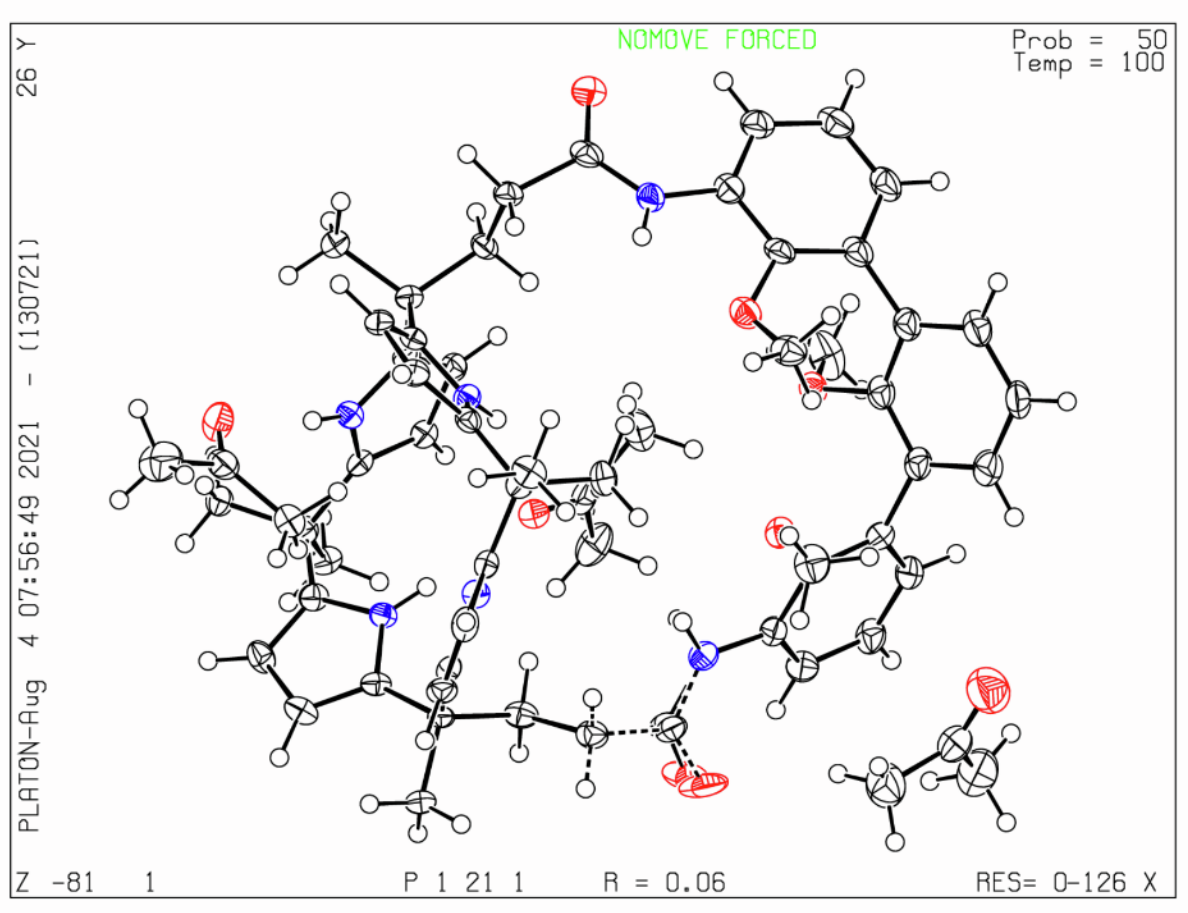

Figure S68. View of complex of **1**. Displacement ellipsoids are scaled to the 50% probability level.

Table S6 Crystal data and structure refinement for 1.

Identification code	**1**
Empirical formula	$C_{62}H_{76}N_6O_8$
Formula weight	1033.28
Temperature/K	100.15
Crystal system	monoclinic
Space group	$P2_1$
a/Å	11.0294(3)
b/Å	20.1804(7)
c/Å	12.8523(4)
α/°	90
β/°	100.224(3)
γ/°	90
Volume/Å^3	2815.22(15)
Z	2
ρ_{calc}g/cm^3	1.219
μ/mm^{-1}	0.646
F(000)	1108.0
Crystal size/mm^3	0.102 × 0.089 × 0.085
Radiation	CuKα (λ = 1.54184 Å)
2Θ range for data collection/°	6.988 to 151.458
Index ranges	$-13 \leq h \leq 13$, $-25 \leq k \leq 25$, $-15 \leq l \leq 16$
Reflections collected	13893
Independent reflections	13893 [R_{int} = ?, R_{sigma} = 0.0740]
Data/restraints/parameters	13893/14/714
Goodness-of-fit on F^2	1.056
Final R indexes [I>=2σ (I)]	R_1 = 0.0573, wR_2 = 0.1406
Final R indexes [all data]	R_1 = 0.0735, wR_2 = 0.1460
Largest diff. peak/hole / e Å^{-3}	0.31/-0.29
Flack parameter	0.1(2)
CCDC number	2063566

X-ray experimental for compound 2

Crystals of compound **2** grew as colorless blocks from the slow evaporation of a $CH_2Cl_2/CH_3CN/CH_3OH$ solution of receptor **2**. A suitable crystal was selected and the data were collected on an Agilent Technologies SuperNova Dual Source diffractometer using a μ-focus Cu Kα radiation source (λ = 1.5418 Å) with collimating mirror monochromators at 100 K using an Oxford Cryostream low temperature device. Details of the crystal data, data collection and structure refinement are listed in Table S7 and in the corresponding CIF file. Data collection, unit cell refinement and data reduction were performed using Agilent Technologies CrysAlisPro V 1.171.37.31.6.[11] Using Olex2,[12] the structure was solved with the ShelXT structure solution program using Direct Methods and refined with the ShelXL refinement package using least squares minimization.[13, 14] Tables of positional and thermal parameters, bond lengths and angles, torsion angles and figures are in the corresponding CIF file, which may be obtained from the Cambridge Crystallographic Data Centre; CCDC deposition number: 2063567.

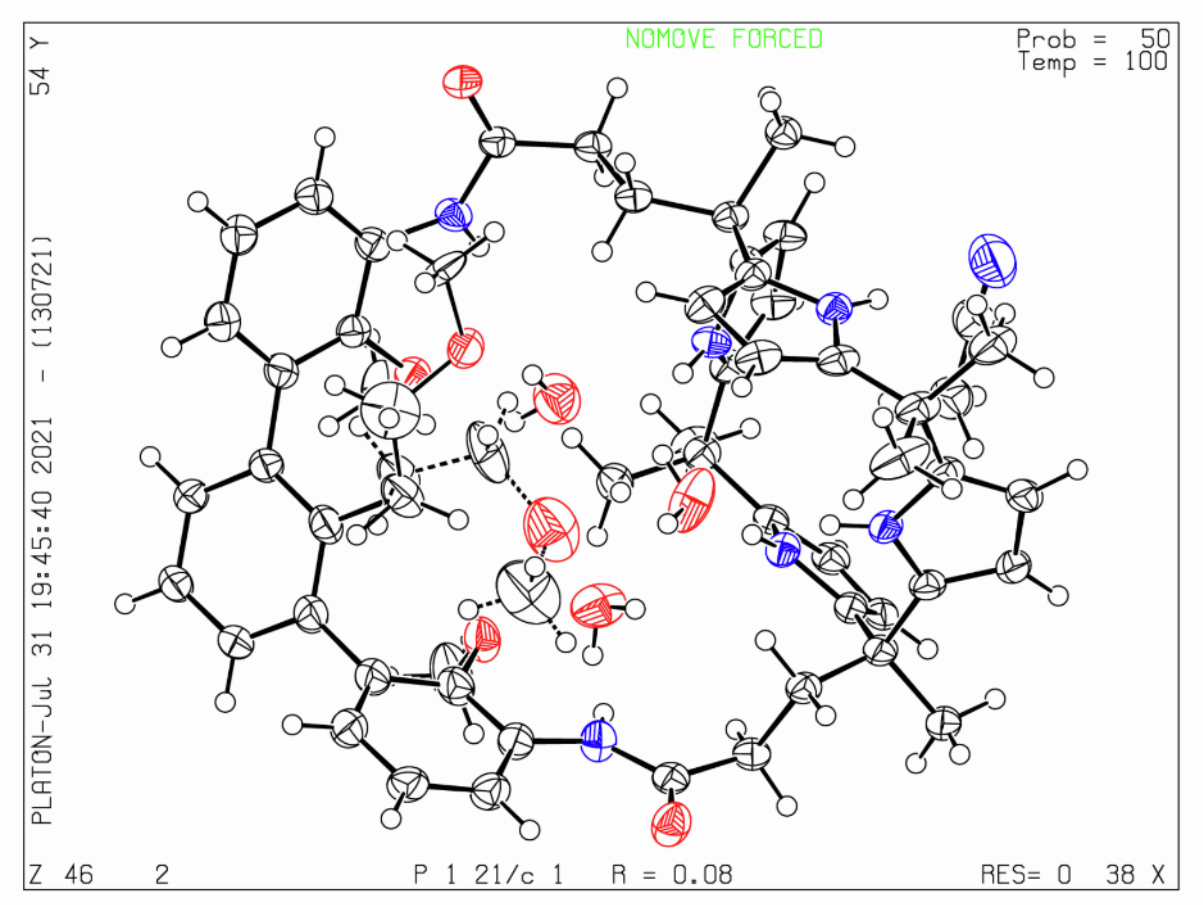

Figure S69. View of complex of **2**. Displacement ellipsoids are scaled to the 50% probability level.

Table 1 Crystal data and structure refinement for 2.

Identification code	2
Empirical formula	$C_{57}H_{69.56}N_7O_{8.28}$
Formula weight	985.23
Temperature/K	100.01(19)
Crystal system	monoclinic
Space group	$P2_1/c$
a/Å	18.9018(5)
b/Å	13.2365(3)
c/Å	21.1241(4)
α/°	90
β/°	90.1149(19)
γ/°	90
Volume/Å^3	5285.1(2)
Z	4
ρ_{calc}g/cm^3	1.238
μ/mm^{-1}	0.673
F(000)	2107.0
Crystal size/mm^3	0.25 × 0.15 × 0.054
Radiation	Cu Kα (λ = 1.54184)
2Θ range for data collection/°	4.674 to 136.466
Index ranges	$-22 \le h \le 22$, $-15 \le k \le 11$, $-24 \le l \le 25$
Reflections collected	25867
Independent reflections	9453 [R_{int} = 0.0555, R_{sigma} = 0.0628]
Data/restraints/parameters	9453/630/708
Goodness-of-fit on F^2	1.220
Final R indexes [I>=2σ (I)]	R_1 = 0.0767, wR_2 = 0.1989
Final R indexes [all data]	R_1 = 0.1060, wR_2 = 0.2199
Largest diff. peak/hole / e Å^{-3}	1.02/-0.46

Table S7 Crystal data and structure refinement for 2.

Identification code	**2**
Empirical formula	$C_{57}H_{69.56}N_7O_{8.28}$
Formula weight	985.23
Temperature/K	100.01(19)
Crystal system	monoclinic
Space group	$P2_1/c$
a/Å	18.9018(5)
b/Å	13.2365(3)
c/Å	21.1241(4)
α/°	90
β/°	90.1149(19)
γ/°	90

Volume/Å^3	5285.1(2)
Z	4
ρ_{calc}g/cm^3	1.238
μ/mm^{-1}	0.673
F(000)	2107.0
Crystal size/mm^3	0.25 × 0.15 × 0.054
Radiation	Cu Kα (λ = 1.54184 Å)
2Θ range for data collection/°	4.674 to 136.466
Index ranges	-22 ≤ h ≤ 22, -15 ≤ k ≤ 11, -24 ≤ l ≤ 25
Reflections collected	25867
Independent reflections	9453 [R_{int} = 0.0555, R_{sigma} = 0.0628]
Data/restraints/parameters	9453/630/708
Goodness-of-fit on F^2	1.220
Final R indexes [I>=2σ (I)]	R_1 = 0.0767, wR_2 = 0.1989
Final R indexes [all data]	R_1 = 0.1060, wR_2 = 0.2199
Largest diff. peak/hole / e Å^{-3}	1.02/-0.46
CCDC	2063567

X-ray experimental for 1·NaCl

Crystals of the complex **1**·NaCl grew as colorless blocks via the slow evaporation of a $CH_2Cl_2/CH_3CN/CH_3OH$ solution of receptor **1** in the presence of NaCl. A suitable crystal was selected and the data were collected on an Agilent Technologies SuperNova Dual Source diffractometer using a μ-focus Cu Kα radiation source (λ = 1.5418 Å) with collimating mirror monochromators at 100 K using an Oxford Cryostream low temperature device. Details of the crystal data, data collection and structure refinement are listed in Table S8 and in the corresponding CIF file. Data collection, unit cell refinement and data reduction were performed using Agilent Technologies CrysAlisPro V 1.171.37.31.6.[11] Using Olex2,[12] the structure was solved with the ShelXT structure solution program using Direct Methods and refined with the ShelXL refinement package using least squares minimization.[13, 14] Tables of positional and thermal parameters, bond lengths and angles, torsion angles and figures are in the corresponding CIF file, which may be obtained from the Cambridge Crystallographic Data Centre; CCDC deposition number: 2063568.

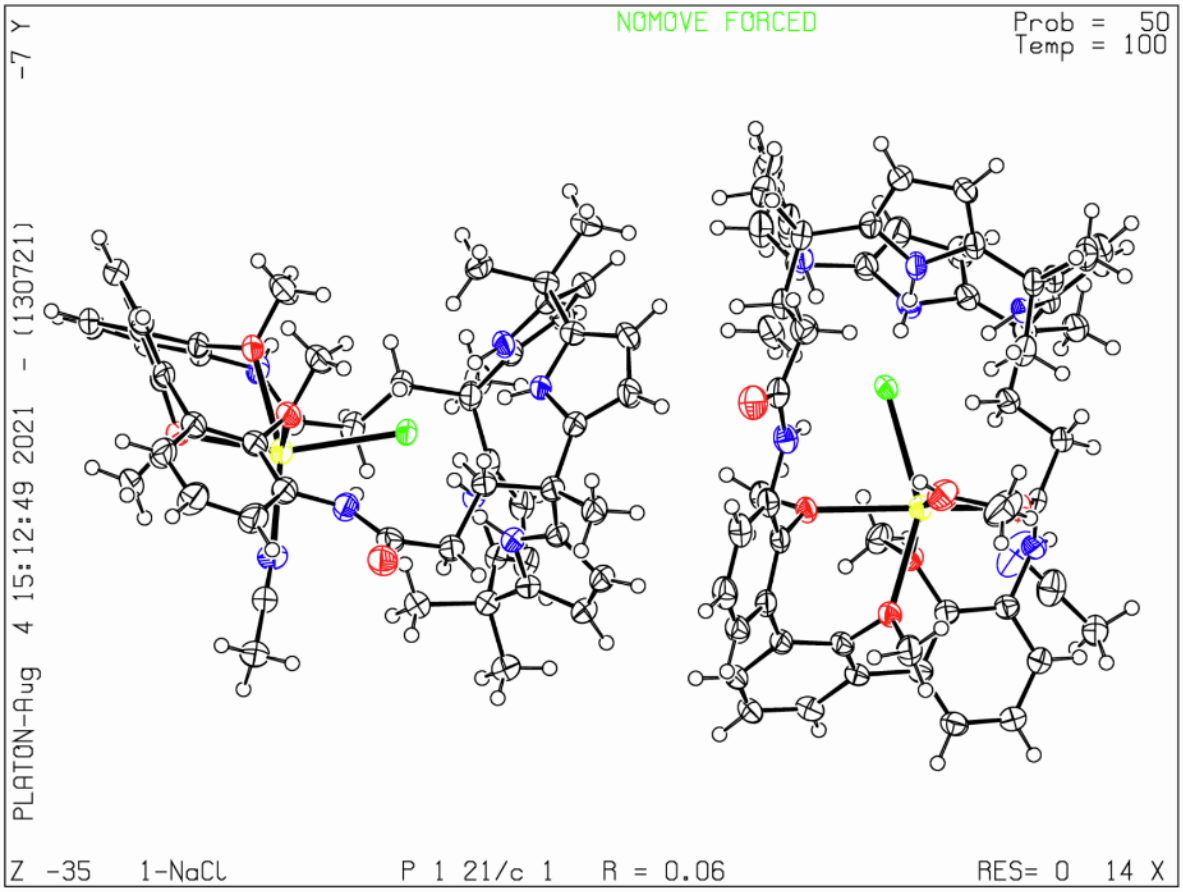

Figure S70. View of complex of **1·NaCl**. Displacement ellipsoids are scaled to the 50% probability level.

Table S8 Crystal data and structure refinement for 1-NaCl.

Identification code	**1**-NaCl
Empirical formula	$C_{111}H_{126}Cl_2N_{14}Na_2O_{11}$
Formula weight	1949.13
Temperature/K	100(2)
Crystal system	monoclinic
Space group	$P2_1/c$
a/Å	18.2277(3)
b/Å	28.2330(6)
c/Å	20.0705(6)
α/°	90
β/°	91.270(2)
γ/°	90
Volume/Å^3	10326.2(4)
Z	4
ρ_{calc}g/cm^3	1.254
μ/mm^{-1}	1.185
F(000)	4136.0
Crystal size/mm^3	0.168 × 0.147 × 0.114
Radiation	CuKα (λ = 1.54184 Å)
2Θ range for data collection/°	4.85 to 147.796
Index ranges	$-22 \leq h \leq 22$, $-34 \leq k \leq 35$, $-22 \leq l \leq 24$
Reflections collected	98683
Independent reflections	20463 [R_{int} = 0.0691, R_{sigma} = 0.0544]
Data/restraints/parameters	20463/3/1285
Goodness-of-fit on F^2	1.035
Final R indexes [I>=2σ (I)]	R_1 = 0.0605, wR_2 = 0.1388
Final R indexes [all data]	R_1 = 0.0904, wR_2 = 0.1544
Largest diff. peak/hole / e Å^{-3}	0.56/-0.49
CCDC number	2063568

X-ray experimental for 1·KCl

Crystals of the complex **1**·KCl grew as colorless blocks via the slow evaporation of a $CH_2Cl_2/CH_3CN/CH_3OH$ solution of receptor **1** in the presence of KCl. A suitable crystal was selected and the data were collected on an Agilent Technologies SuperNova Dual Source diffractometer using a μ-focus Cu Kα radiation source (λ = 1.5418 Å) with collimating mirror monochromators at 100 K using an Oxford Cryostream low temperature device. Details of the crystal data, data collection and structure refinement are listed in Table S9 and in the corresponding CIF file. Data collection, unit cell refinement and data reduction were performed using Agilent Technologies CrysAlisPro V 1.171.37.31.6.[11] Using Olex2,[12] the structure was solved with the ShelXT structure solution program using Direct Methods and refined with the ShelXL refinement package using least squares minimization.[13, 14] Tables of positional and thermal parameters, bond lengths and angles, torsion angles and figures are in the corresponding CIF file, which may be obtained from the Cambridge Crystallographic Data Centre; CCDC deposition number: 2063569.

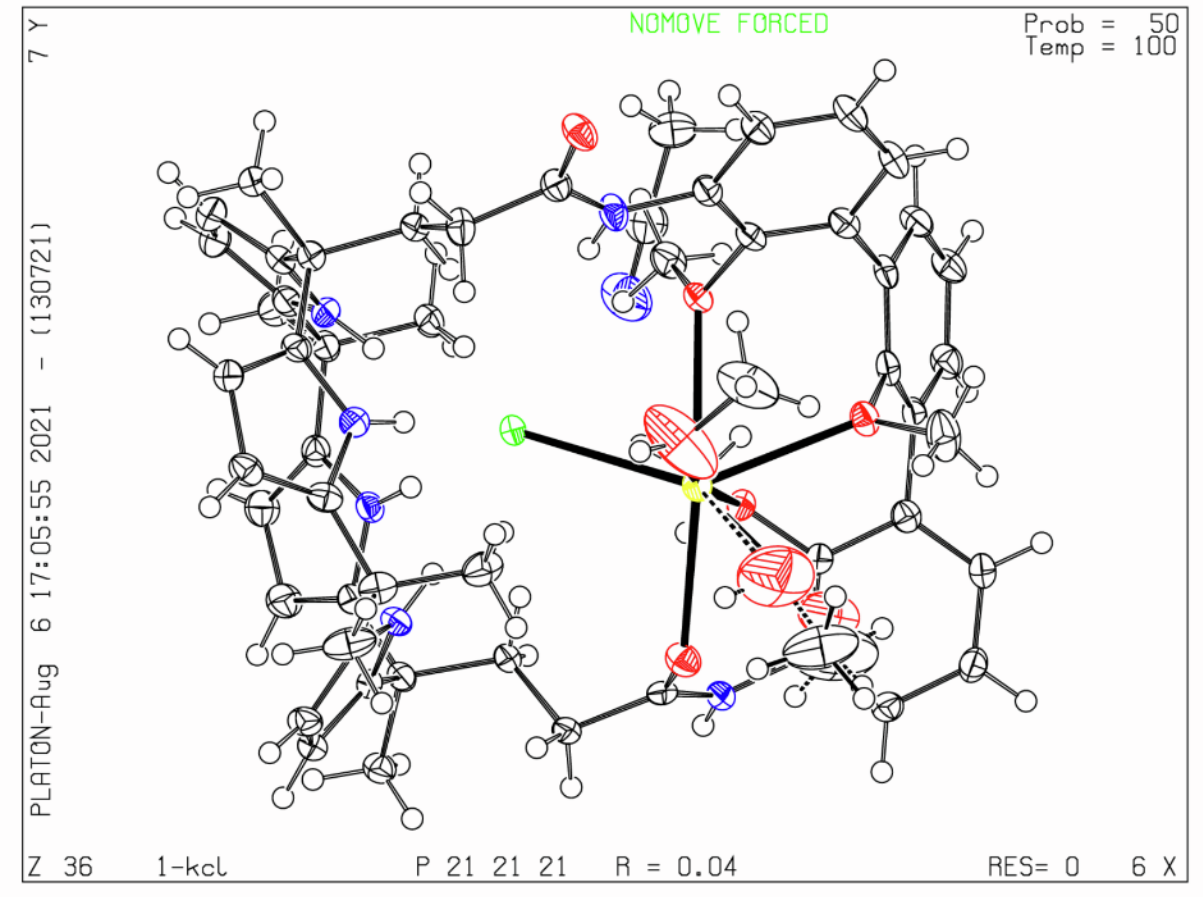

Figure S71. View of complex of **1**·KCl. Displacement ellipsoids are scaled to the 50% probability level.

Table 1 Crystal data and structure refinement for 1-KCl.

Identification code	1-KCl
Empirical formula	$C_{57}H_{69}ClKN_7O_7$
Formula weight	1038.74
Temperature/K	100.02(12)
Crystal system	orthorhombic
Space group	$P2_12_12_1$
a/Å	14.90813(17)
b/Å	18.24827(19)
c/Å	19.8943(2)
α/°	90
β/°	90
γ/°	90
Volume/Å^3	5412.20(10)
Z	4
ρ_{calc}g/cm^3	1.275
μ/mm^{-1}	1.785
F(000)	2208.0
Crystal size/mm^3	0.181 × 0.098 × 0.051
Radiation	Cu Kα (λ = 1.54184)
2Θ range for data collection/°	6.572 to 146.988
Index ranges	-16 ≤ h ≤ 18, -22 ≤ k ≤ 21, -24 ≤ l ≤ 24
Reflections collected	62127
Independent reflections	10756 [R_{int} = 0.0256, R_{sigma} = 0.0157]
Data/restraints/parameters	10756/74/696
Goodness-of-fit on F^2	1.077
Final R indexes [I>=2σ (I)]	R_1 = 0.0362, wR_2 = 0.0973
Final R indexes [all data]	R_1 = 0.0369, wR_2 = 0.0979
Largest diff. peak/hole / e Å^{-3}	0.73/-0.41
Flack parameter	0.005(2)

Table S9 Crystal data and structure refinement for 1-KCl.

Identification code	**1**-KCl
Empirical formula	$C_{57}H_{69}ClKN_7O_7$
Formula weight	1038.74
Temperature/K	100.02(12)
Crystal system	orthorhombic
Space group	$P2_12_12_1$

a/Å	14.90813(17)
b/Å	18.24827(19)
c/Å	19.8943(2)
α/°	90
β/°	90
γ/°	90
Volume/Å^3	5412.20(10)
Z	4
ρ_{calc}g/cm^3	1.275
μ/mm^{-1}	1.785
F(000)	2208.0
Crystal size/mm^3	0.181 × 0.098 × 0.051
Radiation	Cu Kα (λ = 1.54184 Å)
2Θ range for data collection/°	6.572 to 146.988
Index ranges	-16 ≤ h ≤ 18, -22 ≤ k ≤ 21, -24 ≤ l ≤ 24
Reflections collected	62127
Independent reflections	10756 [R_{int} = 0.0256, R_{sigma} = 0.0157]
Data/restraints/parameters	10756/74/696
Goodness-of-fit on F^2	1.077
Final R indexes [I>=2σ (I)]	R_1 = 0.0362, wR_2 = 0.0973
Final R indexes [all data]	R_1 = 0.0369, wR_2 = 0.0979
Largest diff. peak/hole / e Å^{-3}	0.73/-0.41
Flack parameter	0.005(2)
CCDC number	2063569

X-ray experimental for 2·NaCl

Crystals of the complex **2**·NaCl grew as colorless blocks via the slow evaporation of a $CH_2Cl_2/CH_3CN/CH_3OH$ solution of receptor **2** in the presence of NaCl. A suitable crystal was selected and the data were collected on an Agilent Technologies SuperNova Dual Source diffractometer using a μ-focus Cu Kα radiation source (λ = 1.5418 Å) with collimating mirror monochromators at 100 K using an Oxford Cryostream low temperature device. Details of the crystal data, data collection and structure refinement are listed in Table S10 and in the corresponding CIF file. Data collection, unit cell refinement and data reduction were performed using Agilent Technologies CrysAlisPro V 1.171.37.31.6.[11] Using Olex2,[12] the structure was solved with the ShelXT structure solution program using Direct Methods and refined with the ShelXL refinement package using least squares minimization.[13, 14] Tables of positional and thermal parameters, bond lengths and angles, torsion angles and figures are in the corresponding CIF file, which may be obtained from the Cambridge Crystallographic Data Centre; CCDC deposition number: 2063570.

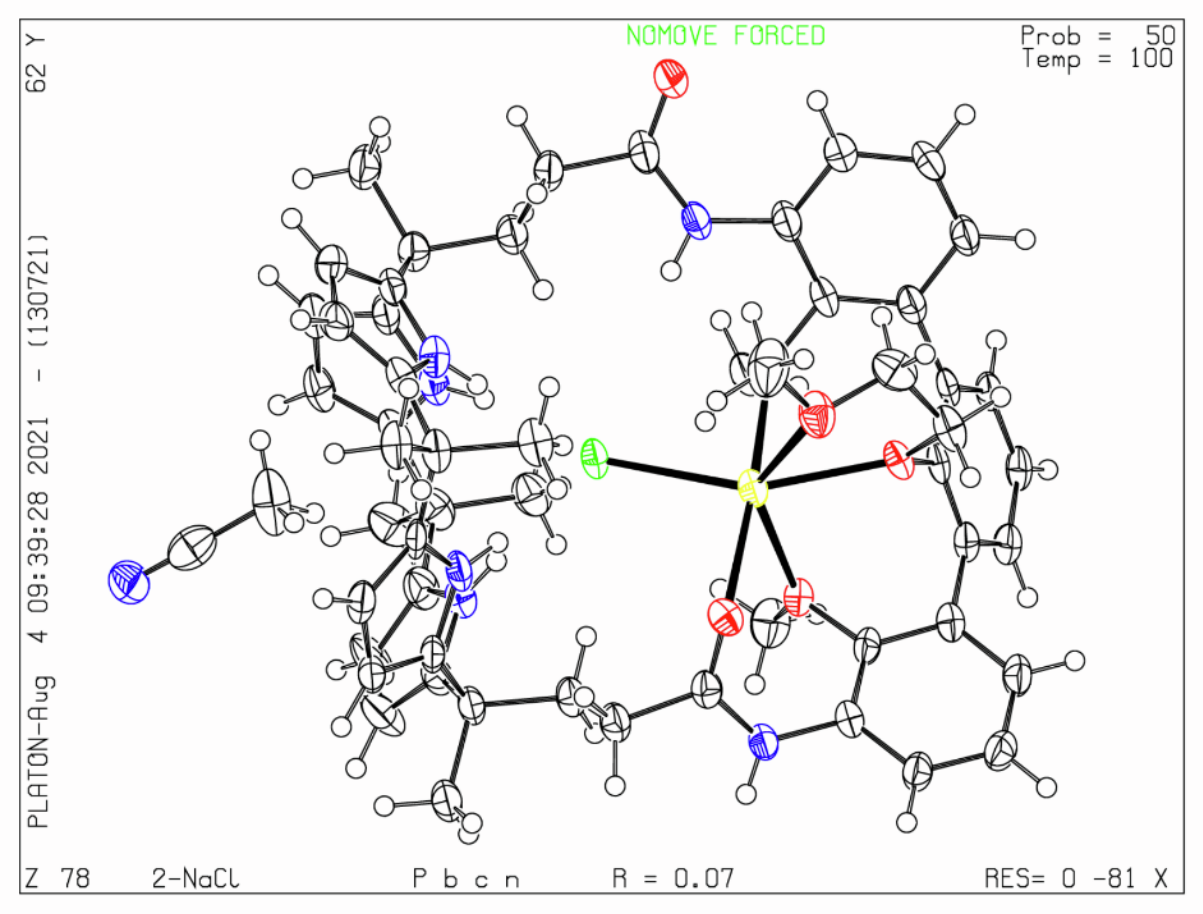

Figure S72. View of complex of **2**·NaCl. Displacement ellipsoids are scaled to the 50% probability level.

Table S10 Crystal data and structure refinement for 2-NaCl.

Identification code	**2**-NaCl
Empirical formula	$C_{48}H_{58}N_8O_5NaCl$
Formula weight	885.46
Temperature/K	100.02(11)
Crystal system	orthorhombic
Space group	Pbcn
a/Å	17.9030(5)
b/Å	23.0933(6)
c/Å	26.5693(7)
α/°	90
β/°	90
γ/°	90
Volume/Å^3	10984.8(5)
Z	10
ρ_{calc}g/cm^3	1.339
μ/mm^{-1}	1.332
F(000)	4700.0
Crystal size/mm^3	0.232 × 0.076 × 0.031
Radiation	Cu Kα (λ = 1.54184 Å)
2Θ range for data collection/°	7.656 to 136.5
Index ranges	-21 ≤ h ≤ 13, -19 ≤ k ≤ 27, -21 ≤ l ≤ 31
Reflections collected	31212
Independent reflections	10007 [R_{int} = 0.0996, R_{sigma} = 0.1143]
Data/restraints/parameters	10007/0/659
Goodness-of-fit on F^2	1.048
Final R indexes [I>=2σ (I)]	R_1 = 0.0744, wR_2 = 0.1567
Final R indexes [all data]	R_1 = 0.1250, wR_2 = 0.1876
Largest diff. peak/hole / e Å^{-3}	0.60/-0.30
CCDC number	2063570

X-ray experimental for 2·KCl

Crystals of the complex **2**·KCl grew as colorless blocks by the slow evaporation of a $CH_2Cl_2/CH_3CN/CH_3OH$ solution of receptor **2** in the presence of KCl. A suitable crystal was selected and the data were collected on a Rigaku AFC12 diffractometer with a Saturn 724+ CCD with MoKα irradiation (λ = 0.71073 Å). The crystal was kept at 100.15 K during data collection. Using Olex2,[12] the structure was solved with the ShelXT structure solution program using Direct Methods and refined with the ShelXL refinement package using least squares minimization.[13, 14] Tables of positional and thermal parameters, bond lengths and angles, torsion angles and figures are in the corresponding CIF file, which may be obtained from the Cambridge Crystallographic Data Centre; CCDC deposition number: 2063571.

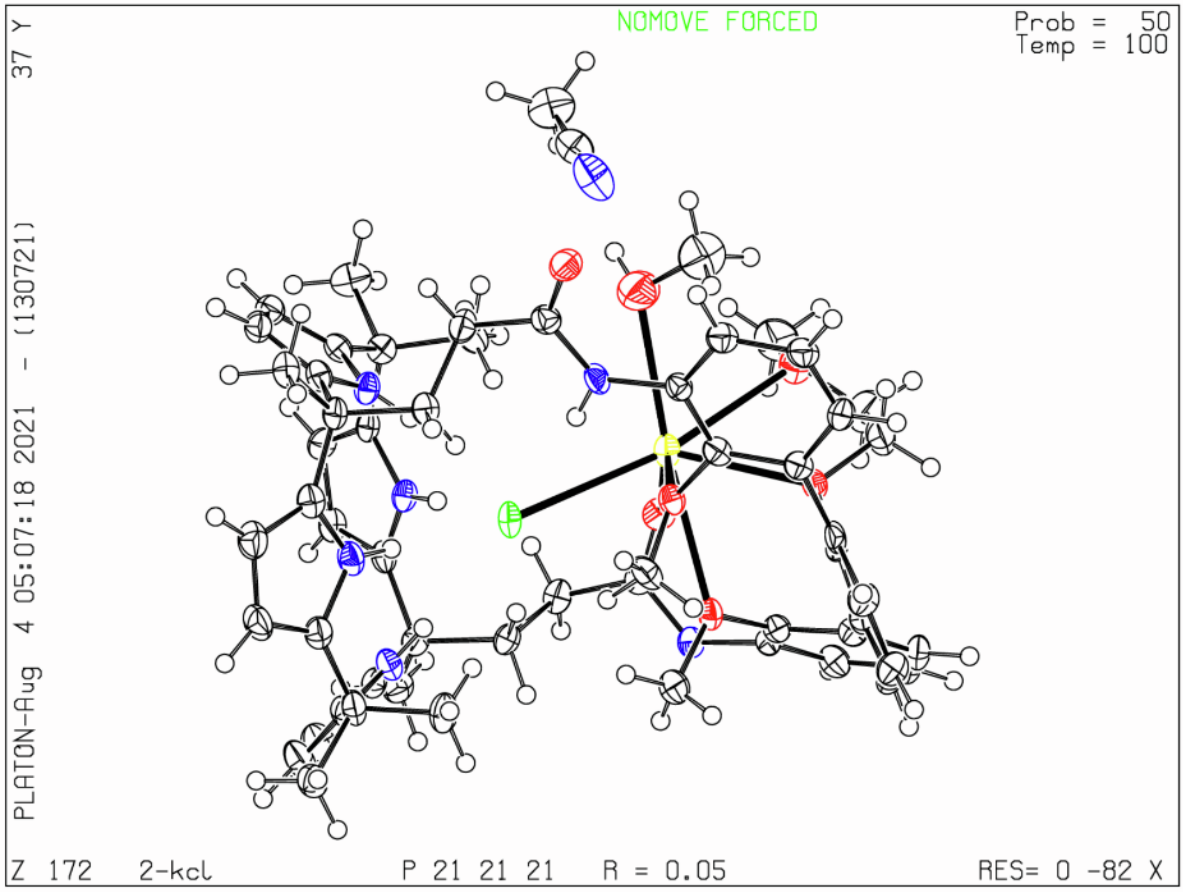

Figure S73. View of complex of **2**·KCl. Displacement ellipsoids are scaled to the 50% probability level.

Table S11 Crystal data and structure refinement for 2-KCl.

Identification code	**2**-KCl
Empirical formula	$C_{58}H_{69}ClKN_7O_7$
Formula weight	1050.75
Temperature/K	100.15
Crystal system	orthorhombic
Space group	$P2_12_12_1$
a/Å	14.9323(16)
b/Å	18.2620(19)
c/Å	19.934(2)
α/°	90
β/°	90
γ/°	90
Volume/Å^3	5435.9(10)
Z	4
ρ_{calc}g/cm^3	1.284
μ/mm^{-1}	0.206
F(000)	2232.0
Crystal size/mm^3	0.096 × 0.088 × 0.085
Radiation	MoKα (λ = 0.71075 Å)
2Θ range for data collection/°	4.46 to 50.7
Index ranges	$-17 \leq h \leq 17$, $-21 \leq k \leq 21$, $-24 \leq l \leq 24$
Reflections collected	62736
Independent reflections	9912 [R_{int} = 0.0630, R_{sigma} = 0.0493]
Data/restraints/parameters	9912/3/682
Goodness-of-fit on F^2	1.048
Final R indexes [I>=2σ (I)]	R_1 = 0.0504, wR_2 = 0.1076
Final R indexes [all data]	R_1 = 0.0630, wR_2 = 0.1125
Largest diff. peak/hole / e Å^{-3}	0.41/-0.21
Flack parameter	0.45(5)
CCDC number	2063571

7. HRMS Analyses and NMR Spectra

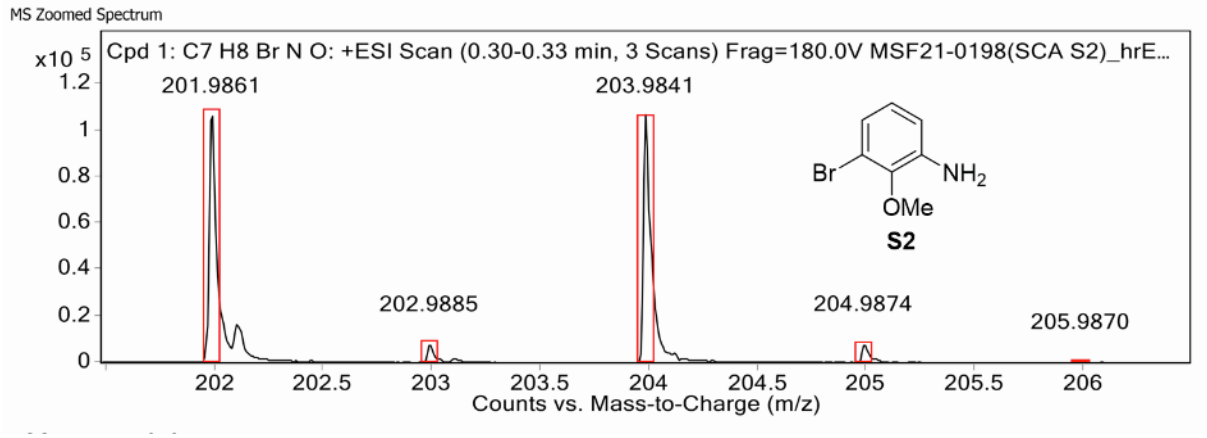

Figure S74. HRMS spectrum of compound S2

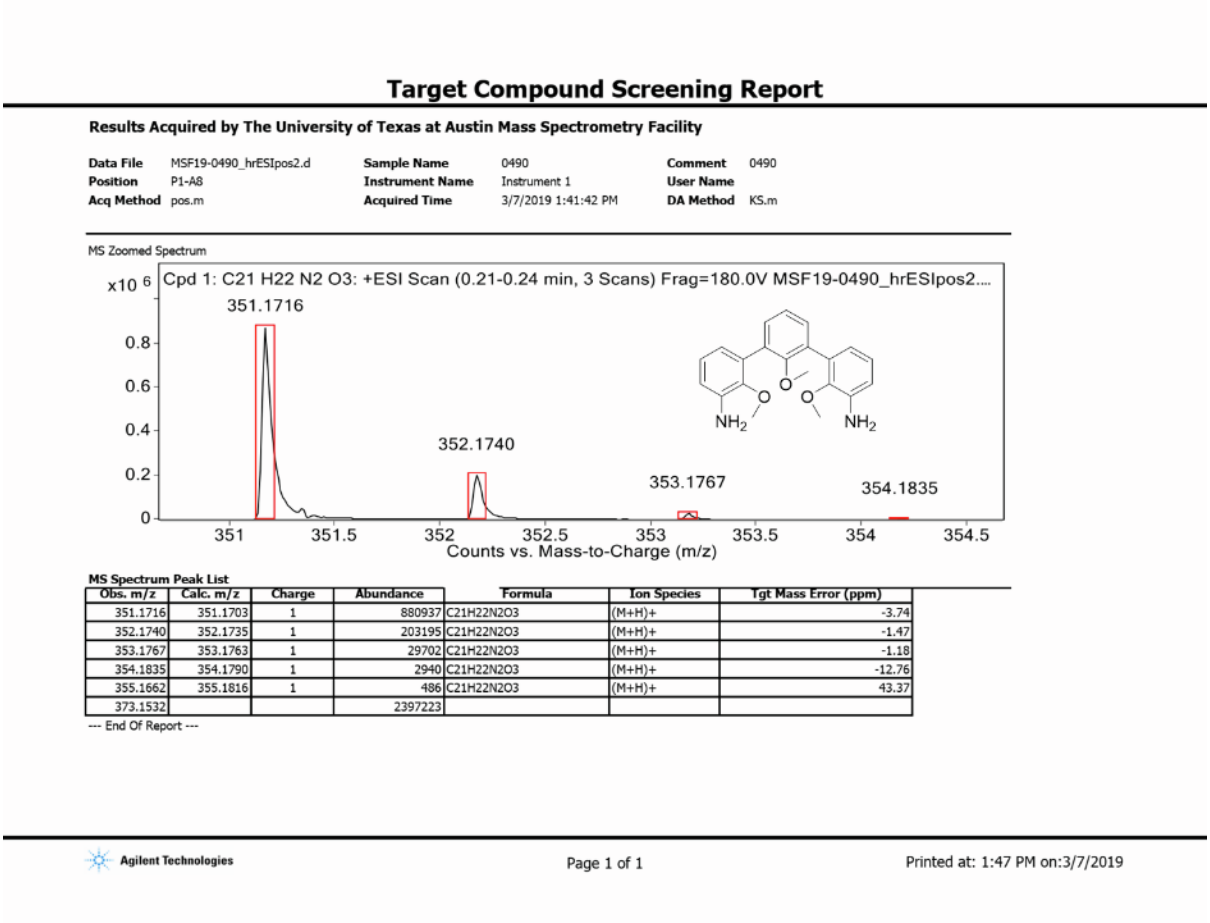

Target Compound Screening Report

Results Acquired by The University of Texas at Austin Mass Spectrometry Facility

Data File	MSF19-0490_hrESIpos2.d	**Sample Name**	0490	**Comment**	0490
Position	P1-A8	**Instrument Name**	Instrument 1	**User Name**	
Acq Method	pos.m	**Acquired Time**	3/7/2019 1:41:42 PM	**DA Method**	KS.m

MS Zoomed Spectrum

Cpd 1: C21 H22 N2 O3: +ESI Scan (0.21-0.24 min, 3 Scans) Frag=180.0V MSF19-0490_hrESIpos2....

x10 6 — 351.1716 — 352.1740 — 353.1767 — 354.1835

Counts vs. Mass-to-Charge (m/z)

MS Spectrum Peak List

Obs. m/z	Calc. m/z	Charge	Abundance	Formula	Ion Species	Tgt Mass Error (ppm)
351.1716	351.1703	1	880937	C21H22N2O3	(M+H)+	-3.74
352.1740	352.1735	1	203195	C21H22N2O3	(M+H)+	-1.47
353.1767	353.1763	1	29702	C21H22N2O3	(M+H)+	-1.18
354.1835	354.1790	1	2940	C21H22N2O3	(M+H)+	-12.76
355.1662	355.1816	1	486	C21H22N2O3	(M+H)+	43.37
373.1532			2397223			

--- End Of Report ---

Agilent Technologies — Page 1 of 1 — Printed at: 1:47 PM on:3/7/2019

Figure S75. HRMS analysis of compound S4

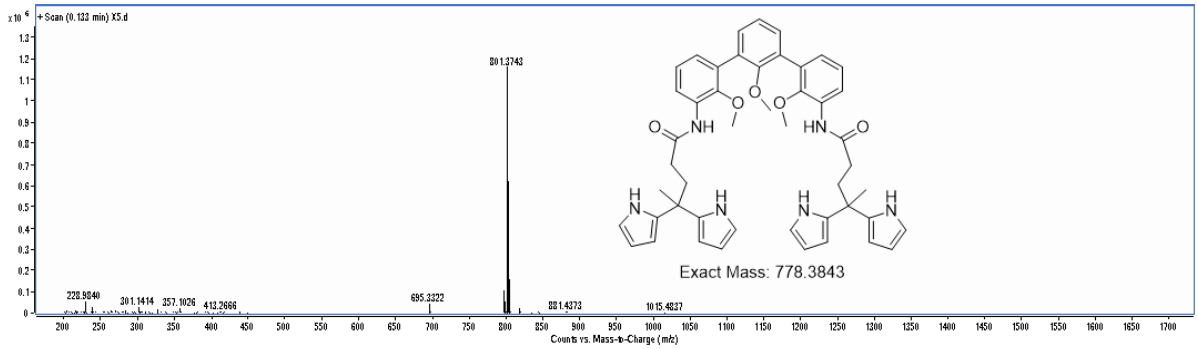

Figure S76. HRMS analysis of compound 4

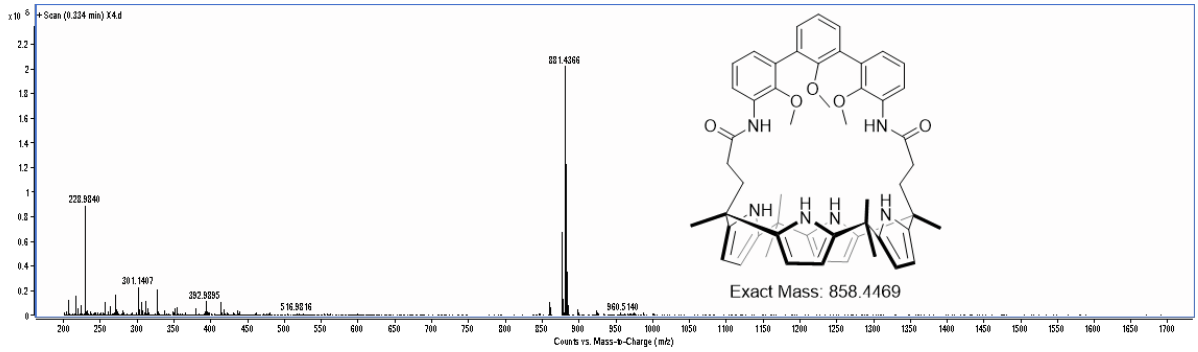

Figure S77. HRMS analysis of compound 1

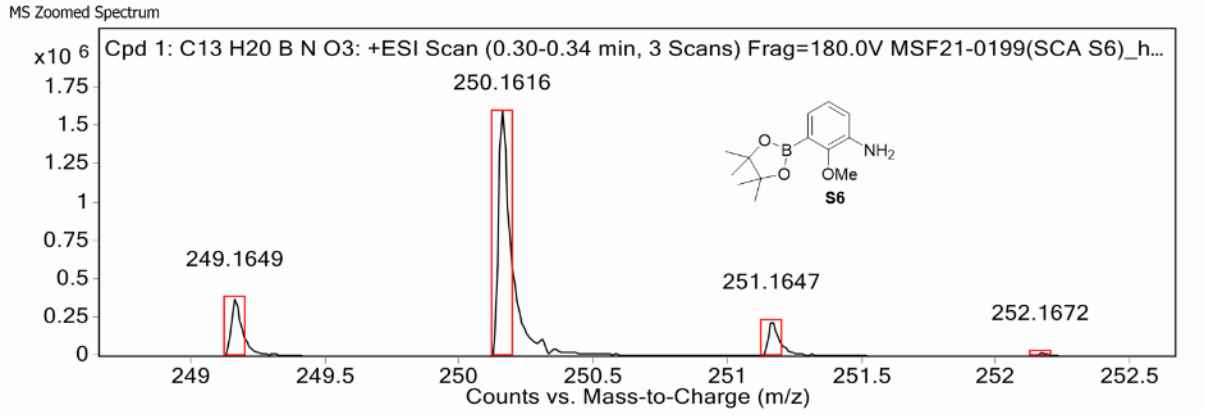

Figure S78. HRMS analysis of compound S6

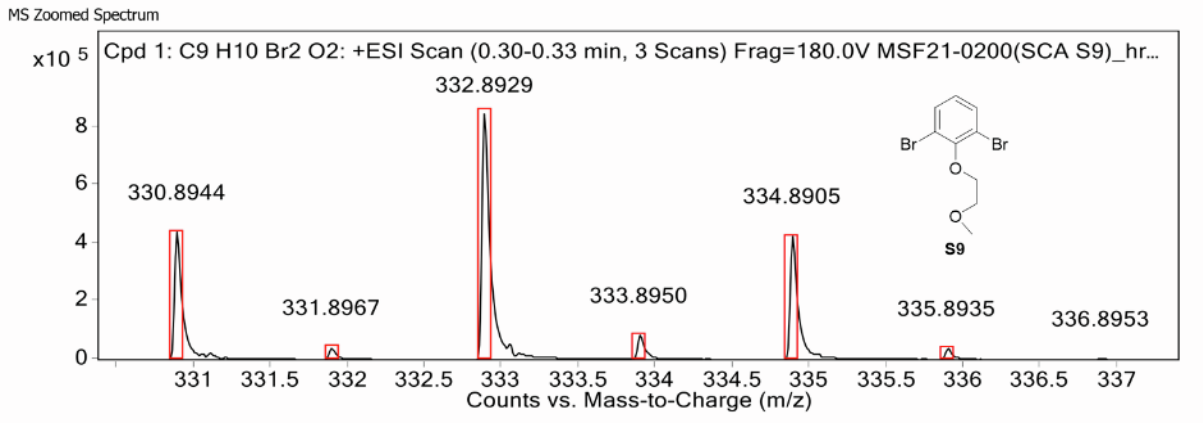

Figure S79. HRMS analysis of compound S9

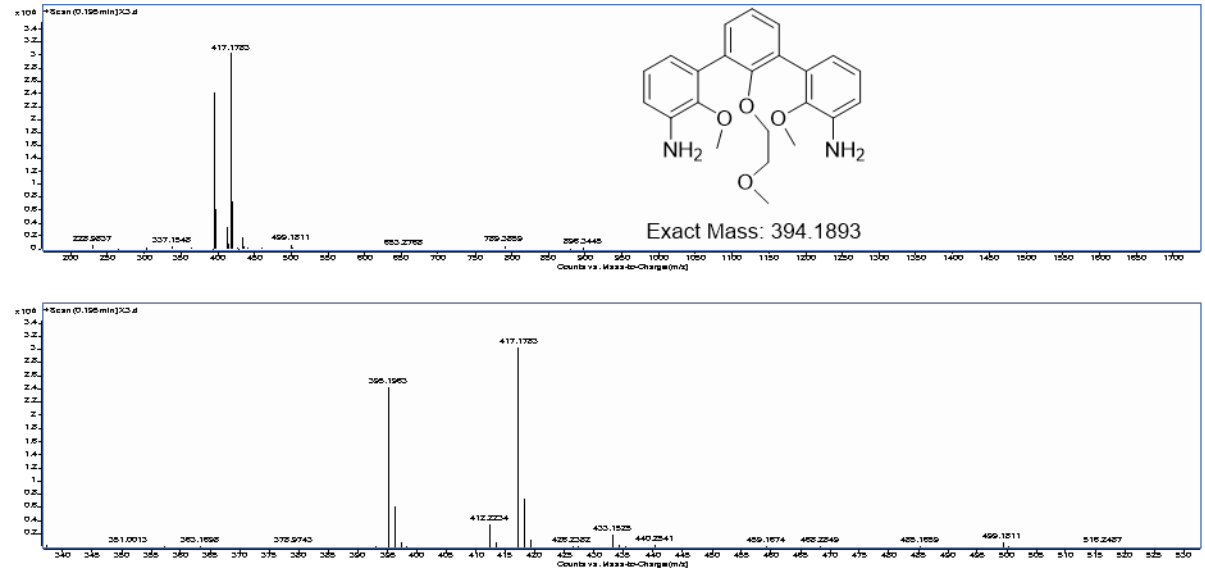

Figure S80. HRMS spectrum of compound S10

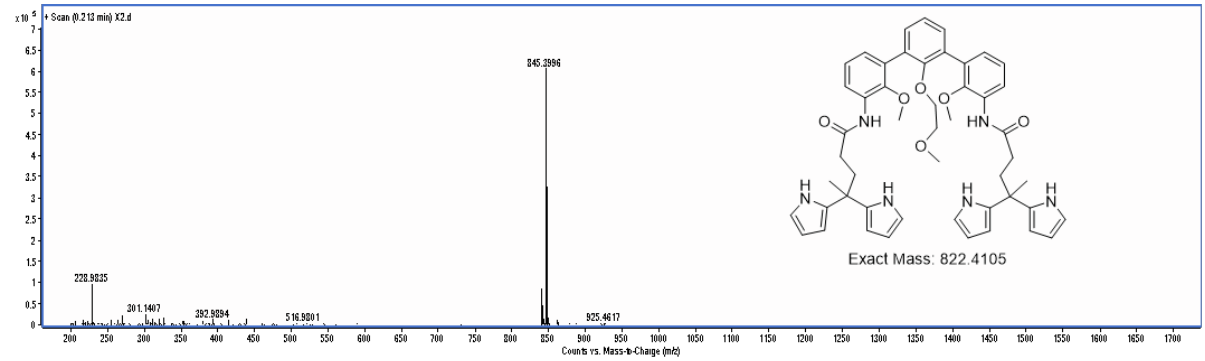

Figure S81. HRMS spectrum of compound S11

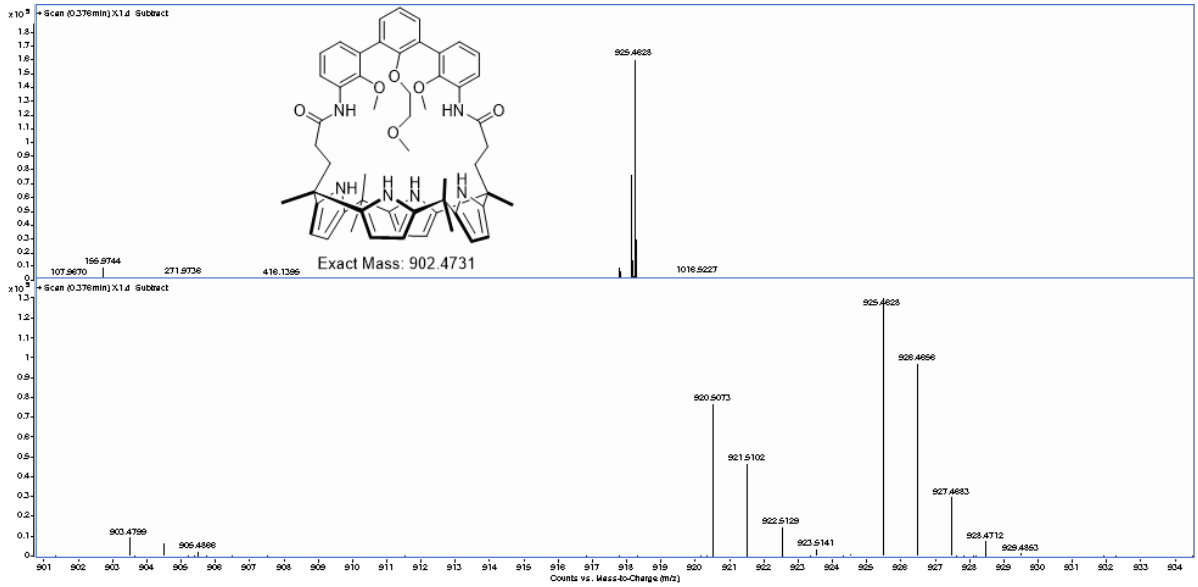

Figure S82. HRMS spectrum of compound 2

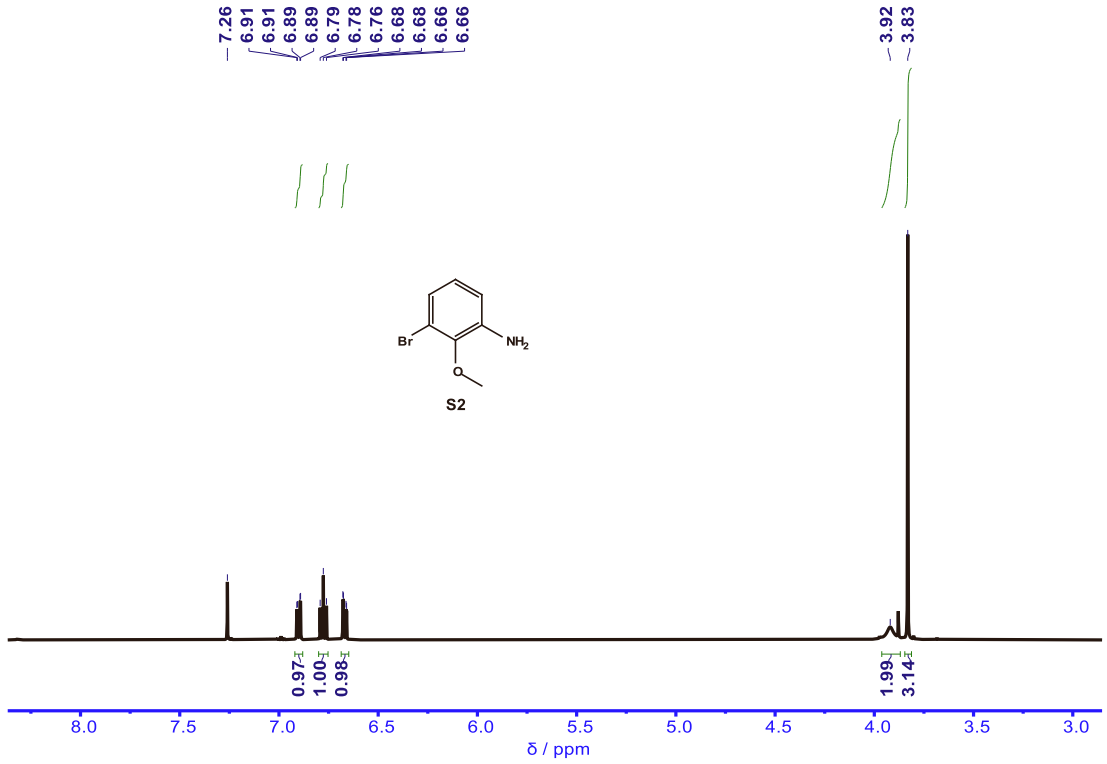

Figure S83. ^{1}H NMR spectrum of **S2** recorded in $CDCl_3$ at 298 K.

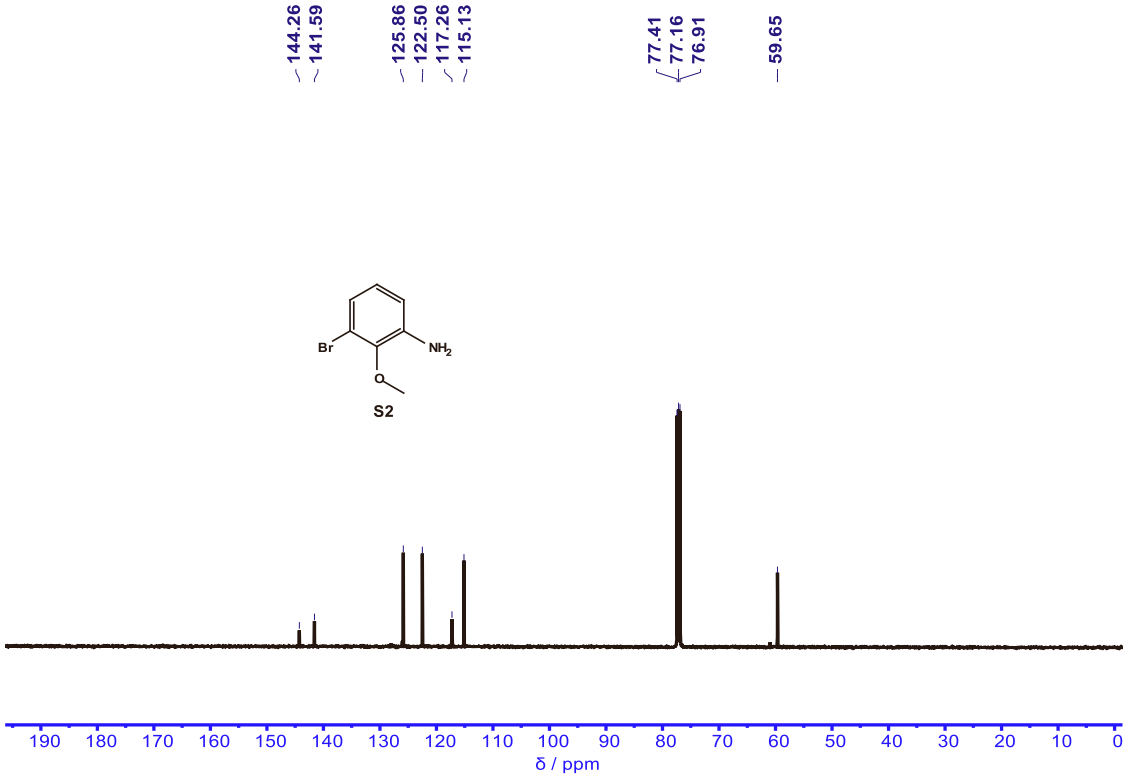

Figure S84. ^{13}C NMR spectrum of **S2** recorded in $CDCl_3$ at 298 K.

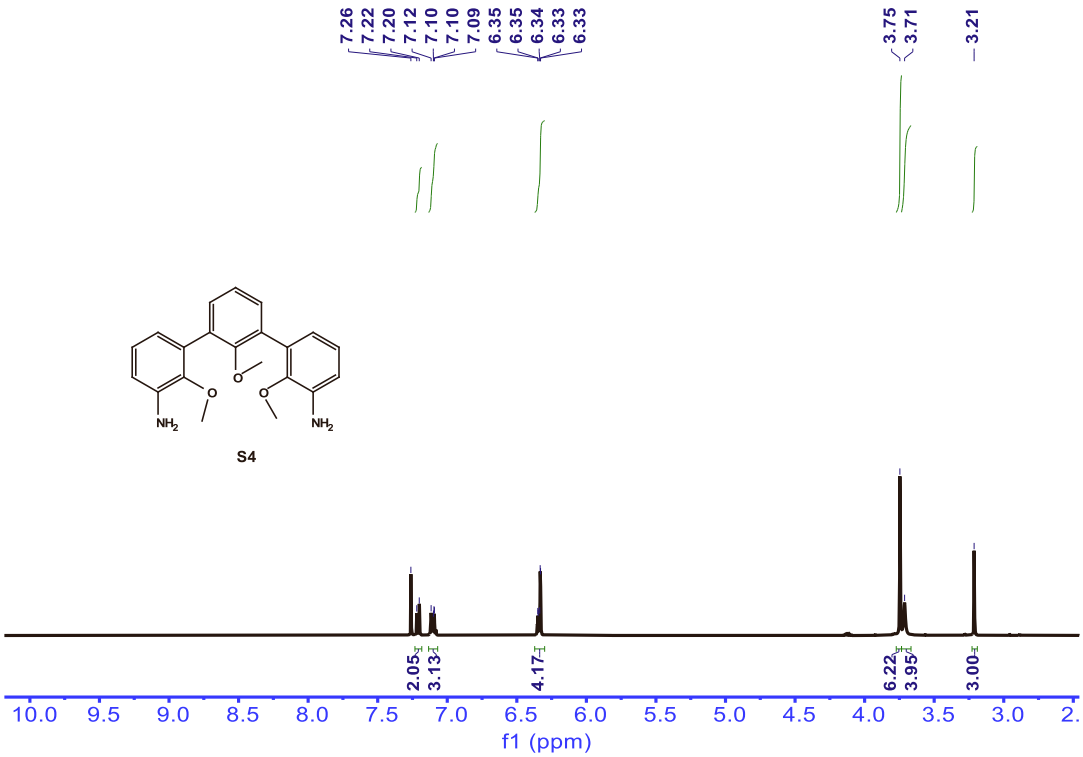

Figure S85. ^{1}H NMR spectrum of **S4** recorded in $CDCl_3$ at 298 K.

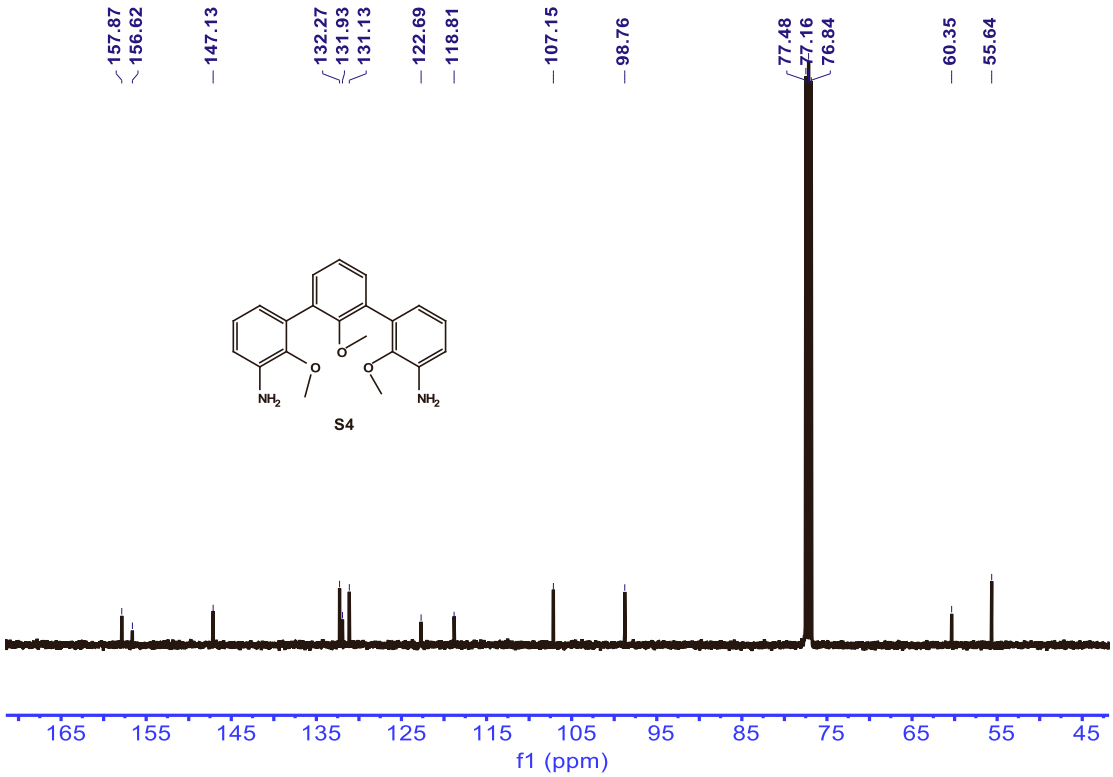

Figure S86. ^{13}C NMR spectrum of **S4** recorded in $CDCl_3$ at 298 K.

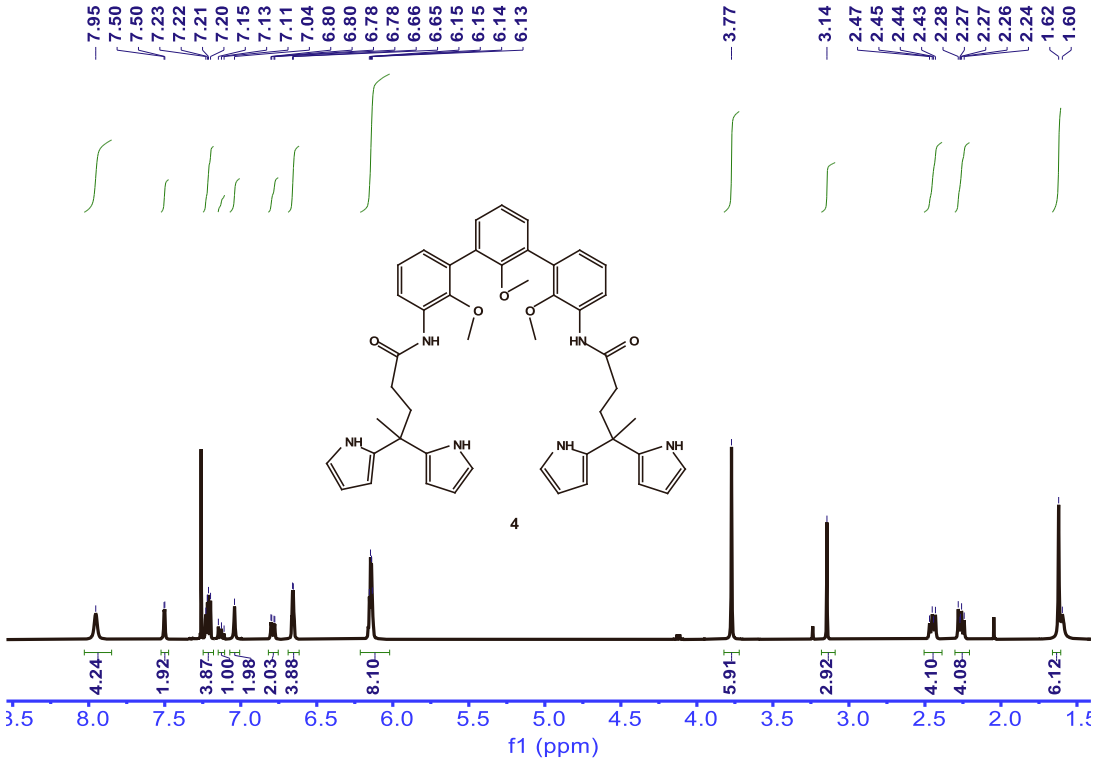

Figure S87. ^{1}H NMR spectrum of **4** recorded in $CDCl_3$ at 298 K.

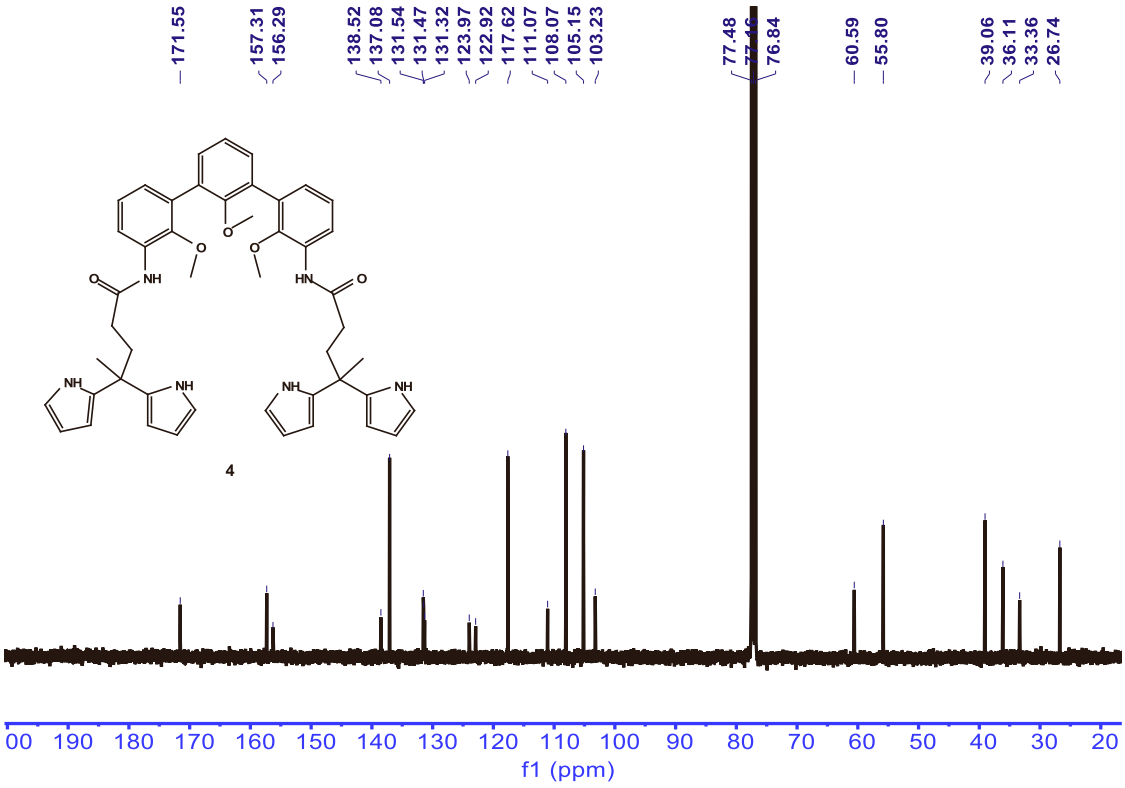

Figure S88. ^{13}C NMR spectrum of **4** recorded in $CDCl_3$ at 298 K.

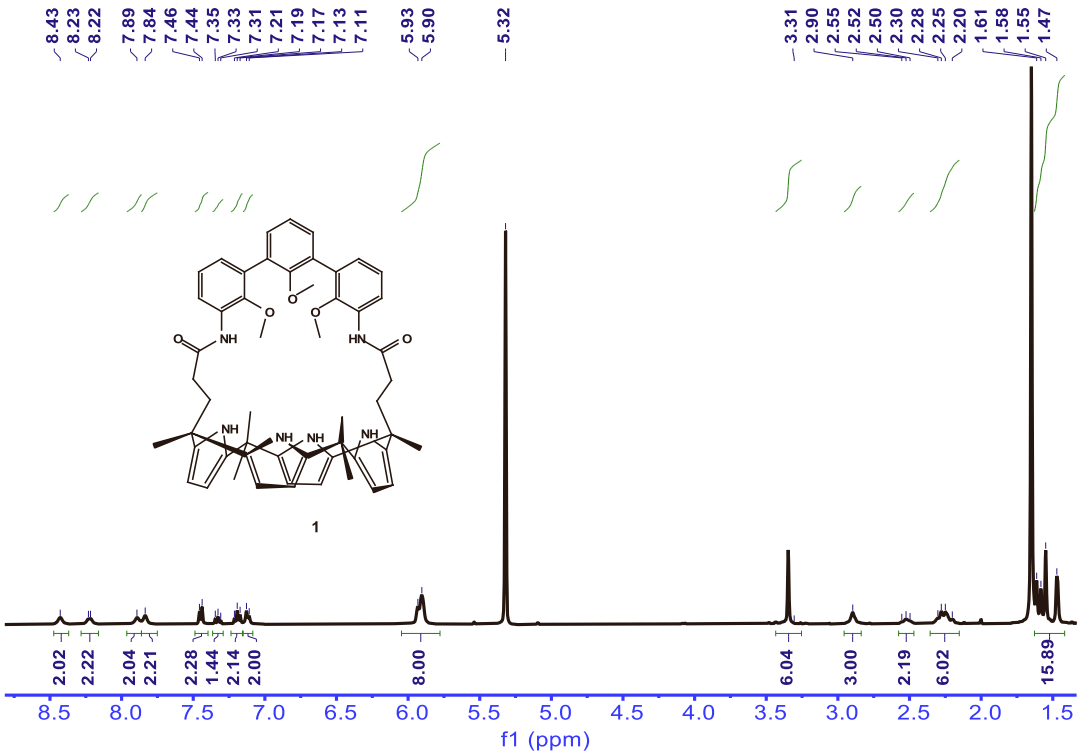

Figure S89. ^{1}H NMR spectrum of **1** recorded in CD_2Cl_2.

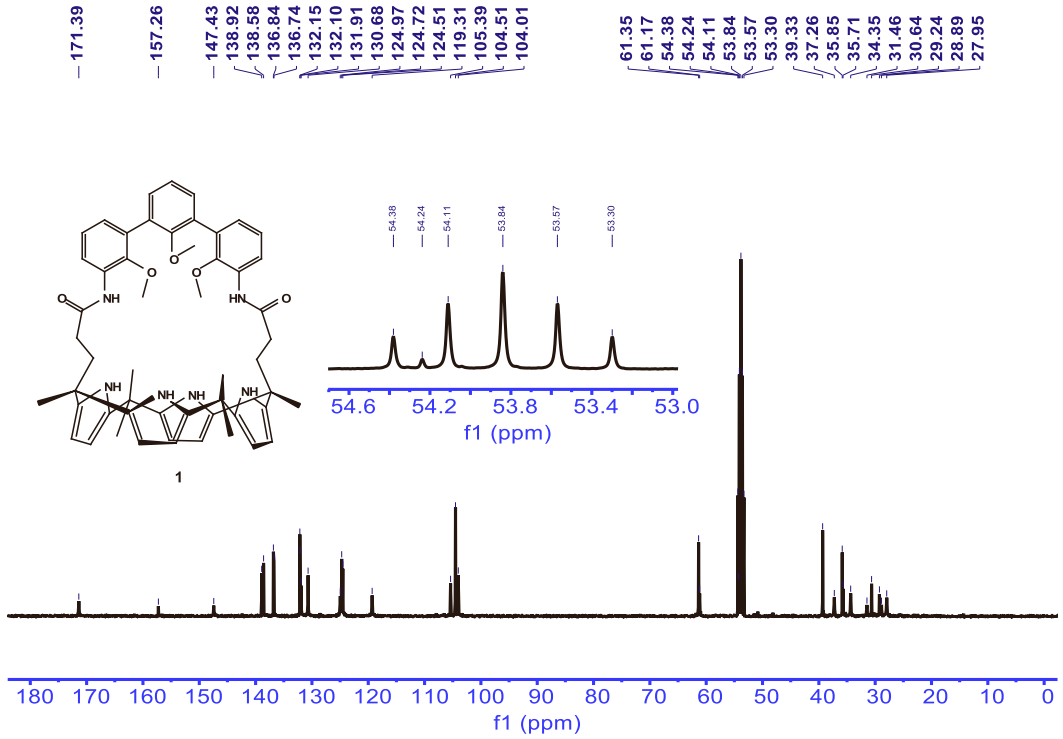

Figure S90. ^{13}C NMR spectrum of **1** recorded in CD_2Cl_2.

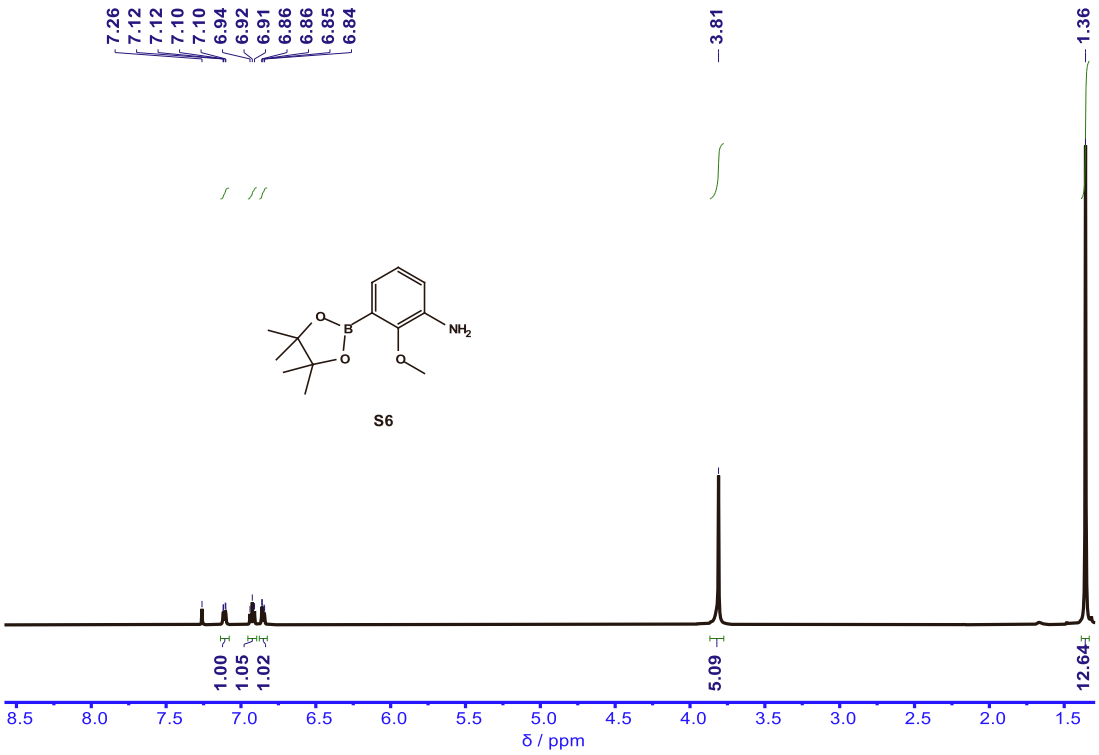

Figure S91. ^{1}H NMR spectrum of **S6** recorded in $CDCl_3$.

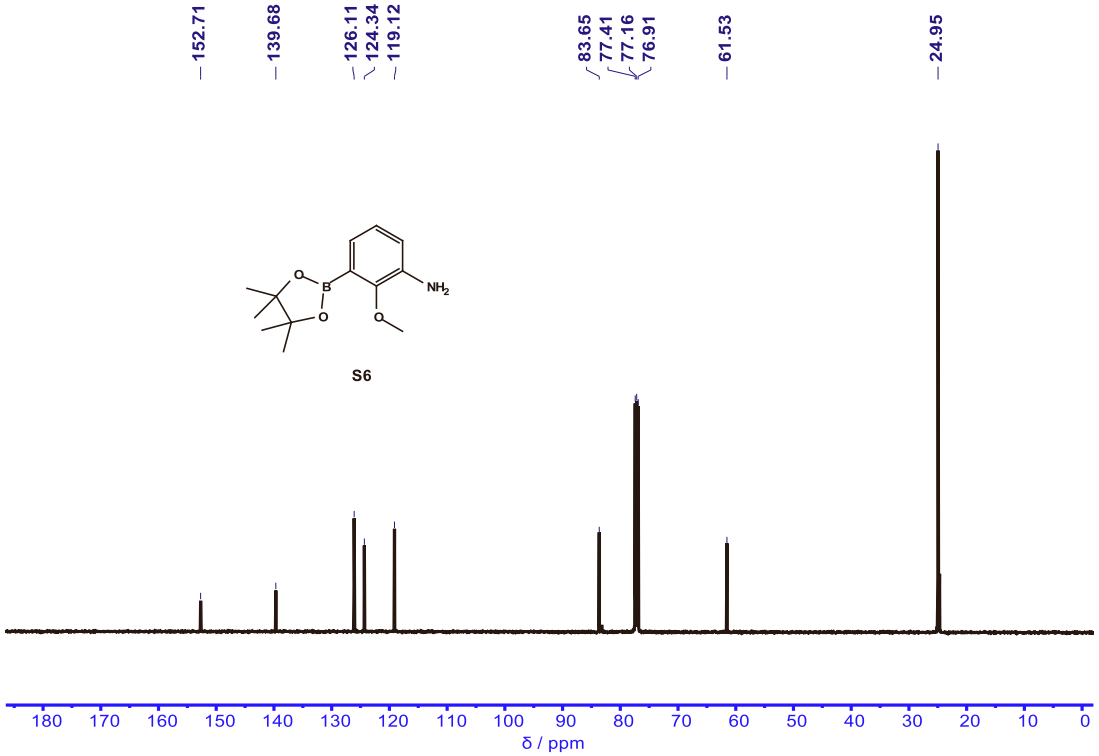

Figure S92. ^{13}C NMR spectrum of **S6** recorded in $CDCl_3$.

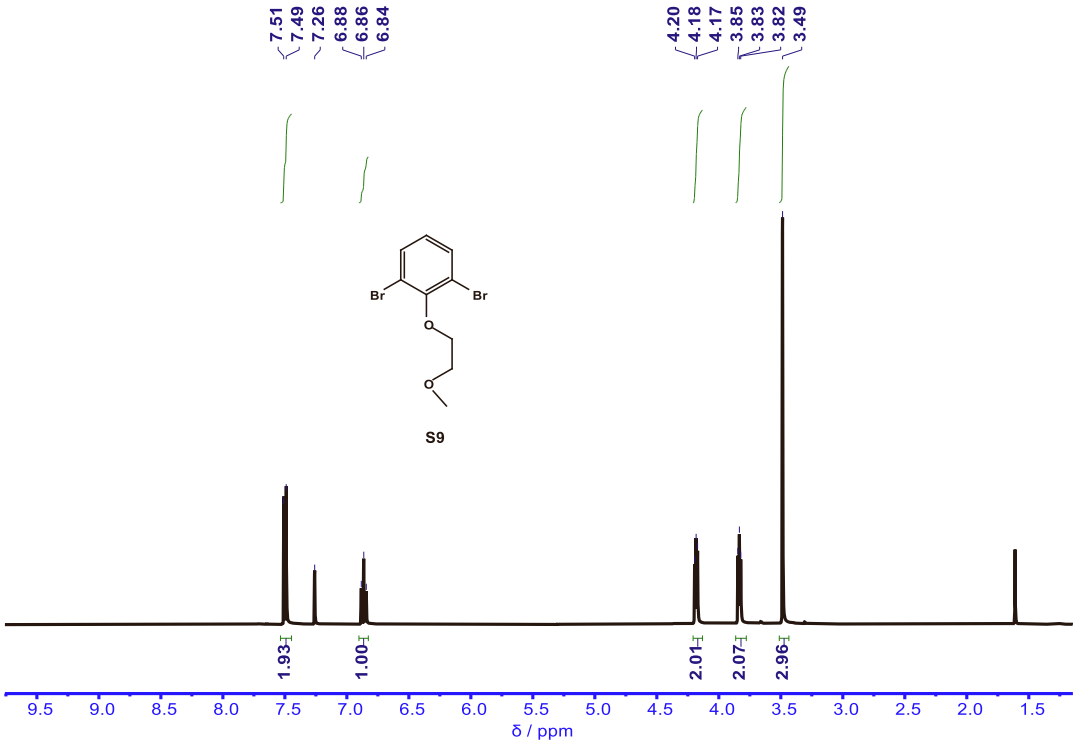

Figure S93. ^{1}H NMR spectrum of **S9** recorded in $CDCl_3$.

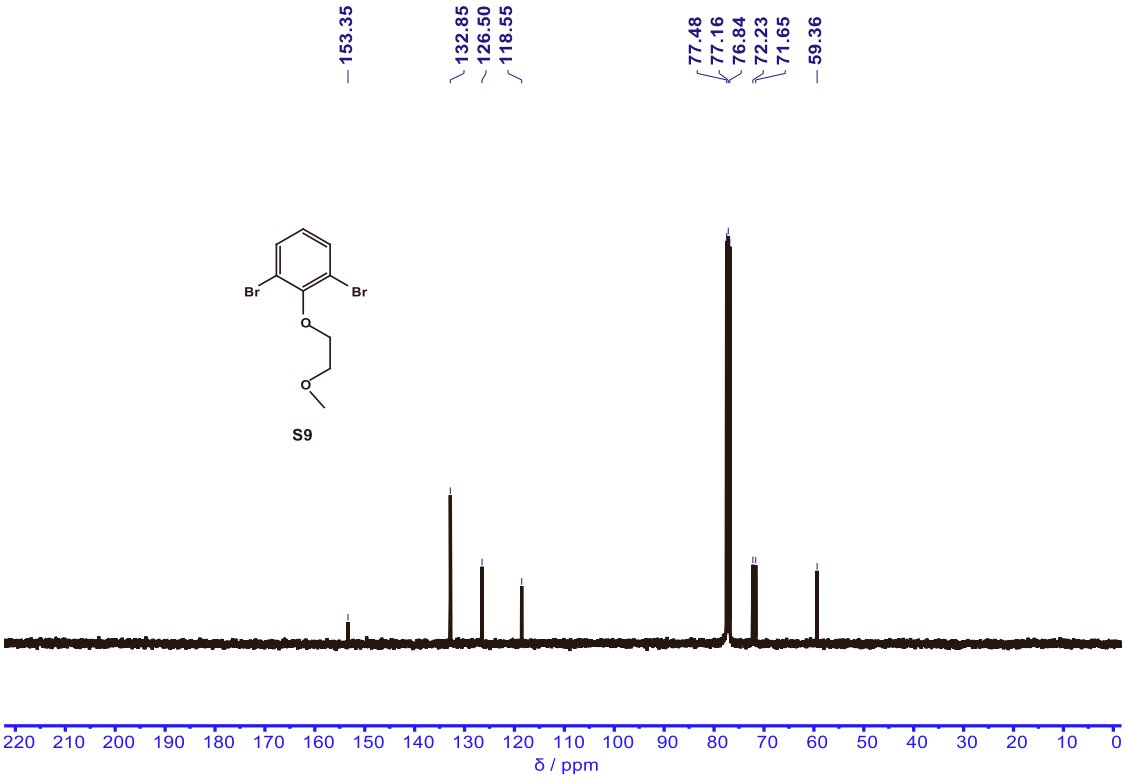

Figure S94. ^{13}C NMR spectrum of **S9** recorded in $CDCl_3$.

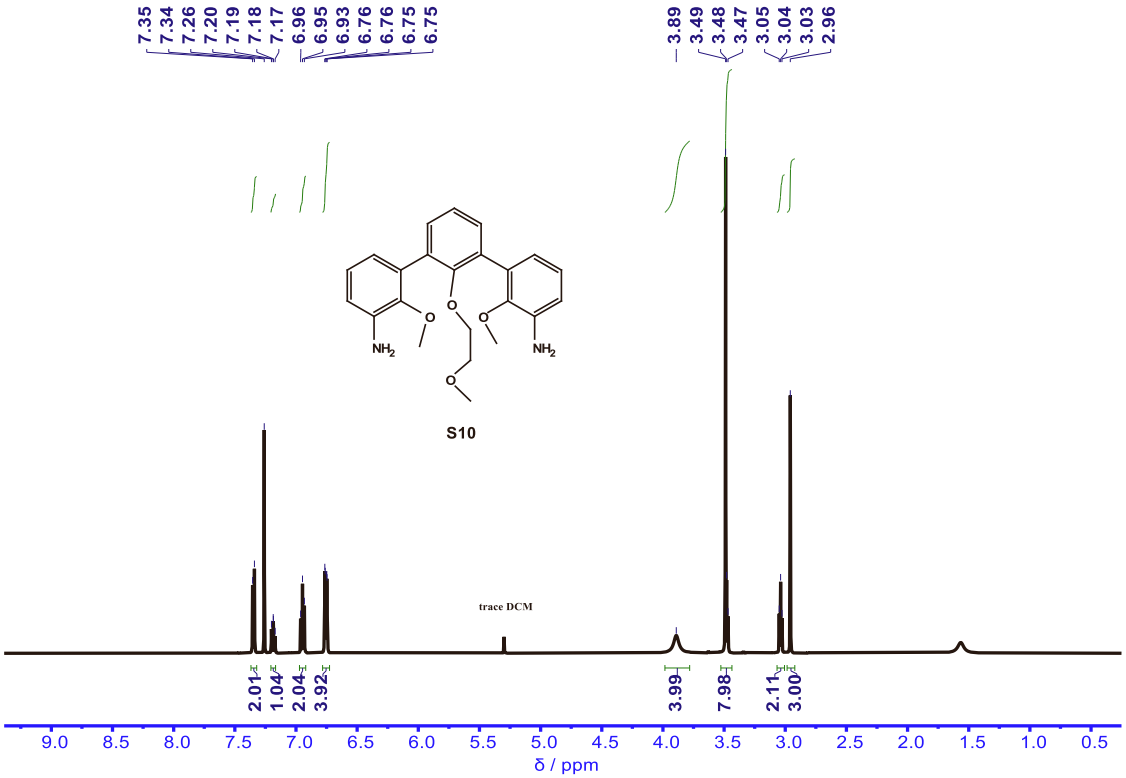

Figure S95. ^{1}H NMR spectrum of **S10** recorded in $CDCl_3$.

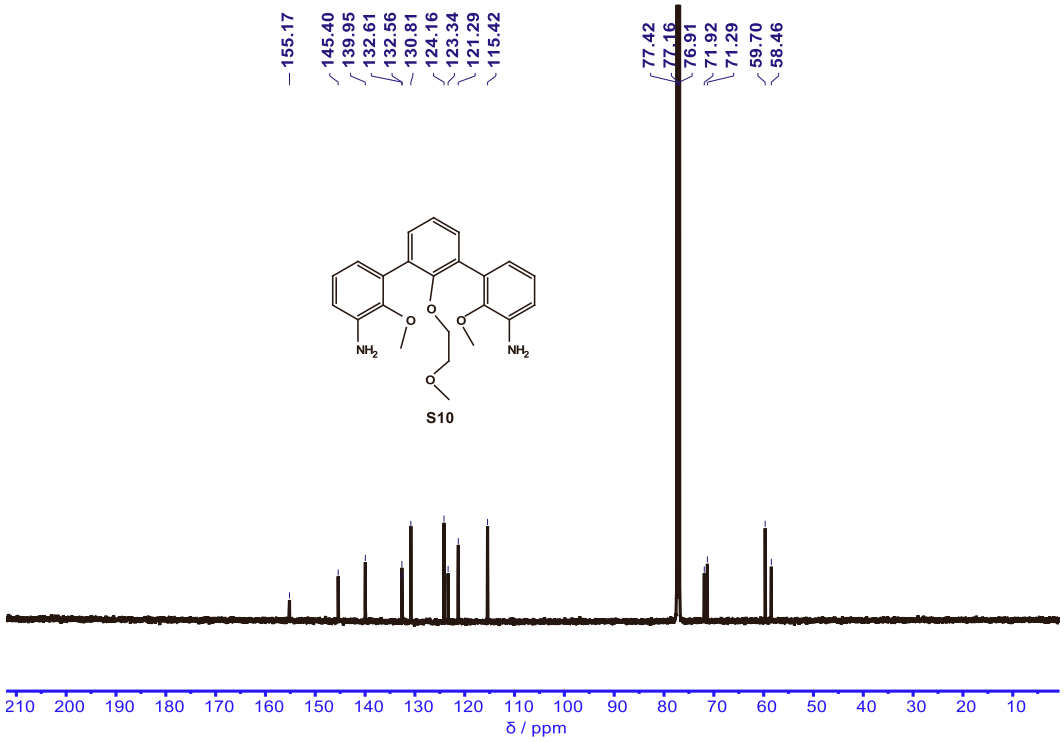

Figure S96. ^{13}C NMR spectrum of **S10** recorded in $CDCl_3$.

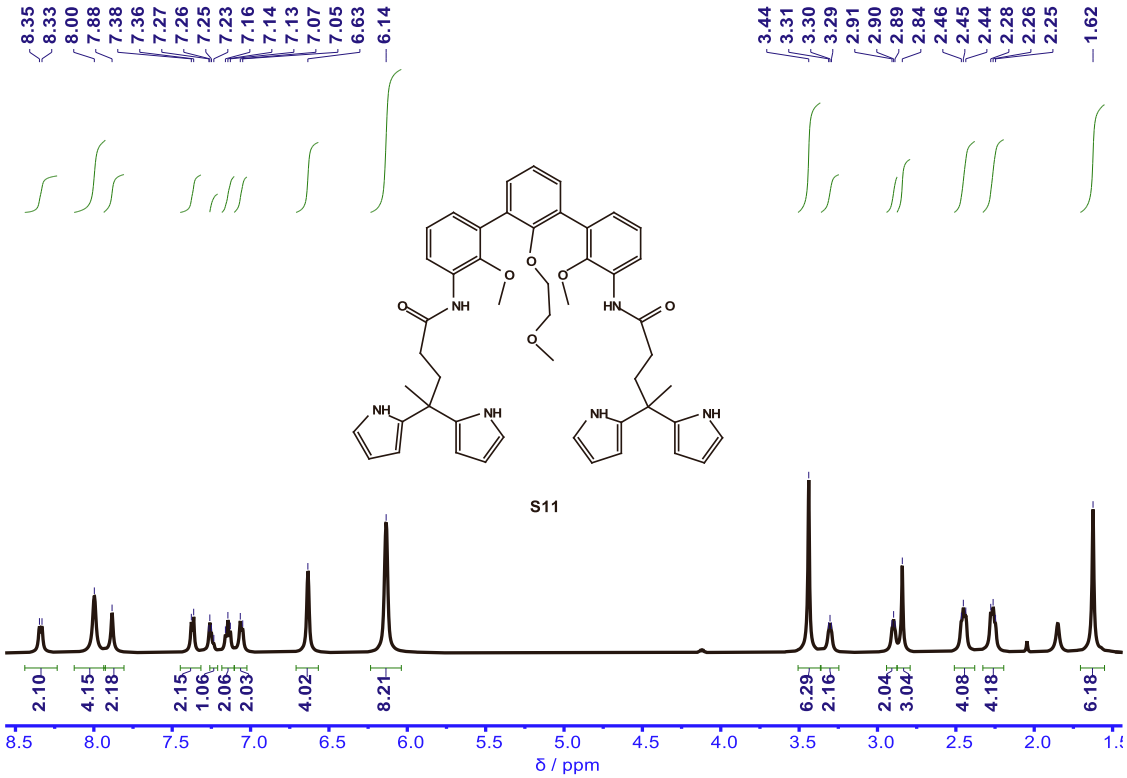

Figure S97. ^{1}H NMR spectrum of **S11** recorded in $CDCl_3$.

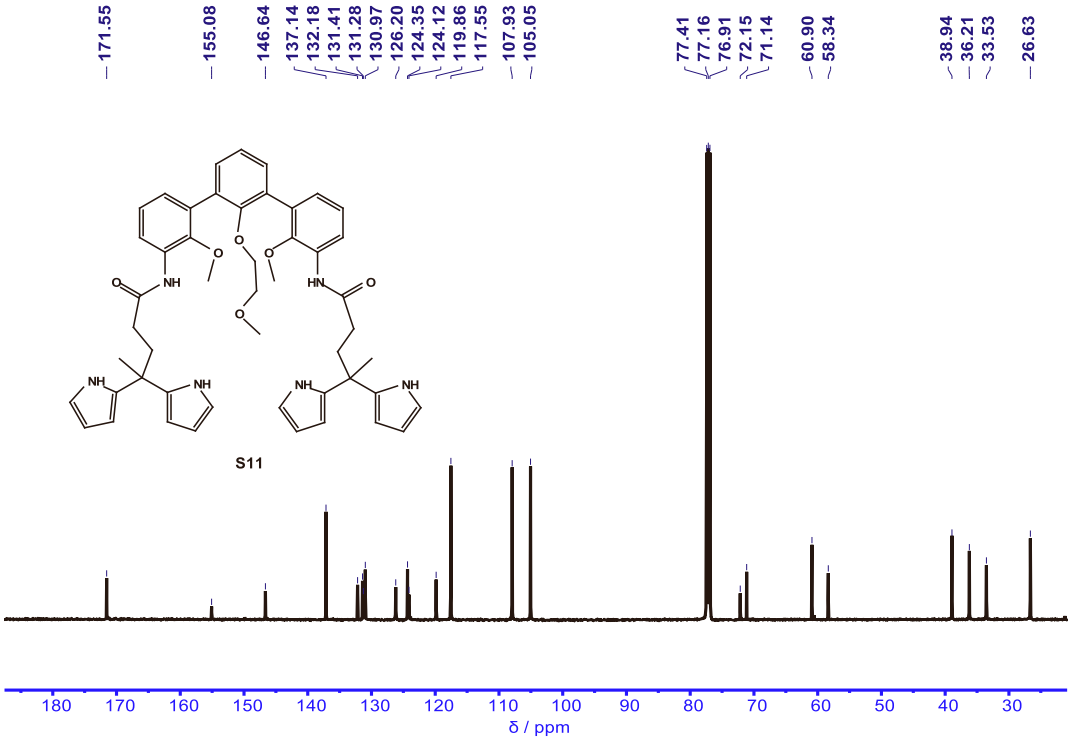

Figure S98. ^{13}C NMR spectrum of **S11** recorded in $CDCl_3$.

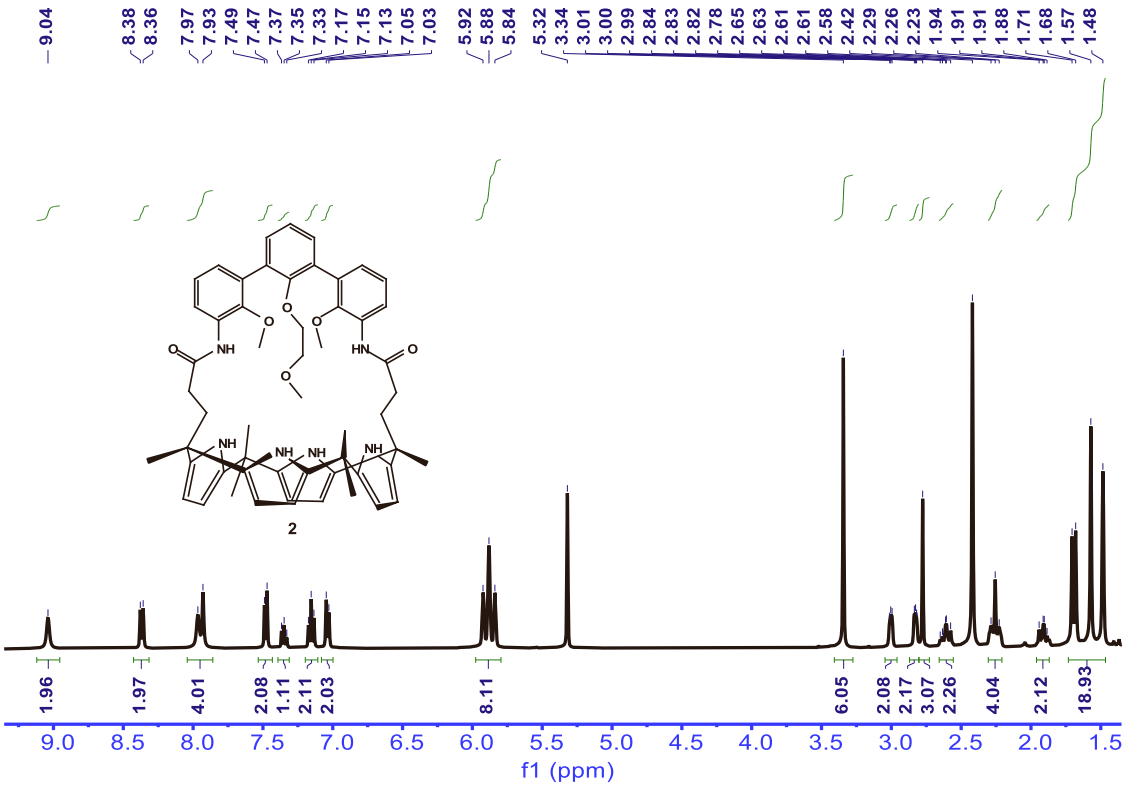

Figure S99. ^{1}H NMR spectrum of **2** recorded in CD_2Cl_2.

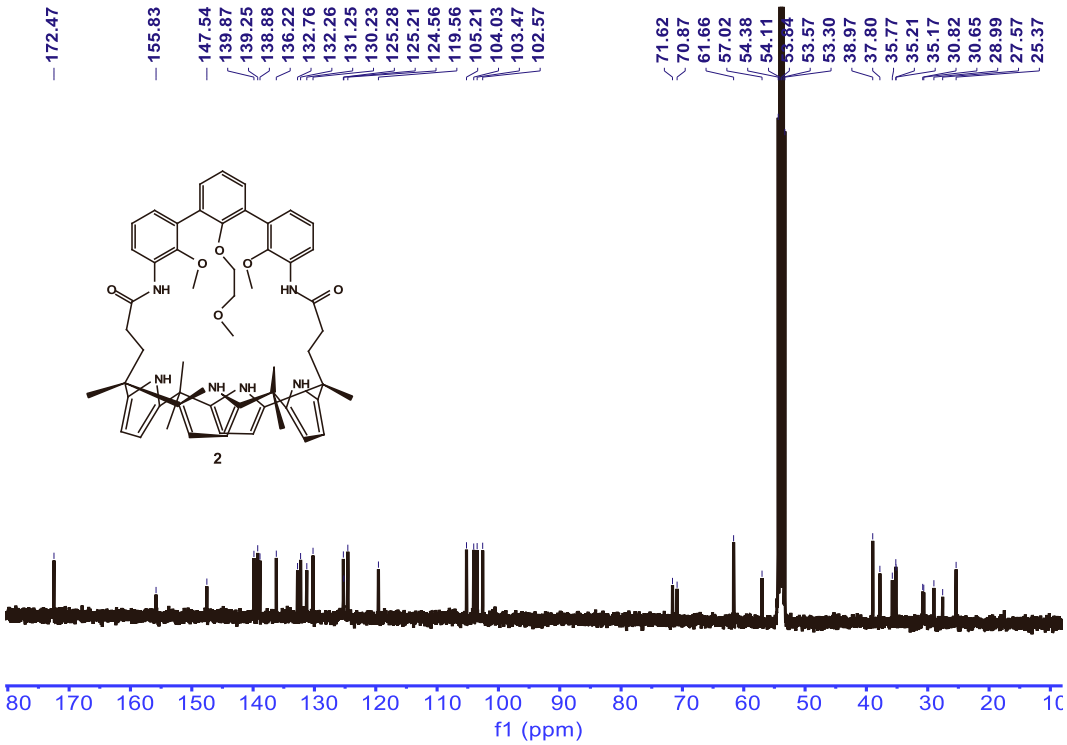

Figure S100. ^{13}C NMR spectrum of **2** recorded in CD_2Cl_2.

8. Binding Energies and Geometrical Coordinates of the Optimized Complexes

1•NaCl complex

Number of negative frequencies: 0

Counterpoise corrected energy =	-3380.454005533743
BSSE energy =	0.033415415374
sum of fragments =	-3380.125584159937
complexation energy =	-227.06 kcal/mole (raw)
complexation energy =	-206.09 kcal/mole (corrected)

Cartesian coordinates:

Symbol	X	Y	Z
Cl	0.59362500	0.14663800	0.24205900
Na	-1.88630100	-0.25643700	-0.49723200
O	-4.09120100	0.38935500	-0.91512300
O	-3.09311900	-1.76523900	0.82051700
N	2.48807300	-1.95344100	-1.69697200
H	1.88093200	-1.33751900	-1.16803100
O	0.02251800	5.96976200	-0.92188200
O	-2.18292900	1.86860600	0.67084100
O	-1.65542700	-2.28136800	-1.54143900
C	-4.87148500	4.18773500	-0.31187400
H	-5.95605700	4.24314800	-0.31030400
C	0.69490000	-3.66062000	0.04529100
H	0.34884900	-4.14799000	0.96532600
H	0.52508800	-2.58869900	0.17836500
N	3.41189800	1.14968500	1.85534400
H	2.53657700	0.86443000	1.43395500
C	3.12657400	-1.60364200	-2.87060800

N	3.23529500	1.33790900	-1.52806400
H	2.43312500	0.97332600	-1.02761100
C	2.77534100	-3.26125700	-1.35281600
C	3.83571200	-2.71580100	-3.28110600
H	4.44725200	-2.78494400	-4.16914500
N	2.69608300	-2.15461300	1.68137000
H	2.07809500	-1.46388900	1.27223800
C	-4.24208000	3.03241000	0.17109000
C	3.44589200	-1.95282900	2.82346700
C	0.29675400	4.79671200	-0.71528300
C	4.00201500	0.52282000	2.93554700
C	-5.41059100	-1.85538900	0.16782700
C	5.01502500	2.55643400	-2.03180300
H	5.80680800	3.29077100	-1.99360400
C	2.91806300	-3.41678700	1.16331300
N	-2.54608300	-4.13685300	-0.56399600
H	-2.40440200	-5.12660000	-0.41280400
C	2.22831500	-3.92752900	-0.09753800
C	-1.83023800	2.00053100	2.06158300
H	-2.73502300	2.01002800	2.67891600
H	-1.25949800	2.91980300	2.22694400
H	-1.20490400	1.14049600	2.30193500
N	-0.66706900	3.84923100	-0.39452000
H	-0.35295800	2.90269200	-0.20453900
C	-1.50770100	-3.43248500	-1.12992500
C	2.46698700	-5.44632700	-0.19919100

H	2.05021800	-5.95544000	0.67580800
H	3.53542400	-5.67135000	-0.24285500
H	2.00681100	-5.85579300	-1.10298600
C	-3.87247700	-3.64111300	-0.46852400
C	-2.71677200	5.17713400	-0.83842900
H	-2.12514000	5.99682600	-1.21814800
C	1.88986700	-0.35484600	3.98414300
H	1.28497100	-0.18218500	3.08787500
H	1.83107200	0.54447300	4.60738900
H	1.44539200	-1.19294300	4.53327800
C	3.68273900	0.86691100	-2.74814800
C	-6.46250800	-2.59421600	-0.38718900
H	-7.46162000	-2.16857100	-0.38915900
C	-4.10719400	5.24457100	-0.80093000
H	-4.60011700	6.13771400	-1.17345400
C	4.66627300	4.36282600	0.27432500
H	5.72630600	4.10298800	0.21758500
H	4.50071700	4.91201300	1.20600800
H	4.44242500	5.02168900	-0.56836500
C	-0.16475600	-4.13116200	-1.15235900
H	0.33189000	-3.85153900	-2.08593100
H	-0.28440900	-5.22049700	-1.14357300
C	3.78701500	3.09652500	0.24071400
C	-2.84207000	2.98158400	0.16169300
C	-5.62241000	-0.48875600	0.71931300
C	-6.23244200	-3.84743700	-0.95462100

H	-7.05658000	-4.41003000	-1.38179200
C	4.03665700	2.36915000	-1.07525300
C	-2.05953400	4.03057300	-0.36205700
C	-4.12630000	-2.42416900	0.17965200
C	4.16965500	2.22618500	1.43496000
C	-5.04060500	1.89669200	0.70940100
C	-6.51443000	-0.25298700	1.77274700
H	-7.06254000	-1.08910500	2.19781800
C	4.79523000	1.61666600	-3.07552600
H	5.38810800	1.51236100	-3.97288600
C	5.16367700	1.21876700	3.20740200
H	5.86578100	0.99634800	3.99818400
C	-6.68468400	1.03280900	2.28296100
H	-7.37771800	1.20459800	3.10094000
C	-4.93815800	-4.35581800	-1.02341900
H	-4.74131600	-5.30023500	-1.52320700
C	-2.93066200	-2.12901500	2.20019300
H	-2.05632600	-1.58355000	2.55886300
H	-2.75447400	-3.20557700	2.29547800
H	-3.81426500	-1.84257100	2.78070900
C	1.46066300	0.11288000	-3.65430000
H	0.94592700	-0.65855500	-4.23837800
H	1.34351100	1.07623500	-4.16360800
H	0.96241800	0.18468700	-2.68216300
C	3.61414700	-3.75251600	-2.33456400
H	4.03441100	-4.74765600	-2.37015900

C	-4.92277700	0.60347800	0.17774200
C	1.72140400	4.27105100	-0.84604000
H	2.32206800	5.15235500	-1.07764100
H	1.76412500	3.61294500	-1.72336100
C	-5.94386100	2.09266400	1.76453000
H	-6.04687200	3.08887500	2.18455300
C	2.28383900	3.52266800	0.37639500
H	1.67280700	2.63476600	0.56477800
H	2.19723600	4.15018900	1.27226200
C	3.37146700	-0.67000700	3.64414100
C	2.96797100	-0.23463900	-3.52081600
C	-4.73403500	0.58696800	-2.18439200
H	-5.08379700	1.62000000	-2.27926400
H	-5.57341400	-0.10695800	-2.30087900
H	-3.98143700	0.38012300	-2.94772900
C	4.11618900	-0.89766600	4.97345200
H	3.66683800	-1.73215000	5.52039100
H	4.05938600	0.00071200	5.59515700
H	5.17169500	-1.12947200	4.80533900
C	3.55888000	-0.29790100	-4.94223000
H	4.62576300	-0.53747200	-4.92144600
H	3.43624300	0.66641000	-5.44413100
H	3.04763500	-1.06656300	-5.52965100
C	5.26826600	2.28263500	2.27079700
H	6.06753800	3.00796000	2.22082100
C	3.82863100	-4.03177700	2.00042600

H	4.22111800	-5.03229000	1.88747100
C	4.15902300	-3.11659100	3.03668200
H	4.84348600	-3.29978400	3.85242800

1•KCl complex

Number of negative frequencies: 0

Counterpoise corrected energy = -3818.031461855805
BSSE energy = 0.033472533241
sum of fragments = -3817.745531583994
complexation energy = -200.43 kcal/mole (raw)
complexation energy = -179.42 kcal/mole (corrected)

Cartesian coordinates:

Symbol	X	Y	Z
K	-1.74091000	-0.14200000	-1.25932600
Cl	0.68344300	0.11001700	0.39010400
O	-2.17346300	1.89289100	0.65257900
O	-4.32561500	0.42648700	-0.98136900
O	-0.06072300	5.99957400	-1.01798400
N	-2.45472500	-4.26230900	-0.35850700
H	-2.28419000	-5.18014600	0.03014900
O	-2.91300100	-1.70488900	0.67516000
N	3.47850300	1.18960500	1.83532600
H	2.63691400	0.83850400	1.39359200
N	2.51372000	-1.92642100	-1.65891000
H	2.04179200	-1.29093000	-1.02530700
N	3.15798900	1.39643000	-1.50959400
H	2.36590400	1.03882100	-0.98706000
N	-0.72424000	3.90558100	-0.37362200
H	-0.39856800	2.98445000	-0.10081600
O	-1.63940900	-2.67372700	-1.76715400
N	2.77629300	-2.15082600	1.69345800
H	2.05328600	-1.51471600	1.37612300

C	-2.87280000	2.99820000	0.19274200
C	4.08961600	0.60202500	2.92443900
C	2.23444500	3.57819600	0.38131400
H	2.14762000	4.19663300	1.28332200
H	1.63714600	2.67956700	0.56812800
C	3.02109600	-1.57322300	-2.89378600
C	3.60295100	-2.70968600	-3.42153400
H	4.09203300	-2.78439700	-4.38203500
C	-2.12020100	4.06730000	-0.33461500
C	4.15910900	2.32429600	1.43901200
C	2.76407300	-3.25758500	-1.38712800
C	2.05615500	-0.39118500	4.02169000
H	1.99513400	0.47842100	4.68535500
H	1.65870800	-1.26524800	4.55075700
H	1.41312900	-0.19577300	3.15786000
C	4.33701500	-0.87833000	4.90709400
H	5.39622500	-1.04827200	4.69433100
H	3.94950900	-1.75428300	5.43590800
H	4.25859200	-0.00784700	5.56530600
C	0.22944700	4.84622200	-0.73565700
C	3.62819900	-1.89476700	2.75115900
C	3.74348200	3.16702200	0.23506700
C	-5.49765700	-0.54133300	0.88122200
C	-4.94788800	0.58623700	0.24936200
C	3.98075700	2.41697600	-1.07107600
C	4.60884400	4.44328100	0.22966100

H	4.37573100	5.07631000	-0.62985300
H	5.67108000	4.19184300	0.17689000
H	4.44143500	5.01691700	1.14629800
C	2.31807200	-3.93098600	-0.09562300
C	4.71772500	1.62776000	-3.06547700
H	5.30329200	1.50492800	-3.96537900
C	3.44050600	-3.76357700	-2.48076500
H	3.79249000	-4.77904300	-2.59519800
C	-5.75147900	2.01791500	2.00651100
H	-5.81614300	3.00327500	2.45891500
C	2.62350500	-5.43858200	-0.19219500
H	2.12569500	-5.88786800	-1.05597800
H	2.29056900	-5.95093600	0.71598400
H	3.69627000	-5.61188100	-0.30541000
C	3.06192800	-3.37468700	1.11611100
C	-3.77571200	-3.74075300	-0.26159600
C	3.36962400	-0.20636600	-4.94224400
H	4.43179400	-0.46394700	-4.97717800
H	3.24092600	0.77632600	-5.40510000
H	2.82015000	-0.94691200	-5.53142900
C	-1.44994300	-3.69239300	-1.10461700
C	1.66502600	4.33635000	-0.83362100
H	2.25588500	5.22833700	-1.04874000
H	1.72921800	3.69252700	-1.72091200
C	3.53302700	-0.63946500	3.61417100
C	-6.16378500	-4.01245500	-0.52832100

H	-7.01126300	-4.62158300	-0.82678400
C	4.95890400	2.57474800	-2.03310500
H	5.76275500	3.29638800	-2.00738400
C	-4.87108200	-4.51653300	-0.64882200
H	-4.69978700	-5.51008500	-1.05346900
C	-1.86933000	1.93963800	2.05969800
H	-2.78445100	1.81880700	2.64876200
H	-1.38966800	2.89070800	2.31547600
H	-1.17520500	1.12109900	2.24608100
C	-4.19918400	5.23570100	-0.73678000
H	-4.71752400	6.11979300	-1.09632500
C	-5.28824000	-1.91446500	0.33537900
C	5.18634400	1.38511300	3.23012400
H	5.88530600	1.21213300	4.03588500
C	2.84710800	-0.18276800	-3.49312200
C	-6.36815100	-2.71797000	-0.05194000
H	-7.37461700	-2.31558000	0.01815600
C	-2.80747700	5.19957300	-0.80087900
H	-2.23983600	6.03249900	-1.18918400
C	3.59294100	0.90215600	-2.72611000
C	-5.01267400	1.86540100	0.82507100
C	0.77657000	-3.73673700	0.10537600
H	0.55340500	-2.66693100	0.16251700
H	0.49705800	-4.16822400	1.07450000
C	-4.93413900	4.16505300	-0.22918100
H	-6.01895600	4.20631600	-0.19394900

C	4.11825700	-3.90847700	1.82969600
H	4.59429100	-4.86071500	1.64450300
C	4.47152900	-2.98466000	2.84899600
H	5.25771900	-3.11386500	3.57887300
C	5.22971900	2.46126400	2.30254200
H	5.97202300	3.24592300	2.27562800
C	-2.50776900	-1.93735700	2.03262900
H	-2.31058500	-3.00157900	2.20077800
H	-3.27864300	-1.58826100	2.72891700
H	-1.58692000	-1.37007100	2.17385300
C	-4.27343900	3.02111800	0.23662100
C	-6.37244400	0.92552300	2.60958200
H	-6.94201100	1.06142300	3.52395000
C	-3.99086800	-2.45309500	0.25714400
C	-0.09100800	-4.35960000	-1.01876700
H	0.40051900	-4.19809100	-1.98271800
H	-0.19595300	-5.44036000	-0.86848200
C	1.33472900	0.17102700	-3.54735300
H	0.78928600	-0.59422300	-4.11182500
H	1.19106100	1.14336200	-4.03292000
H	0.90406100	0.22829100	-2.54172400
C	-6.22423300	-0.34822900	2.06404500
H	-6.65932600	-1.21073700	2.56100500
C	-5.20674300	0.64771300	-2.09104800
H	-4.61902700	0.47877200	-2.99691600
H	-5.58415500	1.67593200	-2.08705400

H	-6.04424900	-0.05847500	-2.06672200

2•NaCl complex

Number of negative frequencies: 0

Counterpoise corrected energy = -3534.228247682795
BSSE energy = 0.035024175328
sum of fragments = -3533.887286906162
complexation energy = -235.93 kcal/mole (raw)
complexation energy = -213.96 kcal/mole (corrected)

Cartesian coordinates:

Symbol	X	Y	Z	
Cl	0.69842800	0.12899500	0.13505400	1
O	-2.06309500	1.79892400	0.77697800	2
O	-4.08669800	0.29420000	-0.64143300	2
O	0.02685100	5.91767500	-0.90114900	2
N	-2.33478500	-4.14618300	-0.45101500	2
H	-2.11931000	-5.10523200	-0.21350200	2
O	-2.79858300	-1.72947200	0.86954400	2
N	3.37973600	1.16867200	1.99317100	2
H	2.56308500	0.84674000	1.48848100	2
N	2.75958700	-1.93362800	-1.61232200	2
H	2.13064500	-1.30616700	-1.12280900	2
N	3.44775100	1.37407800	-1.38530700	2
H	2.59621700	1.00857300	-0.97408300	2
N	-0.63748500	3.79966000	-0.33191600	2
H	-0.31387100	2.85468300	-0.15040700	2
O	-1.62534300	-2.33765700	-1.64159300	2
N	2.70594300	-2.13785600	1.76615100	2
H	2.10221900	-1.45376600	1.32557800	2
C	-2.76478300	2.91617900	0.34697000	2

C	3.89990400	0.55817500	3.11769900	2
C	2.27812400	3.51318400	0.46629400	2
H	2.11900300	4.14021700	1.35263800	2
H	1.69097000	2.60470700	0.62683100	2
C	3.50272400	-1.59015200	-2.72508400	2
C	4.21236600	-2.71809900	-3.08952500	2
H	4.89130900	-2.79657800	-3.92631500	2
C	-2.02552400	3.97704000	-0.21469700	2
C	4.12334200	2.28055700	1.64650000	2
C	2.98431500	-3.25135700	-1.26024500	2
C	1.74621000	-0.37067300	4.01884300	2
H	1.63179000	0.51947300	4.64738800	2
H	1.28011100	-1.22304200	4.52671400	2
H	1.20068000	-0.19416400	3.08563200	2
C	3.91609300	-0.88727800	5.14128200	2
H	4.98473500	-1.09508100	5.03640200	2
H	3.45101400	-1.73796800	5.64854700	2
H	3.80178400	0.00112700	5.76937100	2
C	0.31226400	4.75041900	-0.67635900	2
C	3.39673200	-1.92969800	2.94396600	2
C	3.80052000	3.14233000	0.42841800	2
C	-5.39608400	-0.59272700	1.14268200	2
C	-4.80255700	0.51907900	0.52048700	2
C	4.18010800	2.42251600	-0.86058900	2
C	4.62750400	4.43984200	0.52618500	2
H	4.44170100	5.09047800	-0.33225600	2

H	5.69795600	4.22091600	0.55035600	2
H	4.37177700	4.98161400	1.44173400	2
C	2.34864300	-3.90606700	-0.04092800	2
C	5.17047300	1.65304100	-2.74967800	2
H	5.86218200	1.54591100	-3.57287400	2
C	3.88711600	-3.75671700	-2.17587600	2
H	4.28505300	-4.76153300	-2.18677200	2
C	-5.70957600	1.98879700	2.19073300	2
H	-5.80157300	2.98416000	2.61554400	2
C	2.57571400	-5.42773500	-0.12164800	2
H	2.16603500	-5.83633300	-1.04992100	2
H	2.10154100	-5.92796000	0.72898500	2
H	3.64201400	-5.66541700	-0.10013900	2
C	2.97153700	-3.39442200	1.25478200	2
C	-3.65960400	-3.69154400	-0.21370900	2
C	4.17080300	-0.27854300	-4.72925100	2
H	5.22828400	-0.51887400	-4.58757100	2
H	4.10585700	0.68663800	-5.24003300	2
H	3.72959900	-1.04598200	-5.37243800	2
C	-1.38426300	-3.44155900	-1.15138000	2
C	1.74463500	4.23479300	-0.78557100	2
H	2.34345600	5.11659100	-1.02092700	2
H	1.80931300	3.56137000	-1.64983700	2
C	3.25212300	-0.65686400	3.77055100	2
C	-6.04993900	-4.02314800	-0.35937800	2
H	-6.89635000	-4.63730300	-0.65047700	2

C	5.25873000	2.60980800	-1.70265800	2
H	6.03449500	3.35252900	-1.58402600	2
C	-4.75362900	-4.47454200	-0.59293700	2
H	-4.57931400	-5.42857300	-1.08267700	2
C	-1.64449200	1.88029800	2.15150800	2
H	-2.51544800	1.84028100	2.81454300	2
H	-1.08739900	2.80614900	2.32942700	2
H	-0.98911900	1.02685400	2.32231900	2
C	-4.10157500	5.18944400	-0.48158000	2
H	-4.62339200	6.08626000	-0.80253600	2
C	-5.18314300	-1.95688400	0.58531000	2
C	5.00151900	1.30161800	3.49415500	2
H	5.63966700	1.10392900	4.34353100	2
C	3.42293400	-0.21774300	-3.38361400	2
C	-6.26141100	-2.76534900	0.20475700	2
H	-7.27192100	-2.38974300	0.33620000	2
C	-2.71699400	5.12751800	-0.62609800	2
H	-2.15636900	5.95369300	-1.03816200	2
C	4.03753500	0.89188200	-2.53927600	2
C	-4.90287400	1.81305900	1.05686700	2
C	0.81331200	-3.62243100	0.02395000	2
H	0.64643700	-2.54964900	0.15149800	2
H	0.42244600	-4.10736700	0.92749300	2
C	-4.82518000	4.12461900	0.05109400	2
H	-5.90647600	4.17904500	0.13723500	2
C	3.85032700	-3.99917400	2.13203000	2

H	4.26259700	-4.99338800	2.03455900	2
C	4.11644800	-3.08357700	3.18660300	2
H	4.76211500	-3.26086200	4.03468200	2
C	5.14101100	2.37760100	2.57543900	2
H	5.90833500	3.13798000	2.59944200	2
C	-2.38457200	-2.04668700	2.20717400	2
H	-2.16746100	-3.11604900	2.30126000	2
H	-3.15861100	-1.75985600	2.92763100	2
H	-1.47362400	-1.47454700	2.38723000	2
C	-4.16017300	2.96223700	0.46641800	2
C	-6.35786400	0.90927500	2.78796100	2
H	-6.97301000	1.06641600	3.66875600	2
C	-3.88013400	-2.46018000	0.42161700	2
C	-0.00828600	-4.07656800	-1.20548900	2
H	0.47864800	-3.73500800	-2.12233400	2
H	-0.08215900	-5.16976500	-1.24483300	2
C	1.93992400	0.12367800	-3.68530400	2
H	1.50074700	-0.64905400	-4.32697600	2
H	1.87489500	1.08969500	-4.19972300	2
H	1.33796600	0.18491500	-2.77302800	2
C	-6.18534600	-0.37681300	2.27936900	2
H	-6.65133300	-1.22726600	2.76904900	2
C	-4.71122300	0.71134000	-1.86508600	2
H	-4.72189500	1.80501200	-1.92228500	2
H	-5.74151500	0.33596800	-1.90533200	2
Na	-1.79751100	-0.19996700	-0.70513800	3

C	-3.91096400	0.11798000	-3.00388100 2
H	-3.92873500	-0.98090800	-2.95079800 2
H	-4.36372500	0.43079000	-3.95751900 2
O	-2.57346200	0.58497500	-2.91405200 2
C	-1.77960900	0.17114300	-4.02295100 2
H	-0.79469800	0.62022000	-3.89443000 2
H	-1.68233900	-0.92176700	-4.04670700 2
H	-2.21941600	0.52511900	-4.96551300 2

2•KCl complex

Number of negative frequencies: 0

Counterpoise corrected energy = -3971.803472304384
BSSE energy = 0.036314834655
sum of fragments = -3971.506806715970
complexation energy = -208.95 kcal/mole (raw)
complexation energy = -186.16 kcal/mole (corrected)

Cartesian coordinates:

Symbol	X	Y	Z
Cl	-0.87910500	0.10379700	-0.49787400
O	1.97433500	1.85513800	-0.98116500
O	4.23266100	0.34827300	0.50962500
O	-0.00418700	5.99184500	0.77379200
N	2.27123700	-4.28003000	0.05995000
H	2.05389700	-5.18914800	-0.32573800
O	2.67947900	-1.72630000	-0.99972000
N	-3.73867800	1.19068400	-1.79850300
H	-2.87115800	0.84162700	-1.40774100
N	-2.59252300	-1.90487100	1.66219200
H	-2.14294900	-1.27833100	1.00342700
N	-3.23163700	1.41926300	1.52277800
H	-2.47606800	1.04735000	0.95740300
N	0.60725400	3.88569500	0.11687700
H	0.26199400	2.95992600	-0.11322900
O	1.58797900	-2.69048700	1.53772000
N	-3.05023800	-2.15109400	-1.66806700
H	-2.31443300	-1.51084400	-1.39033100
C	2.70845800	2.95956200	-0.58043200

C	-4.41930800	0.59464800	-2.84075000
C	-2.39667600	3.57591700	-0.44212300
H	-2.35981700	4.18993100	-1.35059500
H	-1.82073600	2.67085900	-0.66105400
C	-3.03880500	-1.53915700	2.91683100
C	-3.60638900	-2.66666600	3.47848500
H	-4.05157800	-2.73058100	4.46089800
C	1.99789600	4.03980500	-0.01724600
C	-4.39157600	2.32933900	-1.36860500
C	-2.86798600	-3.23510900	1.41108900
C	-2.45683500	-0.41129600	-4.04991900
H	-2.43135700	0.45573200	-4.71927700
H	-2.09464400	-1.28895300	-4.59799000
H	-1.76349300	-0.21606400	-3.22588700
C	-4.78744800	-0.89481600	-4.79752600
H	-5.83265300	-1.06108200	-4.52177100
H	-4.43398700	-1.77417600	-5.34428100
H	-4.74591900	-0.02747000	-5.46320300
C	-0.31597000	4.83519200	0.52986900
C	-3.95578200	-1.90322600	-2.68206100
C	-3.89783500	3.18132100	-0.20121500
C	5.25622100	-0.60222900	-1.42773100
C	4.76548400	0.53041000	-0.75549400
C	-4.06514000	2.44736800	1.12476500
C	-4.74933600	4.46614500	-0.15930300
H	-4.45729400	5.10770500	0.67560000

H	-5.80864700	4.22644600	-0.03766800
H	-4.63346400	5.02618500	-1.09213800
C	-2.49351300	-3.92047700	0.10299100
C	-4.69322800	1.68479500	3.16614100
H	-5.22621100	1.57728700	4.10005800
C	-3.49783000	-3.72775900	2.53816000
H	-3.85422600	-4.73886700	2.67521700
C	5.46004500	1.95339900	-2.56607200
H	5.50215000	2.93836500	-3.02209900
C	-2.79680200	-5.42630300	0.22923400
H	-2.25590400	-5.86899200	1.07019000
H	-2.51272200	-5.94784400	-0.69027600
H	-3.86269100	-5.59548100	0.39934900
C	-3.30167000	-3.37279400	-1.07100700
C	3.58713500	-3.77627000	-0.14349400
C	-3.27051800	-0.15993300	4.97338500
H	-4.33158700	-0.40794100	5.06492600
H	-3.10953000	0.82359800	5.42431100
H	-2.69757900	-0.90310200	5.53649400
C	1.33443100	-3.69984300	0.88307300
C	-1.74332800	4.33239400	0.73091400
H	-2.31398800	5.22737900	0.98482900
H	-1.74875800	3.68927800	1.62093400
C	-3.90814600	-0.65232400	-3.55534600
C	5.98474400	-4.08496500	-0.07988400
H	6.84511700	-4.70767800	0.14479600

C	-4.98242200	2.62672700	2.14154800
H	-5.77710800	3.35872600	2.15666000
C	4.69921500	-4.56960900	0.14931000
H	4.54726800	-5.56181000	0.56498800
C	1.57387500	1.89258800	-2.36360300
H	2.44435000	1.75631600	-3.01401400
H	1.08706900	2.84632200	-2.59535900
H	0.86029900	1.07992300	-2.49344500
C	4.10315400	5.20426400	0.22693200
H	4.64785100	6.09108400	0.53755000
C	5.07164800	-1.97236200	-0.86638800
C	-5.53325500	1.37625700	-3.08127700
H	-6.28277900	1.19763100	-3.83893600
C	-2.82416200	-0.14699100	3.49893900
C	6.16762200	-2.79312700	-0.57220100
H	7.17062700	-2.40603600	-0.72703100
C	2.71868300	5.17516800	0.38540500
H	2.18138300	6.01585000	0.79927800
C	-3.60038900	0.94083800	2.76700900
C	4.79903700	1.80877800	-1.33803500
C	-0.96520400	-3.73189600	-0.18503100
H	-0.74234200	-2.66336700	-0.26356400
H	-0.74226500	-4.17170900	-1.16507500
C	4.79792700	4.12291100	-0.31271600
H	5.87825300	4.15779700	-0.41998300
C	-4.39097300	-3.91399100	-1.72722900

H	-4.85334100	-4.86701600	-1.51358600
C	-4.79905400	-2.99649900	-2.73172800
H	-5.62094600	-3.13208700	-3.41993100
C	-5.51596400	2.46015400	-2.16187600
H	-6.25434100	3.24603000	-2.09366100
C	2.15351100	-1.95135400	-2.31596700
H	1.93418900	-3.01359700	-2.46933400
H	2.86189200	-1.60550800	-3.07743900
H	1.22785100	-1.37737400	-2.37241000
C	4.10338100	2.97473100	-0.71669700
C	6.02582700	0.85585900	-3.21206900
H	6.53233500	0.98701600	-4.16346300
C	3.77706000	-2.49068400	-0.67727600
C	-0.03689300	-4.34857200	0.89249600
H	-0.46481400	-4.16715700	1.88268900
H	0.04553500	-5.43280100	0.75264600
C	-1.30859800	0.19551100	3.47195000
H	-0.74062900	-0.57329300	4.00924900
H	-1.13257100	1.16871300	3.94537100
H	-0.92903000	0.24631600	2.44596100
C	5.89880500	-0.41686300	-2.65903700
H	6.28722800	-1.28410700	-3.18557100
C	5.05886600	0.81265900	1.59040400
H	4.96750300	1.90042700	1.68652800
H	6.10701500	0.55896900	1.38916600
K	1.64934600	-0.12718400	1.03010800

C	4.62857500	0.12522100	2.86833000
H	4.70049300	-0.96723000	2.75107300
H	5.31465000	0.43141800	3.67414300
O	3.29800700	0.49850000	3.18965400
C	2.87157100	-0.02553200	4.44048200
H	1.84661300	0.31613200	4.59995200
H	2.89102300	-1.12479600	4.43943200
H	3.50526400	0.34488800	5.25852500

9. References

1. He, Q.; Williams, N. J.; Oh, J. H.; Lynch, V. M.; Kim, S. K.; Moyer, B. A.; Sessler, J. L., Selective Solid-Liquid and Liquid-Liquid Extraction of Lithium Chloride Using Strapped Calix[4]pyrroles. *Angew. Chem. Int. Ed.* **2018,** *57*, 11924-11928.
2. Dey, S.; Pal, K.; Sarkar, S., An efficient and eco-friendly protocol to synthesize calix[4]pyrroles. *Tetrahedron Lett.* **2006,** *47*, 5851-5854.
3. Greenwood, J. R.; Leit de Moradei, S. M.; Masse, C. E.; McLean, T. H.; Mondal, S. Imidazopyridines and imidazopyrimidines as TYK2 inhibitors and their preparation. WO2018075937A1, 2018.
4. Chan, J. M. W.; Swager, T. M., Synthesis of arylethynylated cyclohexa-m-phenylenes via sixfold Suzuki coupling. *Tetrahedron Lett.* **2008,** *49*, 4912-4914.
5. He, Q.; Zhang, Z.; Brewster, J. T.; Lynch, V. M.; Kim, S. K.; Sessler, J. L., Hemispherand-Strapped Calix[4]pyrrole: An Ion-pair Receptor for the Recognition and Extraction of Lithium Nitrite. *J. Am. Chem. Soc.* **2016,** *138*, 9779-9782.
6. Gaussian 16, R. A., Frisch, M. J.; Trucks, G. W.; Schlegel, H. B.; Scuseria, G. E.; Robb, M. A.; Cheeseman, J. R.; Scalmani, G.; Barone, V.; Petersson, G. A.; Nakatsuji, H.; Li, X.; Caricato, M.; Marenich, A. V.; Bloino, J.; Janesko, B. G.; Gomperts, R.; Mennucci, B.; Hratchian, H. P.; Ortiz, J. V.; Izmaylov, A. F.; Sonnenberg, J. L.; Williams-Young, D.; Ding, F.; Lipparini, F.; Egidi, F.; Goings, J.; Peng, B.; Petrone, A.; Henderson, T.; Ranasinghe, D.; Zakrzewski, V. G.; Gao, J.; Rega, N.; Zheng, G.; Liang, W.; Hada, M.; Ehara, M.; Toyota, K.; Fukuda, R.; Hasegawa, J.; Ishida, M.; Nakajima, T.; Honda, Y.; Kitao, O.; Nakai, H.; Vreven, T.; Throssell, K.; Montgomery, J. A., Jr.; Peralta, J. E.; Ogliaro, F.; Bearpark, M. J.; Heyd, J. J.; Brothers, E. N.; Kudin, K. N.; Staroverov, V. N.; Keith, T. A.; Kobayashi, R.; Normand, J.; Raghavachari, K.; Rendell, A. P.; Burant, J. C.; Iyengar, S. S.; Tomasi, J.; Cossi, M.; Millam, J. M.; Klene, M.; Adamo, C.; Cammi, R.; Ochterski, J. W.; Martin, R. L.; Morokuma, K.; Farkas, O.; Foresman, J. B.; Fox, D. J. Gaussian, Inc., Wallingford CT, 2016.
7. Xu, X.; Goddard, W. A., *Proc. Natl. Acad. Sci. USA* **2004,** *101*, 2673-2677.
8. Boys, S. F.; Bernardi, F., *Mol. Phys.* **1970,** *19*, 553-566.
9. van Duijneveldt, F. B.; van Duijneveldt-van de Rijdt, J. G. C. M.; van Lenthe, J. H., *Chem. Rev.* **1994,** *94*, 1873-1885.
10. Jowett, L. A.; Gale, P. A., Supramolecular methods: the chloride/nitrate transmembrane exchange assay. *Supramol. Chem.* **2019,** *31*, 297-312.
11. CrysAlisPro. Agilent Technologies. Agilent Technologies UK Ltd., O., UK, SuperNova CCD System,; CrysAlicPro Software System, 2013.
12. Dolomanov, O. V., Bourhis, L.J., Gildea, R.J, Howard, J.A.K. & Puschmann, H., *J. Appl. Cryst.* **2009,** *42*, 339-341.
13. Sheldrick, G. M., SHELXT - Integrated space-group and crystal-structure determination. *Acta Crystallogr. A* **2015,** *71*, 3-8.
14. Sheldrick, G. M., Crystal structure refinement with SHELXL. *Acta Crystallogr. C* **2015,** *71*, 3-8.